



Vigilada Mineducación

**SUBMARINE LANDSLIDES GEOHAZARDS ALONG THE SOUTHERN MARGIN
OF THE COLOMBIAN CARIBBEAN: RELATION TO GROUND CONDITIONS
AND EFFECT ON SHAPING SEAFLOOR GEOMORPHOLOGY**

DARWIN CLEMENTE MATEUS TARAZONA

thesis

Advisor

Jorge A Prieto, PhD.

**UNIVERSIDAD EAFIT
ESCUELA DE CIENCIAS
DOCTORADO EN CIENCIAS DE LA TIERRA
MEDELLÍN**

**SUBMARINE LANDSLIDES GEOHAZARDS ALONG THE SOUTHERN MARGIN
OF THE COLOMBIAN CARIBBEAN: RELATION TO GROUND CONDITIONS
AND EFFECT ON SHAPING SEAFLOOR GEOMORPHOLOGY**

**A dissertation submitted to the Department of Earth Sciences and the School
of Sciences of Universidad EAFIT in partial fulfillment of the requirements for
the degree of Doctor of Earth Sciences**

Committee:

Juan F. Paniagua-Arroyave, Ph.D., Universidad EAFIT, Colombia.

Alfonso Mariano Ramos Cañón, Ph.D., Universidad Javeriana, Colombia.

TABLE OF CONTENTS

LIST OF FIGURES	6
LIST OF TABLES	8
ABSTRACT	9
RESUMEN	12
ACKNOWLEDGMENTS	15
CHAPTER 1:	16
IDENTIFICATION OF SUBMARINE LANDSLIDES IN THE COLOMBIAN CARIBBEAN MARGIN (SOUTHERN SINÚ FOLD BELT) USING SEISMIC INVESTIGATIONS	16
ABSTRACT	17
1. INTRODUCTION	17
1.1. Regional setting	19
1.2. Data collection and analysis	19
2. TERRAIN CLASSIFICATION AND LANDSLIDE IDENTIFICATION	21
2.1. Landslides	21
2.2. Statistics of individual landslides	28
3. DISCUSSION	31
3.1. Relation between terrain types and Landslides	31
3.2. Landslides processes	32
3.3. Possible impact to future infrastructure	33
4. CONCLUSIONS	34
REFERENCES	35
CHAPTER 2:	40
ABSTRACT	41
1. INTRODUCTION	42
1.1. Regional settings	45

2. DATA COLLECTION AND ANALYSIS	47
3. RESULTS.....	49
3.1. Morphometry of landslides.....	49
3.2. Landslides occurrence and their relation with seafloor morphology....	51
3.2.1. Zone 1.....	51
3.2.2. Zone 2.....	53
3.2.3. Zone 3.....	53
3.2.4. Zone 4.....	57
3.3. Submarine landslides and their relation with the Botton Simulator Reflector (BSR).....	58
4. DISCUSSION.....	59
4.1. Landslides and their relation with ground condition	60
4.1.1. Submarine landslides in canyon walls.....	60
4.1.2. Submarine landslides in tectonically Controlled ridges.	61
4.1.3. Submarine landslides in channel-levee systems.....	62
4.1.4. Submarine landslides associated with the continental shelf break.....	62
4.2. Insights on landslides size and their relation with MTCs	63
4.3. Submarine landslides susceptibility map	64
5. CONCLUSIONS	68
ACKNOWLEDGMENTS	69
REFERENCES	69
CHAPTER 3:.....	79
ABSTRACT.....	80
1. INTRODUCTION.....	81
1.1. Theoretical frame	82
1.2. Regional settings	84
2. DATA AND METHODOLOGY	84
3. RESULTS.....	86
3.1. Pore pressure from wells.....	86

3.2. Pore pressure from seismic data..... 89

4. DISCUSSION..... 93

4.2. CONCLUSIONS 95

ACKNOWLEDGMENTS 95

REFERENCES 96

LIST OF FIGURES

CHAPTER 1:

Figure. 1. a) Topographic and Bathymetric map of the Northwest of Colombia showing the study zone (red polygon) and main geological features (Rincón et al, 2021)..	20
Figure. 2. Terrain types.	22
Figure. 3. Geographic distribution of submarine landslides in the study zone..	24
Figure. 4 Rotational landslide.	25
Figure. 5. Translational slides.....	26
Figure. 6 Complex Landslide..	26
Figure. 7. Deformational zone..	27
Figure. 8. MTC.	27
Figure. 9. Plan view of landslide oriented toward movement direction.	28
Figure. 10. Frequency histogram of morphologic parameter for individual landslides.	29
Figure. 11. Processes that affect landslides.....	33

CHAPTER 2:

Figure. 1. Conceptual models and seismic profile examples of Mass movement types... ..	44
Figure. 2. Study zone.....	46
Figure. 3. Conceptual diagram of the south Caribbean Colombian margin	47
Figure. 4 Statistics for Morphometric parameters in landslides.	50
Figure. 5. Conceptual ground model of zone 1.....	52
Figure. 6. Conceptual ground model of zone 2.....	54
Figure. 7. Conceptual ground model of zone 3.....	55
Figure. 8. Conceptual ground model of zone 4.....	56
Figure. 9. MTCs in the subsurface in zone 4.	57
Figure. 10. Relation between submarine landslides and the BSR..	59
Figure. 11. Examples of submarine landslides in canyons walls.....	61

Figure. 12. Examples of submarine landslides in tectonically Controlled ridges.....	62
Figure. 13. Examples of submarine landslides in channel-levee systems and the continental shelf break.....	63
Figure. 14. Physical parameters are involved in the susceptibility assessment..	66
Figure. 15. Landslides Susceptibility map in the South Colombian Caribbean margin..	67

CHAPTER 3:

Figure. 1. Overpressure range according to well tests in the Colombian Caribbean Offshore..	81
Figure. 2. Study area and data..	84
Figure. 3. Examples of wells South Sinú Offshore basin showing low overpressure profiles..	87
Figure. 4 Examples of wells South Sinú Offshore basin showing high overpressure profiles.	87
Figure. 5. Examples of wells North Sinú Offshore basin showing intermediate overpressure profiles.	88
Figure. 6 Normal compaction curve defined for the sedimentary sequence in the Sinú offshore basin.	89
Figure. 7. Interpretation of pore pressure using a seismic cube for the Sinú offshore area.	90
Figure. 8. Easth -West pore pressure distribution.....	90
Figure. 9. South – North pore pressure distribution.....	91
Figure. 10. Lateral pore pressure distribution along a Pliocene-Pleistocene regional discordance surface.	92
Figure. 11. Estimation of pore pressure from 2D Basin Modeling in the South Sinú fold Belt.	93
Figure. 12. Ko adjusted for pore pressure estimation in the Colombian Caribbean margin.	94

LIST OF TABLES

CHAPTER 1:

Table 1. Summary of terrain type characteristics.....	23
Table 2. Summary Summary Correlation coefficient between landslides morphologic parameters.....	30

CHAPTER 2:

Table 1. Submarine landslide types and characteristics used for identification.	48
Table 2. Landslide Wi index.....	65

ABSTRACT

Submarine landslides are a mixture of rock, soil, and fluids moving downslope due to a slope's initial event of mechanical failure. These phenomena play a significant role in the evolution of continental margins. On the one hand, sediment transport processes from the continental shelf to the foot of the continental slope are meaningful. On the other hand, submarine landslides play a critical role in shaping the geomorphology of the seafloor. In addition, they have the potential to affect coastal infrastructure, submarine telecommunications cables, and pipelines, and generate tsunamis and avalanches. Thus, the negative consequences of submarine landslides have been socially and economically significant.

In the Colombian southern Caribbean margin, submarine landslides are closely related to regional tectonic dynamics and show distinctive characteristics in canyon walls, channel-levee systems, tectonically controlled ridges, and continental shelf break. Previous studies have highlighted the importance of landslides as geohazards analyzing the largest landslides observed in the bathymetry or studying their presence in limited areas of the Colombian southern Caribbean.

This study shows a regional analysis of the occurrence of submarine landslides in the southern Colombian Caribbean. The geomorphological analysis was based on a bathymetric model that included seismic cubes and multibeam bathymetric surveys with resolutions ranging between 10 and 100 meters. These data involved areas from the continental shelf break to the foot of the continental rise making it easier to obtain a regional image of the seafloor in which the interpretation of landslide extended toward areas without 3D seismic information. After mapping the geographic distribution of submarine landslides, their relationship with ground conditions, including seafloor geomorphology, slope degree, fault presence, the Bottom Simulator Reflector (BSR), and Mass-Transport Complexes (MTCs), was analyzed. Finally, a preliminary map of landslides susceptibility was carried out following the landslide Weight index (Wi), a method proposed by Van Westen in

1997, and overpressure conditions in the sedimentary sequence were interpreted to see the relationship between both phenomena.

Chapter 1. This chapter presents a detailed geomorphological mapping of submarine landslides carried out using a high-resolution 3D seismic survey. This mapping allowed obtaining a statistical analysis and a complete interpretation of geomorphological characteristics of the seafloor and subsoil patterns to define the morphology of landslides and their distribution of occurrence, and their relationship with structural deformation. Results suggest that landslides in the study area are related to thrust faults and structural ridges of the Southern Sinú Fold Belt (SSFB) that greatly contribute to the filling of intra-slope sub-basins isolated from the continental shelf.

Chapter 2. This chapter shows the mapping of the southern Caribbean seafloor using seismic cube surveys and multibeam bathymetry data in an area encompassing 59,471 km², which allowed analyzing the regional distribution of submarine landslides and simplifying their occurrence through the construction of a conceptual framework for a better insight. Distinctive characteristics were found for submarine landslides associated with canyon walls, channel-levee systems, tectonically controlled ridges, and continental shelf break. Also, can be observed that Mass-Transport Complexes (MTCs) result from the accumulation of mass movement originating both in the continental shelf break and the channel-levee systems. However, the size of MTCs does not represent individual events but rather the accumulation of multiple events. This fact made it possible to estimate a landslide susceptibility map which suggests the following considerations: Firstly, structural ridges and adjacent intra-slope sub-basins related to the South Caribbean Deformed Belt (SCDB) are more likely to be landslide hazards. Secondly, the continental shelf break and channelized systems produce a moderate landslide hazard potential. Thirdly, deep marine systems with a slope less than five degrees (<5°) show the lowest landslide hazard potential.

Chapter 3. This chapter presents the analysis carried out on overpressures in the Sinú Offshore basin, summarizing the observations from well data, seismic data, and basin modeling. Overpressure zones were observed to match low velocities of sound from well logs and seismic cubes. Likewise, wells with the highest overpressures (>15 ppg) are located in the south of the study area, while wells located in the northern part of the basin showed lower overpressure conditions (<15 ppg). It is concluded that overpressures have a more direct relationship with anticlinal-type compression structures than with other geological phenomena, such as high sedimentation, which is certainly more related to landslides and Mass-Transport Complexes (MTCs) characteristic on the surface of the seafloor.

RESUMEN

Los deslizamientos de tierra submarinos son una mezcla de roca, suelo y fluidos que se mueven pendiente abajo debido a un evento inicial de falla mecánica de un talud. Estos fenómenos juegan un papel importante en la evolución de los márgenes continentales. Por un lado, son significativos procesos de transporte de sedimentos desde la plataforma continental hasta la base del talud continental. Por otra parte, ejercen control sobre la geomorfología del fondo marino. Adicionalmente, tienen el potencial de afectar infraestructura costera, cables de telecomunicaciones submarinos, ductos de la industria de hidrocarburos y generar tsunamis y avalanchas. Es por esto por lo que las consecuencias negativas de estos fenómenos han sido económica y socialmente significativas a nivel mundial.

En el margen continental del Mar Caribe colombiano, los deslizamientos submarinos están estrechamente relacionados con la dinámica tectónica regional y presentan características distintivas en paredes de cañones, sistemas de canal-dique, estructuras geológicas tectónicamente controladas, así como, en el quiebre de la plataforma continental. Estudios previos han resaltado la importancia de los deslizamientos como geoamenazas, a partir del análisis de los más grandes eventos observados en la batimetría o a partir del estudio de porciones limitadas del relieve en el Caribe sur colombiano.

En el presente estudio se muestra un análisis regional de la ocurrencia de deslizamientos submarinos en el sur del Caribe colombiano. El análisis geomorfológico se basó en un modelo batimétrico que incluyó cubos sísmicos y levantamientos batimétricos multihaz con resoluciones que oscilan entre 10 m y 100 m. Estos datos involucraron áreas desde el quiebre de la plataforma continental hasta la base del talud continental obteniendo una imagen regional del fondo marino en la que se extendió la interpretación de deslizamientos hacia áreas sin información sísmica 3D. Después de mapear la distribución geográfica de los deslizamientos submarinos se analizó su relación con las condiciones del subsuelo, la

geomorfología del fondo marino, la pendiente batimétrica, la presencia de fallas, el Botton Simulator Reflector (BSR) y los complejos de transporte en masa (MTCs). Finalmente se realizó un mapa preliminar de susceptibilidad a deslizamientos siguiendo el método del índice de peso de deslizamiento (W_i) propuesto por Van Westen en 1997 y se interpretaron las condiciones de sobrepresiones en la secuencia sedimentaria para ver la relación entre los dos fenómenos.

Capítulo 1. En este capítulo se presenta un mapeo geomorfológico detallado de deslizamientos submarinos realizado mediante un levantamiento sísmico 3D de alta resolución que permitió obtener un análisis estadístico y una interpretación completa de las características geomorfológicas del fondo marino y los patrones del subsuelo para definir no solamente la morfología de los deslizamientos y la distribución, sino también su relación con la deformación estructural. Los resultados sugieren que los deslizamientos en el área de estudio están relacionados con las fallas de empuje y las colinas estructurales del Cinturón deformado de Sinu Sur (SDSS) y contribuyen en gran medida al llenado de las sub-cuencas intra-talud aisladas del quiebre de la plataforma continental.

Capítulo 2. En este capítulo se muestra el mapeo del fondo marino del Caribe Sur usando levantamientos de cubo sísmico y datos de batimetría multihaz en un área que cubre 59,471 km² lo que permitió analizar la distribución regional de los deslizamientos submarinos y simplificar su ocurrencia mediante la construcción de un marco conceptual que facilita su comprensión. Se presentan las características distintivas para deslizamientos submarinos asociados con paredes de cañones, sistemas de canal-dique, estructuras geológicas tectónicamente controladas, así como, con el quiebre de la plataforma continental. También se observó que los Complejos de Transporte en Masa (MTCs) son resultado de la acumulación de movimientos en masa que se originaron en el quiebre del talud continental y en los sistemas de canales-dique. Sin embargo, las dimensiones de los MTCs no representan eventos individuales sino acumulación de múltiples eventos. Lo anterior

permitió estimar un mapa de susceptibilidad que sugiere lo siguiente: En primer lugar, que las crestas estructurales y las subcuencas intratalud adyacentes asociadas al Cinturón Deformado del Caribe Sur (SCDB) presentan el mayor peligro de deslizamiento. En segundo lugar, que el quiebre de la plataforma continental y los sistemas canalizados producen un potencial medio de peligro de deslizamiento. En tercer lugar, que los sistemas marinos profundos con pendientes inferiores a cinco grados (5°) exhiben el menor potencial de deslizamientos submarinos.

Capítulo 3. En este capítulo se presenta el análisis realizado sobre las sobrepresiones en la cuenca Sinú Offshore resumiendo las observaciones a partir de información de pozos, información sísmica y modelamiento de cuenca. Se observó que las zonas de sobrepresión coinciden con las bajas velocidades de sonido de los registros de pozo y cubos sísmicos. Así mismo, que los pozos con las sobrepresiones más altas (>15 ppg) se localizan en el sur del área de estudio, mientras que, los pozos localizados en la parte norte de la cuenca presentaron condiciones de sobrepresión menores (< 15 ppg). Se concluye que las sobrepresiones tienen una relación más directa con las estructuras de compresión tipo anticlinales que con otros fenómenos geológicos como, por ejemplo: la alta sedimentación la cual ciertamente está más relacionada con los deslizamientos y Complejos de Transporte en masa (Mass Transport Complexes-MTCs) característicos en superficie del fondo marino.

ACKNOWLEDGMENTS

The author wishes to thank ECOPETROL, EAFIT, COLCIENCIAS (MINTIC) as part of the agreement FP44842-2017 Doctorado Empresa, which allowed the development of the Doctorate program. The author would also like to thank the following people who were essential in carrying out this wonderful academic journey. To Professor Jorge A. Prieto of the EAFIT University for the time to discuss and guide the scope of the research. To Professor William Murphy of the University of Leeds, UK for review and suggestions for improving the manuscripts of the articles. To Mario Guzman, Nestor Fernando Saavedra and Andres Mantilla from Ecopetrol-ICP for their support to enroll in the PhD program. To my parents Clemente Mateus, Floralba Tarazona and my brothers Jefferson, Jael, Mónica, Yessica for their support and humor during the development of the academic program. Finally, I would like to acknowledge and thank my wife Ingrid Herrera, my sons Darwin Santiago and Pablo Alejandro for their love, support and patience during several long nights and weekends dedicated to conducting the research.

CHAPTER 1:

IDENTIFICATION OF SUBMARINE LANDSLIDES IN THE COLOMBIAN CARIBBEAN MARGIN (SOUTHERN SINÚ FOLD BELT) USING SEISMIC INVESTIGATIONS

This work was published as: Mateus Tarazona, D., Prieto J. A., Murphy, W., Naranjo Vesga, J. Identification of submarine landslides in the Colombian Caribbean Margin (Southern Sinú Fold Belt) using seismic investigations. *The Leading Edge* 2021; 40 (12): 914–922. doi: <https://doi.org/10.1190/tle40120914.1>.

ABSTRACT

Submarine landslides can be triggered by several processes and involve a variety of mechanisms. These phenomena are important sediment transport processes but also constitute a significant geohazard. Mapping of the southwestern Caribbean Sea using 3D seismic data has allowed the identification of several submarine landslides in the Colombian Margin in the area dominated by the Southern Sinú Fold Belt (SSFB). A post-tack depth-migrated seismic cube survey with a 12.5 m by 12.5 m bin spacing was used to identify landslides in an area covering 5746 km². Landslides were interpreted using: a seafloor morphologic parameter identification process; and the internal deformation of the slope forming material, as seen from seismic data. A total of 93 landslides were identified and classified based on their movement styles, as follows: 52 rotational, 29 translational, and 12 complex landslides. In addition, 12 distinct deformational zones, and a zone of Mass Transport Complex (MTCs) were identified. Five different ground condition terrain were interpreted based on landslides type and distribution as well as in geological structures and seismic reflection analysis. Two main processes seem to influence landslides in the study area. First, the folding and faulting involved in the Southern Sinú Fold Belt (SSFB) evolution. This process results in oversteepened slopes that starts as deformational zones and then fail as translational or rotational slides. Those individual landslides progressively become complex landslides zones that follow geological structural orientation. Second, the continental shelf break erosion by debris flows which fill in intra-slope subbasins and continental rise with several MTCs. According to the results, risk of damage by landslides increases in distances shorter than 4 km along structural ridges foothills in the whole study zone.

1. INTRODUCTION

Submarine and terrestrial landslides are mass movements occurring downslope due to a mechanical failure (Cruden and Varnes, 1996). Undersea, these

phenomena play an important role shaping morphological features and transporting sediment on continental margins (McAdoo et al., 2000; Masson et al., 2006). They are also important trigger mechanisms for tsunamis and avalanche generation (Nadim et al., 2006; Vanneste et al., 2013; Leslie and Mann, 2016; Heidarzadeh et al., 2019).

The usual definition of landslide i.e. downward and outward movements of soil, rock or some combination of the two, which has clearly defined boundaries at top, bottom, sides and base, can be enlarged for the submarine environment. In the marine environment, landslides classes include whether landslides are frontally constrained (namely the slide mass still sits at least partially within its boundaries) or frontally unconstrained (the sliding mass has completely vacated the landslide scar). A variety of classifications exist for subaerial and submarine landslides (Shanmugam and Wang, 2015). This study adopted the classification suggested by Cruden and Varnes, (1996) in which landslides processes include translational landslides, rotational landslides, and debris flows. Mass Transport Complex (MTCs) is used to describe deposits where the mechanism of emplacement is unclear (Moscardelli et al., 2006; Moscardelli and Wood, 2016). Additionally, the term Deformational zone is utilized to refer to potential landslide zones where a mass movement is ongoing, but where boundaries cannot be clearly defined and where there are no fully formed shear surfaces.

Submarine landslides and MTCs have been studied worldwide in different geological settings (Hampton et al., 1996; McAdoo et al., 2000; Green and Uken, 2008; He et al., 2014; Lamarche et al., 2016; Shanmugam, 2016). Consequences of submarine landslides can be significant in terms of loss of life (Tappin et al., 2001), damage to coastal infrastructure (Carter et al., 2012) and for the Oil and Gas industry where the costs can reach about US\$ 400 million annually (Lamarche et al., 2016).

In the Colombian Caribbean margin, research has been focused on landslide processes and MTCs mainly associated with the Magdalena fan (Romero-Otero, 2009; Ortiz-Karpf et al., 2017; Idárraga-García et al., 2019). Research has also highlighted the significance of submarine landslides as geohazards for offshore

infrastructure (Alfaro and Holz, 2014a; Leslie and Mann, 2016). However, research has addressed the geomorphological characterization of the sea floor in detail in order to identify potential submarine slopes instabilities. In this document the geomorphological mapping of landslides using high resolution 3D Seismic survey is described as are the descriptive statistics of those landslides. Geophysical data are used to identify both geomorphological features on seafloor and sub-surface internal pattern to define both the landslide morphology and deformation characteristics. This combination of observations has allowed the expected type and average size of future landslides in the study zone to be inferred and gives insights for landslides generation processes in the Colombian Caribbean margin.

1.1. Regional setting

The study area (Figure 1) is located in the south west of the South Caribbean Deformed Belt (SCDB), in a zone dominated by the Southern Sinú Fold Belt (SSFB) (Martinez et al., 2015) which is classified as an Accretionary Prism (Ruiz et al., 2000; Bernal-Olaya et al., 2015) and extends from the Urabá Gulf, in the South, to the Santa Marta Offshore region in the North (Flinch et al., 2003). The SCDB is the product of the obliquely collision between the Caribbean plate and the North Andes Plate (Pindell, 1994; Martinez et al., 2015). The Caribbean plate moves easterly and is subducted beneath the North Andes plate (Pindell, 1994; Symithe et al., 2015). This creates a stress field in the Southwest Caribbean resulting in a strike-slip faulting as well as compressional zones (Bird, 2003; Rodríguez et al., 2021). Moreover, the southern part of the study area is also affected by the North-eastern Panama plate movement, which is forming the Panama Fold Belt (PFB) (Alfaro and Holz, 2014a) and the Uramita fault (Figure 1).

1.2. Data collection and analysis

The area under investigation covers a significant range of bathymetry and different geomorphological settings, i.e. from continental slope to continental rise. Intra-slope subbasins and structural ridges are most representative morphology in continental slope while MTCs, canyons and abandoned channel systems cover the continental rise (Rincón et al, 2021). The primary data used in this investigation was

a post-tack depth-migrated seismic cube survey (PSDM) which covers an area of 5,743 km². Sample rate was 2 milliseconds (ms) and the recording length was 15,000 ms with a receiver interval of 12.5m. Seismic cube has a bin spacing of 12.5 m by 12.5 m.

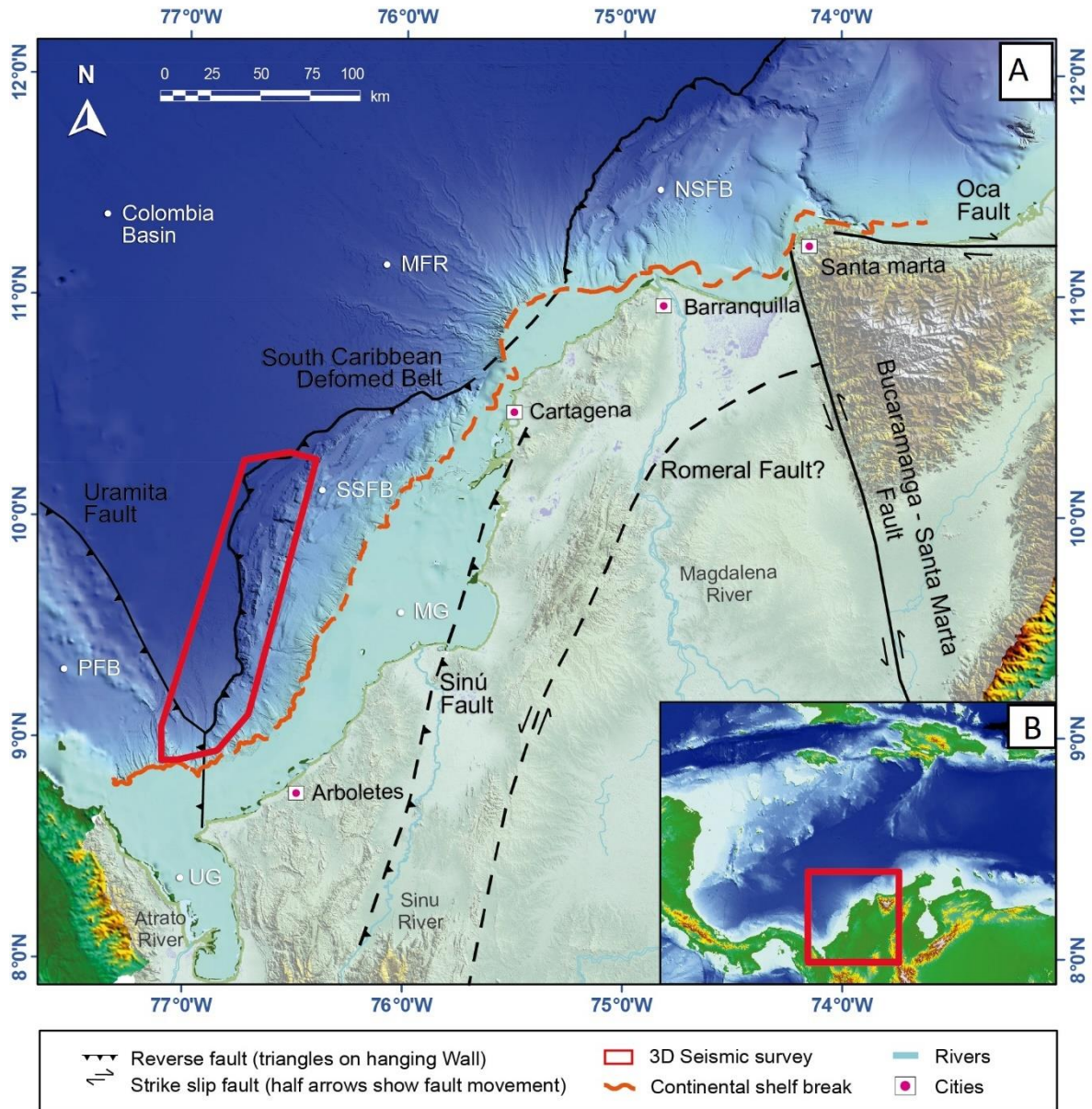


Figure. 1. a) Topographic and Bathymetric map of the Northwest of Colombia showing the study zone (red polygon) and main geological features (Rincón et al, 2021). The South Caribbean Deformed Belt is locally divided in the North Sinú Fold Belt (NSFB), Magdalena Fan River (MFR) and the South Sinú Fold Belt (SSFB) (Martinez et al., 2015). It is also included the Panama Fold Belt location (PFB) (Alfaro and Holz, 2014a) The Golf of Morrosquillo (MG) and the Urabá Golf (UG). b) The red box shows the location of the enlarged information in panel A. Modified from Rincón et al, (2021).

First step for identifying submarine landslides on the study area was to obtain the sea floor surface based on the seismic cube. To accomplish this purpose, the first strong reflector was followed to generate a continuous surface. Then, seismic reflection changes on amplitude, dip and continuity as well as geomorphological features were used to identify landslides (Shanmugam and Wang, 2015; Shanmugam, 2016). The main characteristics that were used for slide identification were: the crown, significant scarps and the geometry of the displaced mass as outlined by He et al., (2014). Somewhat more challenging were features which had the geometry of landslides but the body of the landslide was absent indicating that the slide mass had vacated the landslide scar.

Types of Landslides were defined based on its kinematics (Cruden and Varnes, 1996). Thus:

1) Transitional slides, i.e. planar failure surface, for example along a planar bedding planes. 2) Rotational slides characterized by circular slip surfaces and internal deformation. 3) Complex landslides in which a lateral or vertical superposition of more than one slide masses with different movement mechanisms were identified.

2. TERRAIN CLASSIFICATION AND LANDSLIDE IDENTIFICATION

On the basis of seafloor geomorphology, seismic reflection features and landslide occurrence, it was possible to define five terrain types (Figure 2a) with characteristics as summarizes in Table 1.

2.1. Landslides

In total were identified 93 landslides, 12 deformational zones, and a zone controlled by Mass Transport Complexes (MTCs) besides several mud volcanos (Figure 3). Features were grouped in 52 rotational, 29 translational, and 12 complex landslides. This research took into account quantitative morphological parameters suggested by Clare et al., (2018) which include: total landslide length (L_t), scarp perimeter

length (Ls), scarp width (Ws), total height drop (Ht), slope gradient (S), slope gradient of the heads carp (Ss), area and volume (Figure 4b-d).

Rotational slides. Rotational slides are characterized by a circular slip surface which cut continuous seismic reflections from unaltered material. Highly-deformed, semi continuous to discontinuous seismic facies can be observed within displaced mass. Most of the rotational slides identified are located on oversteepened slopes associated with imbricated thrusts and reverse faults. Figure 4 shows an example which is influenced by a Northeast - Southwest strike-slip fault and by a structural ridge which confine its displaced mass obliquely to the crown. Its horizontal extent (Lt) is 12.5 km and 5.92 km scarp width. In general, minimum area covering rotational landslides is 0.24 km² while maximum area is 52 km². However, in 30 of the 52 rotational slides was not possible to estimate this parameter since the displaced mass was vacate.

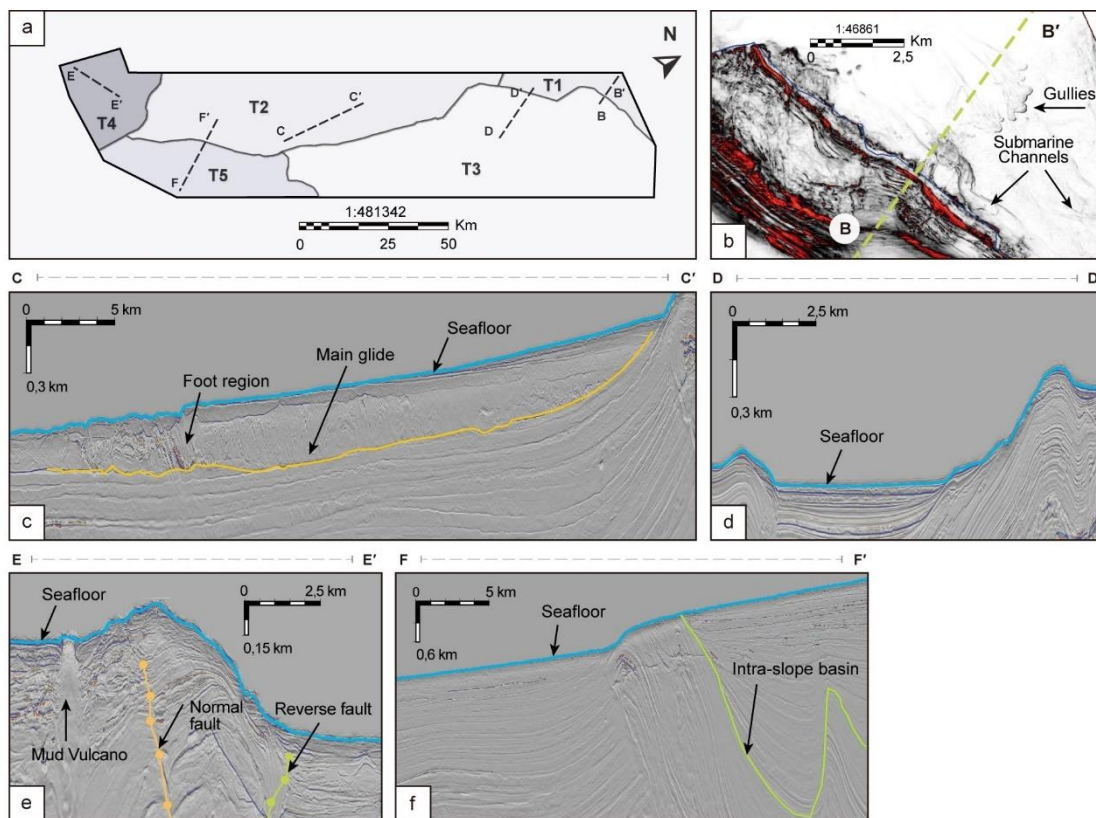


Figure. 2. Terrain types. a) Distribution Plan view of the five terrain types. b) Time slide of variance seismic attribute showing abandoned gullies and channels as main morphological characteristic of terrain type T1, white color means low variance (flat reflectors) whereas red color means high variance on seismic signal. c) Seismic section showing Mass Transport Complex (MTC) on Terrain type T2. Low amplitude and semi-continuous

reflections are a characteristic of syndepositional trusts on foot region. Blue line represents seafloor. d) Overstepped slopes that fail and fill intra-slope basin in terrain type T3. e) Terrain type T4, lime and amber lines represent faults related to the Uramita fault system. f) Terrain type T5 green line represents the base of an intra-slope basin which is filled by MTCs characterized by low amplitude and semi-continuous reflections.

Table 1. Summary of terrain type characteristics.

Terrain Unit	Name	Seismic characteristics	Geomorphological characteristics	Landslide data
T1	Magdalena fan deposits (MFD)	Characterized by flat-lying high-amplitude continuous coherent seismic reflections.	Slope angle in this zone is normally less than 2 degrees and dominated by sedimentation by gravity. The buried channels in section without evidence of surface erosion.(Figure 2b)	No evidence of landslides on this terrain unit.
T2	Colombian basin, domain of MTCs (CB-MTCs).	Sub-horizontal low-amplitude to steeply-dipping chaotic reflections.	Interplate zone showing little or no evidence of compressional tectonics. Superposition of mass transport deposits is evident. (Figure 2c)	Only evidence of the deposits of landslide activity generated from zone 3. Occasional large blocks can emerge from MTCs and be carried into Zone 1.
T3	Southern Sinú Fold Belt (SSFB)	Parallel continuous to discontinuous high amplitude reflections	Seafloor surface is characterized by imbricated folds and high angle reverse faulting which allow the filled of several intra-slope basins. (Figure 2d)	The majority of landslides observed occur in this area. The oversteepening caused by reverse faulting is a significant trigger.
T4	Urabá basin – domain of MTCs (UB-MTCs)	Oblique to discontinuous low amplitude reflectors	Smooth bathymetry with development of gullies and canyons and mud volcanos. Subsurface characterized by folds and high angle reverse faulting (Figure 2e)	Rotational Landslide and slide scar are observed on canyon wall
T5	Southern Sinú Fold Belt (SSFB) – domain of MTCs (SSFB-MTCs)	Sub-horizontal low-amplitude chaotic reflections	Seafloor surface presents hummocky morphology. Subsurface characterized by overfilled intra-slopes basins. (Figure 2f)	Debris flows scars are main landslides observed on seafloor surfaces.

Translational slides. Translational landslides are characterized by a largely planar-failure surface on which displaced mass moves. In the study zone, landslides of this type are associated with structural ridge limbs (Figure 5). Either thin masses were present or the displaced masses had vacated the landslide boundaries, therefore, it was impossible to estimate total length distance (Lt) and other morphometric parameters depending on displaced mass on 20 of the 29 landslides. For those landslides which allowed measurements, the minimum area covering was 0.38km² while the maximum area was 10.87 km². Minimum and maximum total length (Lt) observed was 0.65 km and 1.92 km respectively.

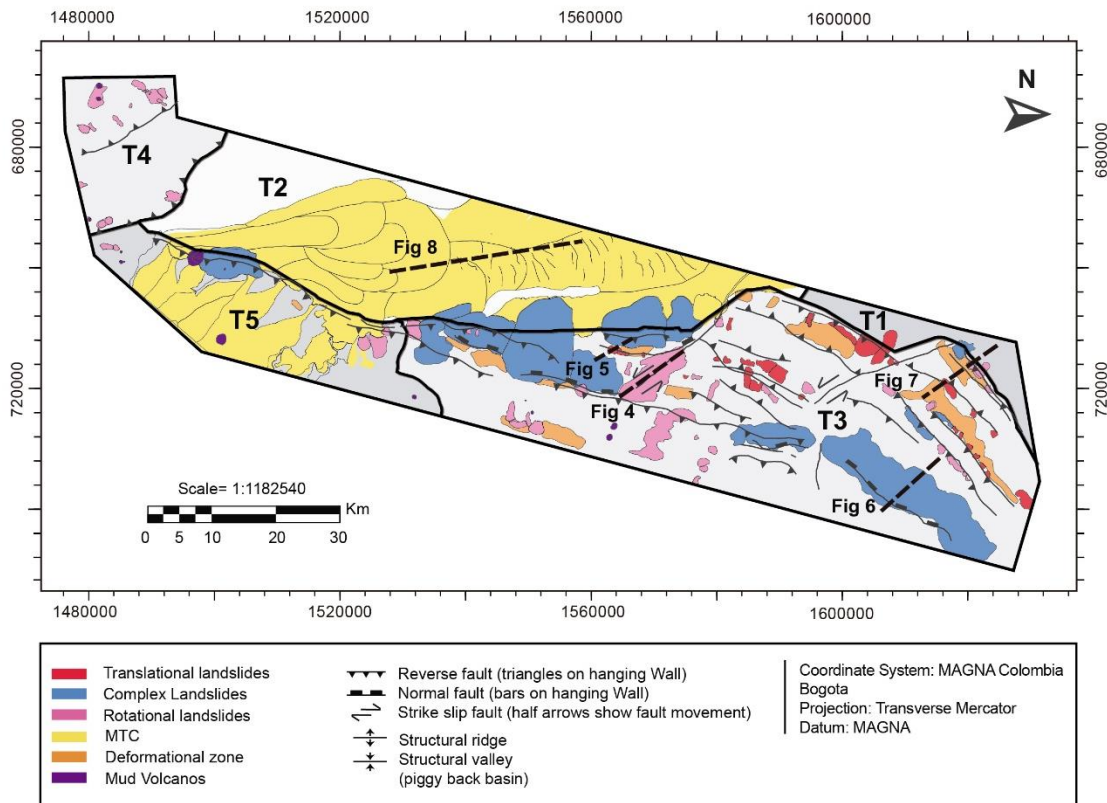


Figure. 3. Geographic distribution of submarine landslides in the study zone. Yellow areas represent Mass Transport Complex (MTC). Blue areas represent complex landslides, red areas represent translational slides, magenta areas represent rotational slides, orange areas represent Deformational zones, and purple areas represent mud volcanos. T1 to T5 represent terrain types and long dashed black lines show the location of Figures 4 to 8.

Complex Landslides. Complex landslides are formed by superposition of lateral or vertical landslides (Hampton et al., 1996; He et al., 2014) and can involve one or both translational and rotational kinematics. In the study area they are associated with regional reverse faulting. Seismic facies vary from lightly disturbed reflections to highly bonded discontinuous reflections (Figure 6). Maximum estimated area was 209 km² and volume of 108 km³.

Deformational zone. Deformational zones are characterized by discontinuous parallel seismic reflections with low to moderate amplitude, which are seen to be affected by normal faulting with small offsets (Figure 7). These zones are located mainly on structural ridge limbs and are associated with landslides scarp perimeters. The normal faults evident in this zone do not extend the full depth of the seismic section and tend to terminate against clear reflectors. It seems likely that these are

progressive slide blocks which have not yet developed into large scale failures of the submarine slope. This, to some extent, would fit the geographic relationship between slide scars and scarps.

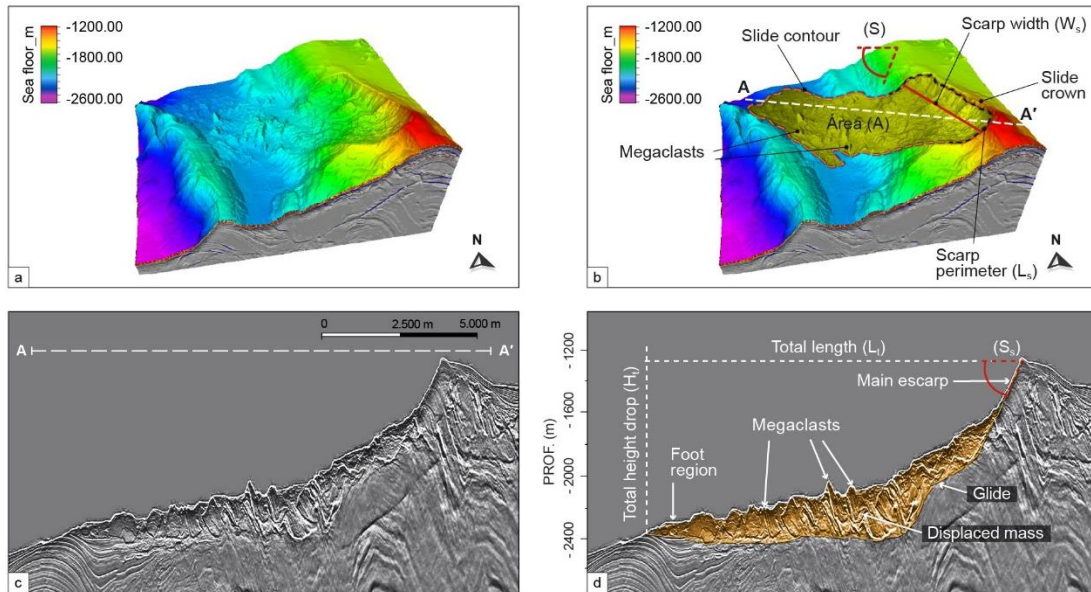


Figure. 4 Rotational landslide. a) Tridimensional view of seafloor surface without interpretation. b) Tridimensional view of a rotational landslide (RS5 in Appendix 1) showing morphological characteristics on seafloor like megaclasts, slide crown and slide contour. This panel also show the Scar perimeter length (L_s), scar width (W_s) and slope gradient. (S) in a typical landslide. c) Seismic section showing main landslide characteristics like failure plane (glide), Displaced mass internal deformation (Copper area), megaclasts food region, total length (L_t), total height drop (H_t) and slope gradient of the heads scarp (S_s). Modified from Rincón et al, (2021)

Mass Transport Complexes (MTCs). Mass transport complexes are deposits of multiple, potentially large, landslides whose scars are unidentified. They present as inter-bedded packages filling intra-slopes basins in terrain type T3 and as the main sedimentation process in terrain type T2 and T5. Figure 8 presents the largest MTC observed in the study zone, it is 64 km horizontal length, 12 km width, maximum deposit thickness of 0.6 km covering an area of nearly 700 km² and a volume of 51 km³. Its basal surface is irregular and presents scours northeast oriented and erosive boundaries. This large MTC induces pressure ridges on seafloor perpendicular to its movement direction.

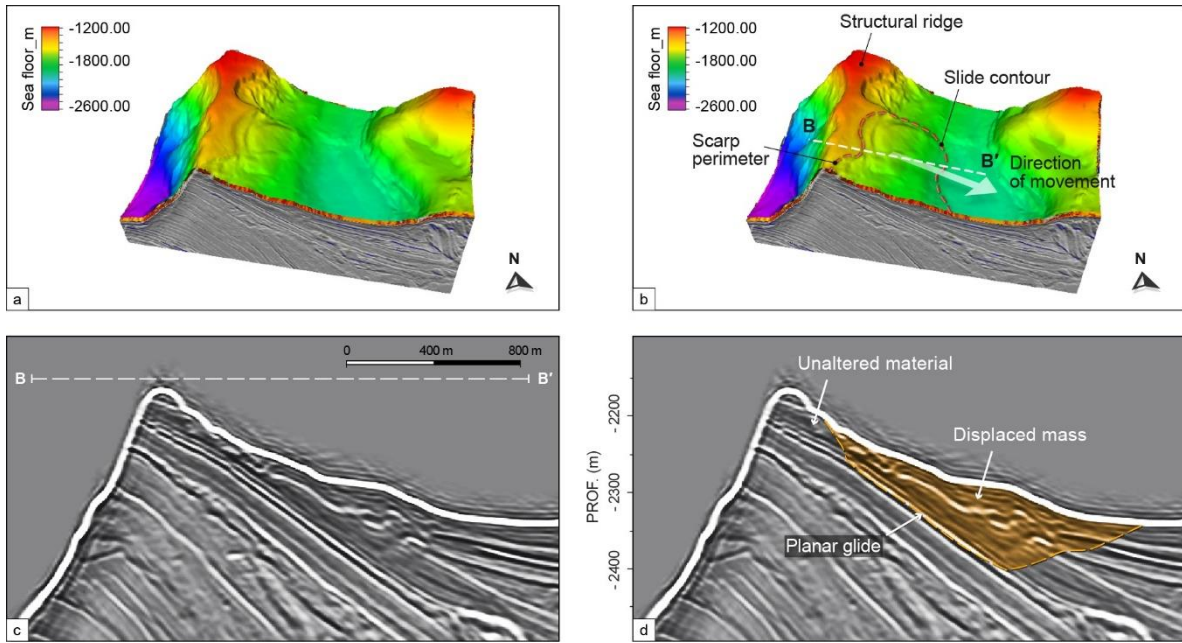


Figure. 5. Translational slides. a) Tridimensional view of seafloor surface without interpretation. b) Tridimensional view of a translational slide highlighting slide contour, direction of movement and Scarp contour. c) Seismic section without interpretation. d) Seismic section showing landslide displaced mass (Copper area) planar glide that moves parallel to bending planes and displaced mass internal deformation. Modified from Rincón et al, (2021).

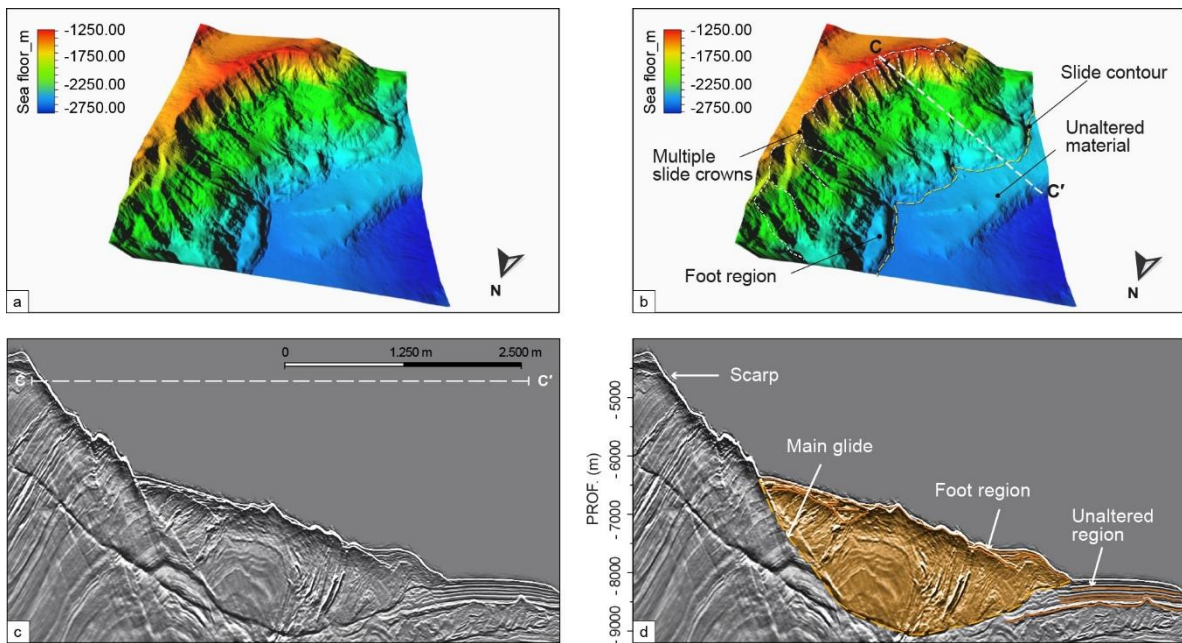


Figure. 6 Complex Landslide. a) Tridimensional view of seafloor surface without interpretation. b) Tridimensional view of a Complex landslide where multiple slide crown, foot region and slide contour are showed. c) Seismic section without interpretation. d) Seismic section of the complex landslide. Copper colored area highlights displaced mass on main glide. Foot region is characterized by folding and reverse faulting as a result of the lateral movement. Unaltered region presents parallel and continuous seismic reflectors at the right side of the landslide. Modified from Rincón et al, (2021).

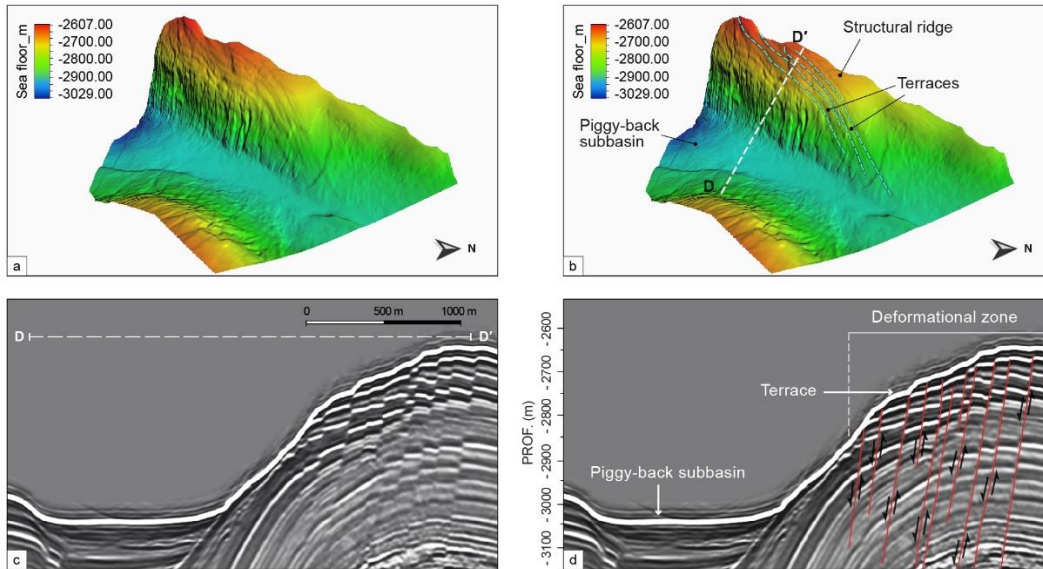


Figure 7. Deformational zone. a) Tridimensional view of seafloor surface without interpretation. b) Tridimensional view of a deformational zone showing terraces resulting of small drops by normal faulting (Jungle green dashed line). c) Seismic section without interpretation. d) Seismic section of the deformational zone highlighting, terraces and normal faulting. Reflectors discontinuity suggest lack of strength in the structural ridge limb which could trigger new landslides in the future. Modified from Rincón et al, (2021).

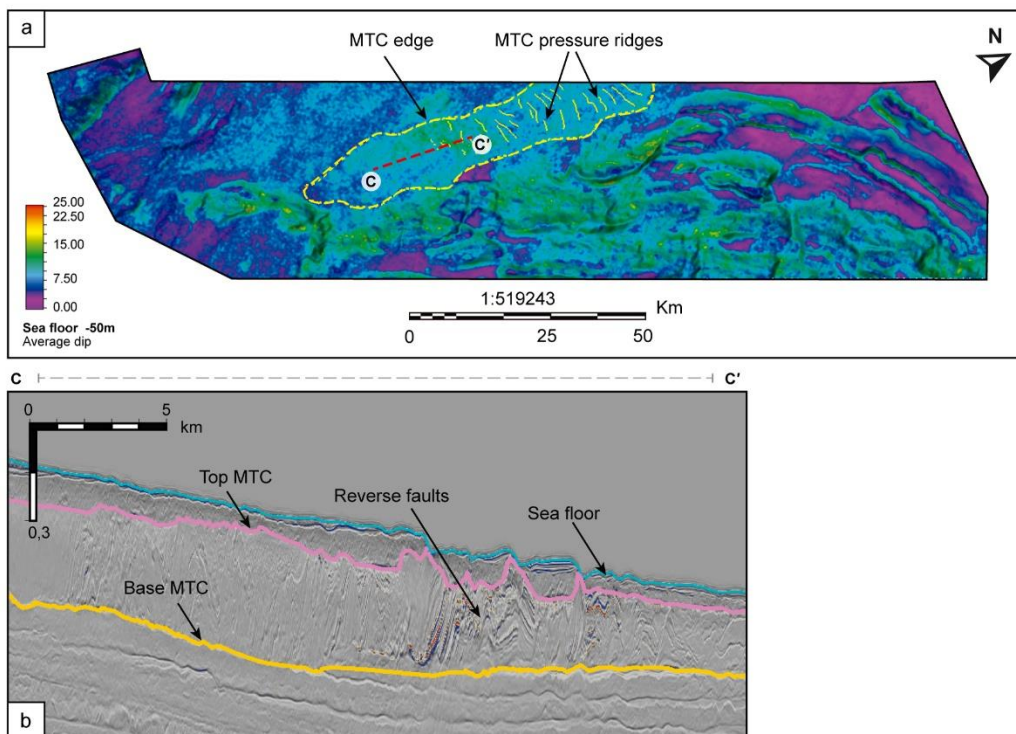


Figure 8. MTC. a) Average dip attribute calculated 50m under seafloor highlights the MTC contour. b) Interpreted limits of the MTC in Cross section C-C' showing low amplitude, semi-continuous reflections as a characteristic of syndepositional compression. Orange line represents the base of the main movement. Magenta line represents the top of the mass movement event.

2.2. Statistics of individual landslides

Figure 9 shows a general view of landslides size. According to this, it is clear that complex landslides and MTCs are significantly larger than individual events, the formers involve tens of kilometers of scarp width and horizontal movement, while most of the individual events present less than 6 km of scarp width and horizontal movement less than 10 km. “Appendix A” presents morphologic parameter measured for all landslides interpreted in the study zone.

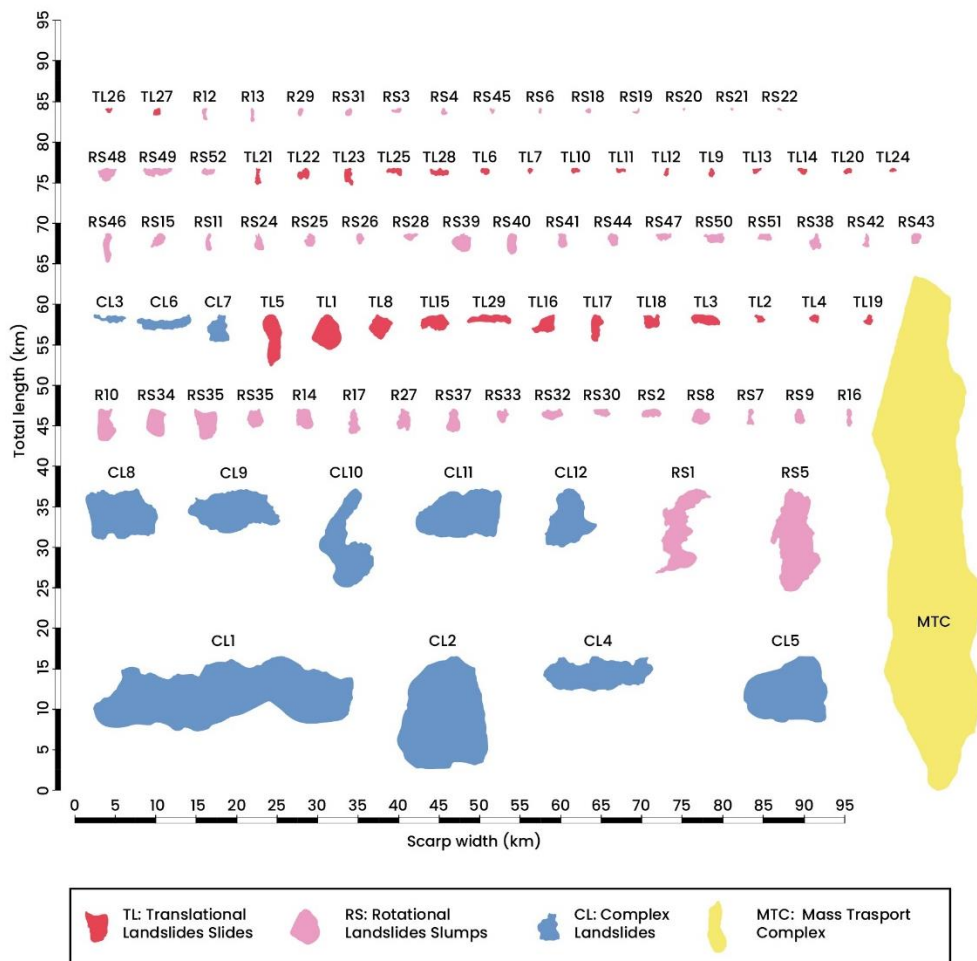


Figure. 9. Plan view of landslide oriented toward movement direction. Yellow polygon represent a MTC, blue polygons represent complex landslides (CL), magenta polygons represent rotational slides (RS), and red polygons represent translational slides (TL). Horizontal movement – Total length (Lt) is graphed in vertical axe and scarp width (Ws) is represented on the horizontal axe of the figure.

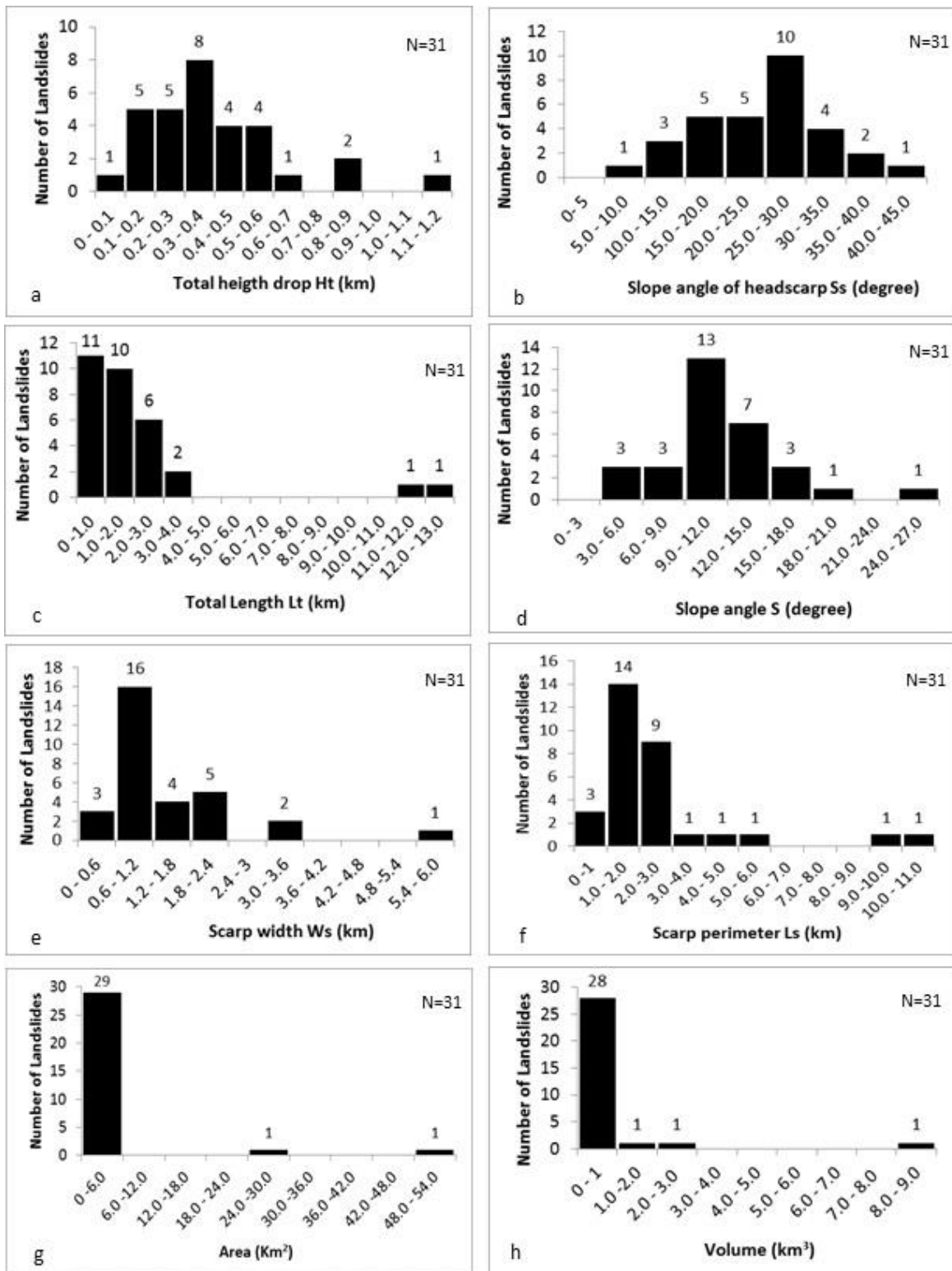


Figure. 10. Frequency histogram of morphologic parameter for individual landslides. a) Total height drop (L_t). b) Slope angle of head scarp (S_s). c) Total length (L_t). d) Slope angle (S). e) Scarp width (W_s). f) Scarp perimeter (L_s). g) Area. h) Volume.

Figure 10 shows frequency histograms for main morphometric parameter of 31 individual landslides. Complex landslides and MTC zones were excluded from this analysis since they involve more than one slide event. Additionally, individual landslides in which displaced mass was vacated from the scar were also excluded. Maximum and minimum total height drop (Ht) found was 1.18 km, and 0.094 km respectively with a mean value of 0.4 km and a standard deviation of 0.240 km. Maximum total length (Lt) reached was 12.5 km in RS5 and the minimum value was 0.54 km in RS22. However, 93% of data (29 landslides) showed Lt less than 4 km. Maximum scarp width observed was 5.9 km and the minimum one was 0.37 km, 90% of the data (28 Slides) showed scarp width less than 2.4 km. Minimum and maximum Slope angle of head scarp (Ss) was 8 and 44 degrees respectively, with an average of 26 degrees, while near to landslides, minimum and maximum non-failed slope angle (S) was 5 and 25 respectively. Minimum volume of individual landslides was 0.004 km³ and maximum 8.54 km³, however 90% of the data was lower than 0.16 km³.

Table 2. Summary Summary Correlation coefficient between landslides morphologic parameters. Ht - Total height drop. Lt -Total Length. Ws - Scarp width. Ls - Scarp perimeter length. Ss - Slope gradient of head scarp. S - Slope gradient. Vol - Volume.

	<i>Ht</i>	<i>Lt</i>	<i>Ws</i>	<i>Ls</i>	<i>Ss</i>	<i>S</i>	<i>Vol</i>	<i>Area</i>
Ht	1,00							
Lt	0,74	1,00						
Ws	0,70	0,75	1,00					
Ls	0,66	0,85	0,83	1,00				
Ss	0,20	0,00	-0,01	-0,18	1,00			
S	0,02	0,18	0,08	0,12	-0,03	1,00		
Vol	0,68	0,82	0,79	0,71	0,02	0,20	1,00	
Area	0,75	0,94	0,85	0,85	-0,01	0,17	0,95	1,00

Table 2. Shows correlation coefficient between landslides morphometric parameters. Good correlation is evident between Total length (Lt), Total height drop (Ht), Scarp width (Ws) and volume. Those relations have been documented worldwide (Hampton et al., 1996; McAdoo et al., 2000; Green and Uken, 2008; He et al., 2014). Correlation between Ws and Lt is certainly useful since it gives the possibility to estimate the maximum distance reached by new landslides through mapping possible crowns on deformational zones.

3. DISCUSSION

The distribution and characteristics of submarine landslides and MTCs in the study area show a clear association with ground condition, which in turn respond to the combination of tectonic deformation and sediment supply (Rincon et al., 2021). For this reason, our interpretation of the connection between subsurface conditions and observed landslides and MTCs is presented below. Similarly, main processes that we believe are controlling the occurrence of submarine landslides in this convergent margin zone are argued. This will contribute to understand submarine landslides generation in this type of geological environment.

3.1. Relation between terrain types and Landslides

In Terrain T1, the absence of observable landslides would suggest that this terrain type is a low landslide risk area. The slow slope angle in the bathymetry ($<2^\circ$) is the result of the high rate of sediments supplied by the Magdalena River that feeds channel-levees, in the continental slope, and smooth the marine relief in the abyssal basin (Flinch et al., 2003; Naranjo-Vesga et al., 2020).

Terrain T2 is the result of two effects: the inter-plate tectonics associated to the collision along the North Andes plate and the Caribbean plate; high sedimentation rates supplied by mass transport events, originated in the continental shelf break. These events feed Mass Transport Complexes (MTCs) that show hummocky appearance (Vanneste et al., 2013) and compressional ridges on seafloor. Rarely translational or rotational slides are present on surface except by those located near foothills which are originated in terrain type T3.

Most of the landslides observed are located in the Terrain T3 (SSFB) which is the result of the collision between the North Andes continental plate and the Caribbean oceanic plate (Ruiz et al., 2000; Martinez et al., 2015; Rodríguez et al., 2021). Translational slides occur mainly in structural limbs where bedding dip concur with the seafloor slope (Figure 5). Whereas individual rotational slides seem to be present in two geological context. First, structural limbs where bedding dip is in opposite direction to the seafloor slope. Second, in canyon walls that cut geological structures

both in T3 and T4. Complex landslides formed by the succession of lateral translational slides are present at the North part of the study zone and involves thin beds along structural limbs (CL3, CL6, CL7 in Figure 9). On the other hand, larger complex landslides, showing a rotational kinematics are associated with main structural ridges and faults that forms the SSFB. (Figure 3). They involve both recent sediments and compacted rocks exposed by reverse faulting. Consequently, coherent movement of rotational landslides are observed (Figure 6).

Terrain T5 seabed is characterize by Mass Transport Complex (MTCs) which are interpreted as a result of multiple debris flows originated at the continental shelf break (Figure 1). The seabed scours reported by Alfaro and Holz, (2014a) and Rincon et al, (2021) allow us to infer that debris flows are the main feeder source of MTCs in this zone. These debris flows are deposited downward filling intra-slope subbasins throughout the continental shelf and eventually reaching the continental rise.

3.2. Landslides processes

Two main processes influence landslides in the study area. First, the folding and faulting involved in the Southern Sinú Fold Belt (SSFB) evolution. This process results in oversteepened slopes that starts as deformational zones (Figure 11a) and then fail as translational (Figure 11b) or rotational slides (Figure 11c). Second, the continental shelf break erosion by debris flows which fill in intra-slope subbasins and continental rise with several MTCs (Figure 11d).

MTCs involve areas of hundreds of square kilometers and tens of cubic kilometers in volume. In terrain T3 these deposits partially fill intra-slope subbasins which avoid MTCs to reach the continental rise, while in terrain T5, MTCs have overfilled intra-slope subbasins, allowing them to travel from the continental shelf break to the continental rise, in terrain T2 (Figure 3). MTCs observed in the seismic record are interpreted as a result of multiple landslides events, as a consequence, must not be interpreted as instantaneous events for geohazards assessment purposes, because it could overestimate volumes involved in mass movements.

The most important features in terms of triggering future landslides are deformational zones in the limbs of structural ridges in terrain T3 (Figure 3) since they involve failed material in a preconditioning stage (Vanneste et al., 2013). These zones cover areas between 1.48 and 47.6 km² identified as slopes with angles between 5° and 15° which is also the slope angle interval where more landslides occur (Figure 10d).

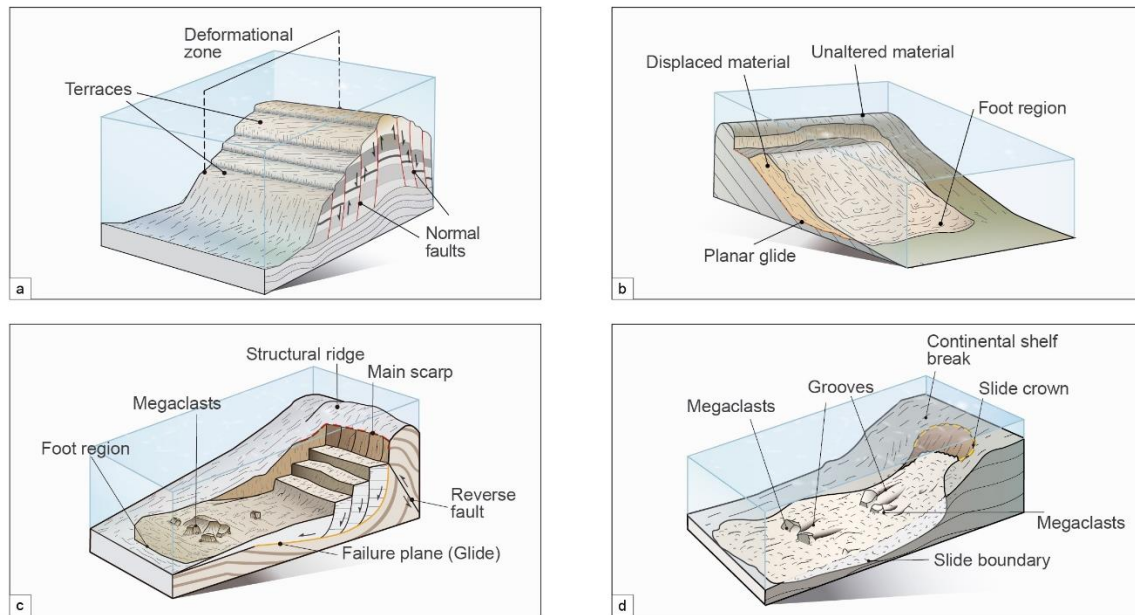


Figure. 11. Processes that affect landslides. a) Deformational zones occur on structural ridge limbs and are interpreted like early stage of landslides. b) Translational slides occur when strong seismic reflector (bedding planes) concurs with slope azimuth. c) Rotational slides occur where bedding dip azimuth is in opposite direction compared with slope azimuth. d) Debris flows occur at continental shelf break and feed MTCs on piggy-back sub-basins and abyssal plain. Modified from Rincón et al, (2021).

3.3. Possible impact to future infrastructure

Preliminary observation of future infrastructure assessment hazards indicates that:

- i) Terrain T1 can generally be considered as low landslide hazard but movements could be triggered extreme events such as earthquakes.
- ii) T2 may be exposed to shallow displacements due to remobilization of MTCs as well as low energy parts of debris flows coming from T5.
- iii) In Terrain T3, displacements due to landslides, debris flows, and fault superficial ruptures should be considered for offshore structure design.
- iv) Terrain T4 may be exposed to landslides in the canyon and gully walls;
- v) T5 should be analyzed including the effect of debris flows originated

at the continental shelf break. vi) Risk of damage caused by rock falls or landslides increases in distances shorter than 4 km along structural ridges foothills in the whole study zone.

4. CONCLUSIONS

Based on seismic interpretation and seafloor morphological analyses 93 landslides were identified. These mass movement were grouped in 52 rotational slides, 29 translational slides and 12 complex landslides. In addition to landslides, 12 deformation zones and a mass transport complex (MTCs) zone were observed.

Rotational landslides reach horizontal displacements as long as 12.5 km thus being the longest ones for the whole study area. These displacements are linked to the SSDB thrust fault and structural ridges. They contribute in great manner to the filling of the intra-slope subbasins isolated from the continental shelf break. On the other hand, complex landslides involve areas exceeding 200 km² and in the same way as rotational landslides they are directly related to the SSDB structures and faults. The above suggests that most landslides in the study area come from tectonic movements inherent to SSDB evolution.

Debris flows consist of events mainly associated to the continental shelf break which involve non-cohesive sediments causing erosive scars (scours) on the seafloor, allowing to infer these landslide are the main feeder of MTCs found in intra-slope subbasins in terrain T5 and in the continental rise in terrain T2.

Five terrain types with different ground condition were defined from landslides distribution, geologic structures and seismic facies interpretation. Terrain type T1 is the flatter area in which morphology is dominated by low energy sedimentation supplied by the Magdalena rivers system. Terrain type T2 is a relative flat area (slope angle <5°) dominated by Mass Transport Complexes, this zone is feeded by the continental shelf break failure. Most landslides observed in this terrain type are located close to hill zones of the terrain type T3. Terrain type T3 is associated with North-East trend thrust faults beneath the SSFB. This region has the steepest hills,

where the majority of landslides were identified. Terrain type T4, located to the southwest of the study region, close to Panama Plate edge, has steeped hills and small landslides. Terrain type T5 is formed by intra-slope subbasins filled by MTCs that over cross it and reach terrain type T2.

The main limitation for the understanding of submarine landslides in the study zone is due to the lack of information on the frequency of occurrence of different types of landslides. This would require the acquisition of new specialized data, such as: deep core piston, underwater vehicle campaigns (Gliders / AUV / ROV), seismic and high resolution bathymetry in different time periods as well as collecting dateable material to constrain the age of landsliding. These are key areas requiring further research to understand landslide risk in the South West Caribbean region.

ACKNOWLEDGEMENTS

This work was undertaken as part of Royal Academy of Engineering - Newton Fund grant IAPP1617/112 and the agreement FP44842-2017 Doctorado Empresa, ECOPETROL, EAFIT, COLCIENCIAS (MINTIC). The data were kindly provided by Ecopetrol. Professors David Hodgson and Bill McCaffrey of the University of Leeds are acknowledged for discussion and advice.

REFERENCES

- Alfaro, E., and M. Holz, 2014a, Seismic geomorphological analysis of deepwater gravity-driven deposits on a slope system of the southern Colombian Caribbean margin: *Marine Petroleum Geology*, 57, 294–311. <https://doi.org/10.1016/j.marpetgeo.2014.06.002>
- Bernal-Olaya, R., J. Sanchez, P. Mann, and M. Murphy, 2015, Along-strike Crustal Thickness Variations of the Subducting Caribbean Plate Produces Two Distinctive Styles of Thrusting in the Offshore South Caribbean Deformed Belt, Colombia, in C. Bartolini and P. Mann, eds., *Petroleum Geology and Potential of the Colombian Caribbean Margin: AAPG Memoir 108*, p. 295–322. <https://doi.org/10.1306/13531941M1083645>

- Bird, P., 2003, An updated digital model of plate boundaries: *Geochemistry, Geophysics, Geosystems*, 4, 1-52. <https://doi.org/10.1029/2001GC000252>
- Carter, L., J. D. Milliman, P. J. Talling, R. Gavey, and R. B. Wynn, 2012, Near-synchronous and delayed initiation of long run-out submarine sediment flows from a record-breaking river flood, offshore Taiwan: *Geophys. Research Letters*, 39, 1-5. <https://doi.org/10.1029/2012GL051172>
- Clare, M., J. Chaytor, O. Dabson, D. Gamboa, A. Georgiopoulou, H. Eady, J. Hunt, C. Jackson, O. Katz, S. Krastel, R. León, A. Micallef, J. Moernaut, R. Moriconi, L. Moscardelli, C. Mueller, A. Normandeau, M. Patacci, M. Steventon, M. Urlaub, D. Völker, L. Wood, and Z. Jobe, 2019, A consistent global approach for the morphometric characterization of subaqueous landslides: *Geological Society, London, Special Publications*, 477, 455-477. <https://doi.org/10.1144/SP477.15>
- Cruden, D.M. and J. D. Varnes, 1996, Landslide types and processes, in D. M. Cruden, D. J. Varnes, eds., *Landslides: Investigation and Mitigation: Transportation Research Board Special Report*.
- Flinch, J.F., J. Amaral, A. Doucet, B. Mouly, C. Osorio, and J.M. Pince, 2003, Structure of the Offshore Sinu Accretionary Wedge. Northern Colombia: 8th Simposio Bolivariano - Exploracion Petrolera en las Cuencas Subandinas, EAGE, Conference Proceedings, 76–83. <https://doi.org/10.3997/2214-4609-pdb.33.Paper8>
- Green, A., and R. Uken, 2008, Submarine landsliding and canyon evolution on the northern KwaZulu-Natal continental shelf, South Africa, SW Indian Ocean: *Marine Geology*, 254, 152–170. <https://doi.org/10.1016/j.margeo.2008.06.001>
- Hampton, M A., H. J. Lee, and L. Jacques, 1996, Submarine landslides: Review of *Geophysics*, 34, 35–59. <https://doi.org/10.1029/95rg03287>
- He, Y., Zhong, G., Wang, L., Kuang, Z., 2014. Characteristics and occurrence of submarine canyon-associated landslides in the middle of the northern continental slope, South China Sea. *Mar. Pet. Geol.* <https://doi.org/10.1016/j.marpetgeo.2014.07.003>
- Heidarzadeh, M., D. R. Tappin, and T. Ishibe, 2019, Modeling the large runup along a narrow segment of the Kaikoura coast, New Zealand following the November 2016 tsunami from a potential landslide: *Ocean Engineering*, 175, 113–121. <https://doi.org/10.1016/j.oceaneng.2019.02.024>
- Idárraga-García, J., D.G. Masson, J. García, H. León, and C.A. Vargas, 2019, Architecture and development of the Magdalena Submarine Fan

- (southwestern Caribbean): *Marine Geology*, 414, 18–33.
<https://doi.org/10.1016/j.margeo.2019.05.005>
- Lamarche, G., J. Mountjoy, S. Bull, T. Hubble, S. Krastel, E. Lane, A. Micallef, L. Moscardelli, C. Mueller, I. Pecher, and S. Woelz, 2016, Submarine mass movements and their consequences: progress and challenges, in G. Lamarche, G., J. Mountjoy, S. Bull, T. Hubble, S. Krastel, E. Lane, A. Micallef, L. Moscardelli, C. Mueller, I. Pecher, and S. Woelz, eds., *Submarine mass movements and their consequences – 7th International Symposium*: Springer, 41,1-13.
- Leslie, S.C., and P. Mann, 2016, Giant submarine landslides on the Colombian margin and tsunami risk in the Caribbean Sea: *Earth and Planetary Science Letters*, 449, 382–394. <https://doi.org/10.1016/j.epsl.2016.05.040>
- Martinez, J.A., J. Castillo, A. Ortiz-Karpf, L. Rendon, J. C. Mosquera, and V. Vega, 2015, Deep water untested oil-play in the Magdalena Fan, Caribbean Colombian Basin, in: C. Bartolini, P. Mann, eds, *Petroleum geology and potential of the Colombian Caribbean Margin*. *American Association of Petroleum Geologists*, 108, 251–260.
<https://doi.org/10.1306/13531955m1083658>
- Masson, D., C. Harbitz, R. Wynn, G. Pedersen, F. Løvholt, F., 2006, Submarine landslides: processes, triggers and hazard prediction. *Philosophical Transactions of the Royal Society. A Mathematical, Physical and Engineering Sciences*, 364, 2009–2039. <https://doi.org/10.1098/rsta.2006.1810>
- McAdoo, B.G., L.F. Pratson, and D.L. Orange, 2000, Submarine landslide geomorphology, US continental slope: *Marine Geology*, 169, 103-136.
[https://doi.org/10.1016/S0025-3227\(00\)00050-5](https://doi.org/10.1016/S0025-3227(00)00050-5)
- Moscardelli, L., and L. Wood, 2016, Morphometry of mass-transport deposits as a predictive tool: *Bulletin of the Geological Society of America*, 128, 47–80.
<https://doi.org/10.1130/B31221.1>
- Moscardelli, L., L. Wood, and P. Mann, 2006, Mass-transport complexes and associated processes in the offshore area of Trinidad and Venezuela: *American Association of Petroleum Geologist Bulletin*, 7, 1059–1088.
<https://doi.org/10.1306/02210605052>
- Nadim, F., O. Kjekstad, P. Peduzzi, C. Herold, and C. Jaedicke, 2006, Global landslide and avalanche hotspot: *Landslides*, 3, 159–173.
<https://doi.org/10.1007/s10346-006-0036-1>
- Naranjo-Vesga, J., A. Ortiz-Karpf, L. Wood, Z. Jobe, J.F. Paniagua-Arroyave, L. Shumaker, D. Mateus-Tarazona, and P. Galindo, 2020, Regional controls in the distribution and morphometry of deep-water gravitational deposits along

- a convergent tectonic margin. *Southern Caribbean of Colombia: Marine and Petroleum Geology*, 121, 1–30. <https://doi.org/10.1016/j.marpetgeo.2020.104639>
- Ortiz-Karpf, A., D. M. Hodgson, C. A-L. Jackson, and W. D. McCaffrey, 2017, Influence of seabed morphology and substrate composition on mass-transport flow processes and pathways: Insights from the Magdalena Fan, Offshore Colombia: *Journal of Sedimentary Research*, 87, 189–209. <https://doi.org/10.2110/jsr.2017.10>
- Pindell, J.L., 1994, Evolution of the Gulf of Mexico and the Caribbean. *Caribbean Geology: An Introduction*. 13–39.
- Rincón, D. A., J. F. Naranjo, D. Mateus Tarazona, C. A. Hernández, H. D. Madero, J. De Bedout, A. Ortiz-Karpf, F. E. Malagón, and C. O. Cabrera, 2021, Geomorfología del fondo marino profundo en la región sur del caribe colombiano. *Ecopetrol; Entrelibros*. DOI: <https://doi.org/10.29047/9789589287361>
- Rodríguez, I., M. Bulnes, J. Poblet, M. Masini, and J. Flinch, 2021, Structural style and evolution of the offshore portion of the Sinu Fold Belt (South Caribbean Deformed Belt) and adjacent part of the Colombian Basin: *Marine and Petroleum Geology*, 125, 1-24. <https://doi.org/10.1016/j.marpetgeo.2020.104862>
- Romero-Otero, G.A., 2009, Deepwater sedimentary processes in an active margin, Magdalena submarine fan, Offshore Colombia: PHD Thesis, University of Oklahoma.
- Ruiz, C., N. Davis, P. Bentham, A. Price, and D. Carvajal, 2000, Structure and tectonic evolution of the South Caribbean Basin, Southern Offshore Colombia: a progressive accretionary prism: VII Simposio Bolivariano - Exploración Petrolera en las Cuencas Subandinas.
- Shanmugam, G., 2016, Slides, slumps, debris flows, turbidity currents, and bottom currents: Reference Module in Earth Systems and Environmental Sciences. <https://doi.org/10.1016/B978-0-12-409548-9.04380-3>
- Shanmugam, G. and Y. Wang, 2015, The landslide problem: *Journal of Palaeogeography*, 4, 109–166. <https://doi.org/10.3724/SP.J.1261.2015.00071>
- Symithe, S., E. Calais, J.B. de Chabaliér, R. Robertson, and M Higgins, 2015, Current block motions and strain accumulation on active faults in the Caribbean. *Journal of Geophysical Research: Solid Earth*, 120, 3748–3774. <https://doi.org/10.1002/2014JB011779>
- Tappin, D.R., P. Watts, G. M. McMurtry, Y. Lafoy, and T. Matsumoto, 2001, The Sissano, Papua New Guinea tsunami of July 1998 - Offshore evidence on the

source mechanism: Marine Geology, 175, 1–23.
[https://doi.org/10.1016/S0025-3227\(01\)00131-1](https://doi.org/10.1016/S0025-3227(01)00131-1)

Vanneste, M., C. F. Forsberg, S. Glimsdal, C.B. Harbitz, D. Issler, T. J. Kvalstad, F. Løvholt, and F. Nadim, 2013, Submarine landslides and their consequences: What do we know, what can we do?, in C. Margottini, P. Canuti, and K. Sassa, eds., *Landslide Science and Practice - Complex Environment*: Springer, 5, 5–17. https://doi.org/10.1007/978-3-642-31427-8_1

CHAPTER 2.

CHARACTERIZATION OF SUBMARINE LANDSLIDES ALONG THE SOUTH CARIBBEAN COLOMBIAN MARGIN: RELATION TO GROUND CONDITIONS, EFFECT ON GEOMORPHOLOGY SHAPING AND LANDSLIDE SUSCEPTIBILITY ASSESSMENT.

This work was published as: D. Mateus Tarazona., J. A. Prieto., W. Murphy., J Naranjo-Vesga., D. Rincon., C. Hernandez., H. D. Madero., A. Mora., and M. Acuña., Submarine landslide susceptibility assessment along the southern convergent margin of the Colombian Caribbean. *The Leading Edge* 2023; 42 (5): 344–359. Doi: <https://doi.org/10.1190/tle42050344.1>

ABSTRACT

Submarine landslides are a mixture of rock, soil, and fluids moving downslope due to a slope's initial event of mechanical failure. This phenomenon plays a critical role in shaping the geomorphology of the seafloor and the transport of sediments from the continental shelf to the continental rise in the southern margin of the Colombian Caribbean. Concerning the above, two fundamental issues can be highlighted: Firstly, Mass Transport Complexes (MTCs) produced by submarine landslides encompass significant portions of the stratigraphic record. Secondly, these mass movements can affect coastal and underwater infrastructure. The mapping of the southern Caribbean seafloor using seismic cube surveys and multibeam bathymetry data in an area encompassing 59,471 km² made it possible to identify 220 submarine landslides whose areas range between 0.1 km² and 209 km². In addition, the regional analysis of landslide distribution and simplifying their occurrence was possible by building a conceptual framework for a better insight. Distinctive characteristics were found for submarine landslides associated with canyon walls, channel-levee systems, tectonically controlled ridges, and continental shelf break. Mass-Transport Complexes result from the accumulation of mass movement originating both in the continental shelf break and the channel-levee systems were also observed. However, the size of MTCs does not represent individual events but rather the accumulation of multiple events. This fact made it possible to estimate a landslide susceptibility map which suggests the following considerations: Firstly, structural ridges and adjacent intra-slope sub-basins related to the South Caribbean Deformed Belt (SCDB) are more likely to be landslide hazards. Secondly, the continental shelf break and channelized systems produce a moderate landslide hazard potential. Thirdly, deep marine systems with a slope less than five degrees (5°) show the lowest landslide hazard potential. This work enriches the understanding of submarine landslide phenomena in the Colombian Caribbean margin and provides insights into future landslide hazards.

1. INTRODUCTION

Submarine and subaerial landslides have their genesis in rock/soil instability that generates mass movements under the influence of gravity (Cruden and Varnes, 1996; Highland and Bobrowsky, 2008; Martelloni et al., 2012; Shanmugam, 2016; Scarselli, 2020). These phenomena play a significant role in the evolution of continental margins due to their ability to mobilize large volumes of rock, debris, or soil downslope (McAdoo et al., 2000; Lastras et al., 2005; Masson et al., 2006; Moscardelli and Wood, 2008; Morley and Leong, 2008; Locat and Lee, 2009; Karpf et al., 2015). Likewise, they have the potential to affect coastal infrastructure (Carter et al., 2012; Kopf et al., 2010), submarine telecommunications cables (Hasegawa and Kanamori, 1987), pipelines (Lamarche et al., 2016), and generate tsunamis and avalanches (Nadim et al., 2006; Abella and Van Westen, 2007; Devoli et al., 2007; Tappin, 2010; Randolph and White, 2012; Vanneste et al., 2013; Glimsdal et al., 2016; Leslie and Mann, 2016; Tappin, 2017; Arikawa, 2018; Heidarzadeh et al., 2019). The negative consequences of submarine landslides have been socially and economically significant (Tappin et al., 2001; Heidarzadeh M., 2018).

Extensive nomenclature to classify mass movements based on diverse characteristics is used. For instance, the frontal confinement (Martinez et al., 2006; Clare et al., 2018), the relation between its deposits and the failure zone (Moscardelli and Wood, 2008), the internal deformation and disaggregation of the deposit (Shanmugam, 2016), or kinematics of failure (Cruden and Varnes, 1996; Highland and Bobrowsky, 2008). This work adopted the classification based on kinematics in which mass movement includes translational landslides (Figure 1A), rotational landslides (Figure 1B), and debris flows (Figure 1C). Additionally, the term complex landslide (Figure 1D) denotes areas affected by the superposition of lateral or vertical landslides (Hampton et al., 1996; He et al., 2014), and the term Mass Movement Complexes (MTCs) (Moscardelli et al., 2006; Moscardelli and Wood, 2008; Moscardelli, 2016) names areas of mass movement deposits where it is not possible to identify the kinematical genesis.

In convergent continental margins, like the Colombian Caribbean Sea, submarine landslides influence geomorphological features and are closely related to tectonic dynamics (Idarraga and Vargas, 2014; Mateus et al., 2021). In this geographic area, geoscience studies have focused on understanding structural geology (Ruiz et al., 2000; Martinez et al., 2015; Sanchez et al., 2019; Galindo and Lonergan, 2020; Rodríguez et al., 2021) and processes that affect sediment transport (Flinch et al., 2003; Ortiz-Karpf et al., 2015; Naranjo-Vesga et al., 2020) due to the interest of the hydrocarbon industry in new resources. Other studies have shown the bathymetric surveys (INVEMAR & ANH, 2010; Vinnels et al., 2010) and their geomorphological interpretation (Rincon et al, 2021). Some authors have also highlighted the importance of landslides as geohazards (Alfaro and Holz, 2014b; Leslie and Mann, 2016), analyzed the largest landslides observed in the bathymetry (Idarraga and Vargas, 2014; Naranjo-Vesga et al., 2020), or studied the presence of them in limited portions of the Colombian southern Caribbean (Alfaro and Holz, 2014a; Mateus et al, 2021).

However, any previous study has regionally analyzed the occurrence of submarine landslides, their relation with the ground condition, and the susceptibility to new events in the entire south Colombian Caribbean continental slope. This work helps to improve the knowledge of downwards processes in convergent continental margins and gives insights into the expected type and the average size of future landslides in the Colombian Caribbean margin.

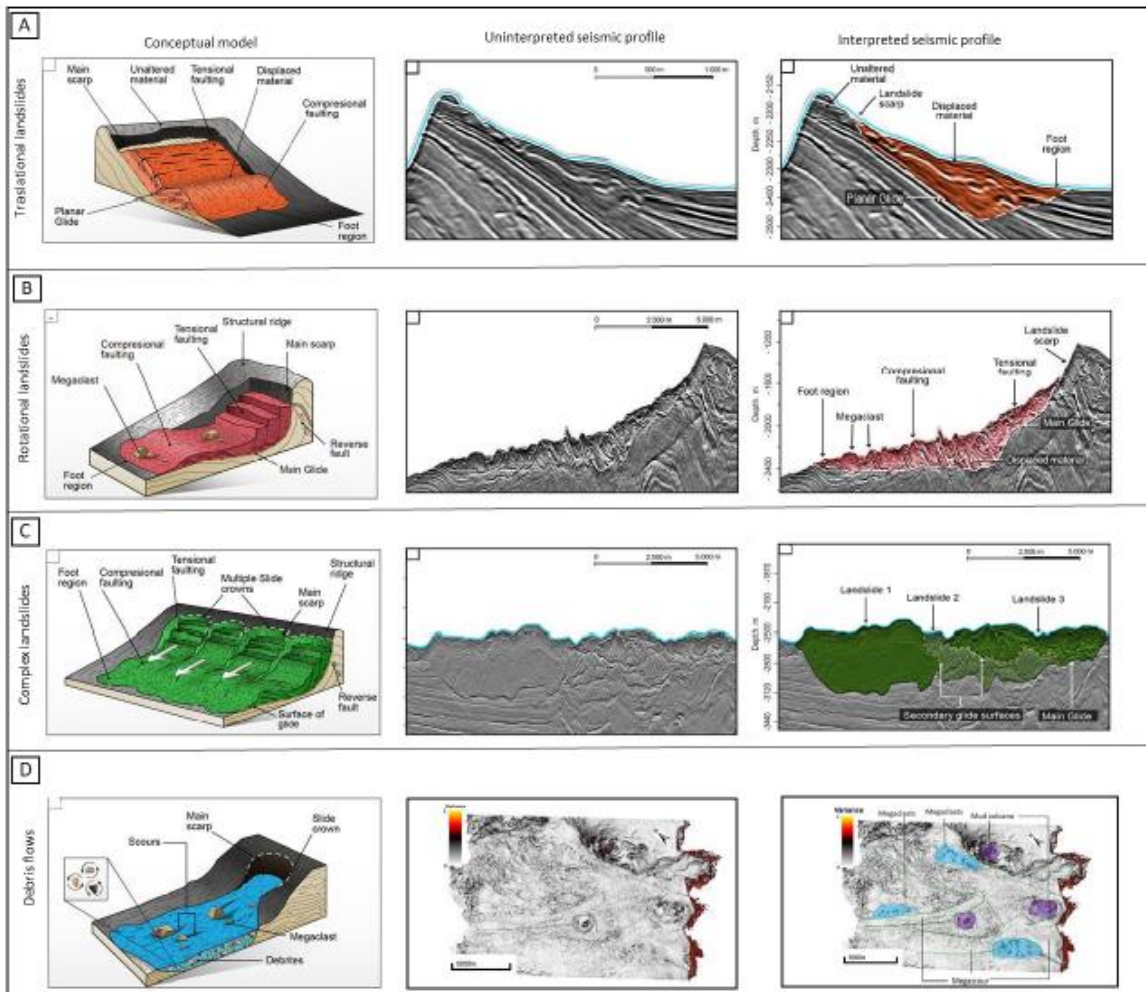


Figure 1. Conceptual models and seismic profile examples of Mass movement types. A) Translational landslides are coherent mass movements with little or no internal deformation (Mulder and Cochonat, 1996; Masson et al., 2006) characterized by presenting a planar glide on which the displaced material moves. This singularity is the main difference with rotational landslides. The displaced material includes an upward tensional faulting zone, contrasting with a compressional faulting zone toward the foot region. The Interpreted seismic profile highlights the displaced mass, unaltered material, escarp, foot region, and the planar glide. B) Rotational landslides are mass movements formed by the failure of a solid or coherent material characterized by a semi-circular sliding surface (Cruden and Varnes, 1996; Highland and Bobrowsky, 2008). The Interpreted seismic profile indicates the scarp, displaced material (tensional and compressional faulting zones), megaclasts, foot region, and main slide surface (Glide). C) complex landslides are formed by the lateral or vertical superposition of sliding events (Hampton et al., 1996; He et al., 2014). They exhibit common landslide elements such as main scarp, glide, displace material (tensional and compressional faulting zones), and foot region. The interpreted seismic profile presents an example of complex landslides highlighting the main glide and secondary surfaces that allow for differentiating at least three separate events that overlap horizontally. D) Debris flows are mainly composed of disaggregated material in which the intergranular movement is greater than the shear movement on the slip surface (Shanmugam, 2016). The bathymetric expressions from these mass movements can present from abundant megaclasts and erosive grooves to irregular surfaces known as hummocky texture (Bornhold and Johns, 1984; Bell et al., 2013; Vanneste et al., 2013). The small box represents the inter-joint movement that differentiates debris flow from rotational and translational landslides. Modified from Rincon et al. (2021). The Interpreted seismic profile presents an example of a debris flow zone highlighting megaclasts and mega scours observed in the variance attribute of a horizontal slide 100 ft below the seafloor.

1.1. Regional settings

The study area is located in the Colombian southern Caribbean margin (Figure 2) and includes sectors in sedimentary basins of Urabá, Sinú Offshore, Guajira Offshore, and Colombia. The study area borders La Aguja Canyon (AC) and the underwater foothills of the Santa Marta massif on the north, the Panama Deformed Belt (PDB) and the Uramita Fault on the south, the continental shelf break on the East, and The Colombia basin on the West.

The geological evolution of the Colombian southern Caribbean continental margin has been influenced tectonically by the convergence of the Caribbean oceanic plate beneath the continental South America plate. This interaction created the South Caribbean Deformed Belt (SCDB) in front of Colombia and Venezuela (Duque-caro., 1979; Corredor., 2003; Pindell and Kennan., 2009; Bernal-Olaya et al., 2015b; Symithe et al., 2015). On the Colombian margin, the SCDB is subdivided into three main zones: the South Sinú Fold Belt (SSFB); the Magdalena Fan Deposit (MFD); and the North Sinú Fold Belt (NSFB) (Flinch et al., 2003; Martinez et al., 2015).

The geomorphology of the study area is strongly associated with co-existing factors such as tectonics, continental sediment supply, and ocean currents (Vinnels et al., 2010; Martinez et al., 2015; Romero-Otero., 2015; Naranjo et al., 2020, 2021; Rincon et al, 2021). Figure 3 shows a conceptual diagram representing four geomorphological domains identified in the study zone. In the NSFB (Zone 1) and SSBN (Zone 3), anticlines become structural ridges that, combined with intraslope sub-basins, act as topographic barriers for the transport of sediments from the continental shelf to the continental rise (Ruiz et al., 2000; Flinch et al., 2003; Vinnels et al., 2010; Martinez et al., 2015; Idarraga et al., 2019; Naranjo-Vesga et al., 2020, 2021; Rincon et al. al, 2021). On the other hand, in the area of influence of the MFD (Zone 2), channel-levee systems and MTCs prevail (Ercilla et al., 2002b; Flinch et al., 2003; Cadena et al., 2015; Martinez et al., 2015; Romero-Otero et al., 2015; Idárraga-García et al., 2019; Naranjo-Vesga et al., 2020, 2021; Rincon et al., 2021), which allow a continuous transfer of sediments from the continental shelf to the

continental rise. Finally, the southern of the SSFB (Zone 4) is affected by the convergence between the Caribbean Ocean plate, the continental South America plate, and the mini plate of Panama (Duque and Caro, 1990,1979; Ruiz et al., 2000; Cortés and Angelier, 2005). This interaction generates structures associated with the Uramita Fault System with a Northwest-Southeast orientation.

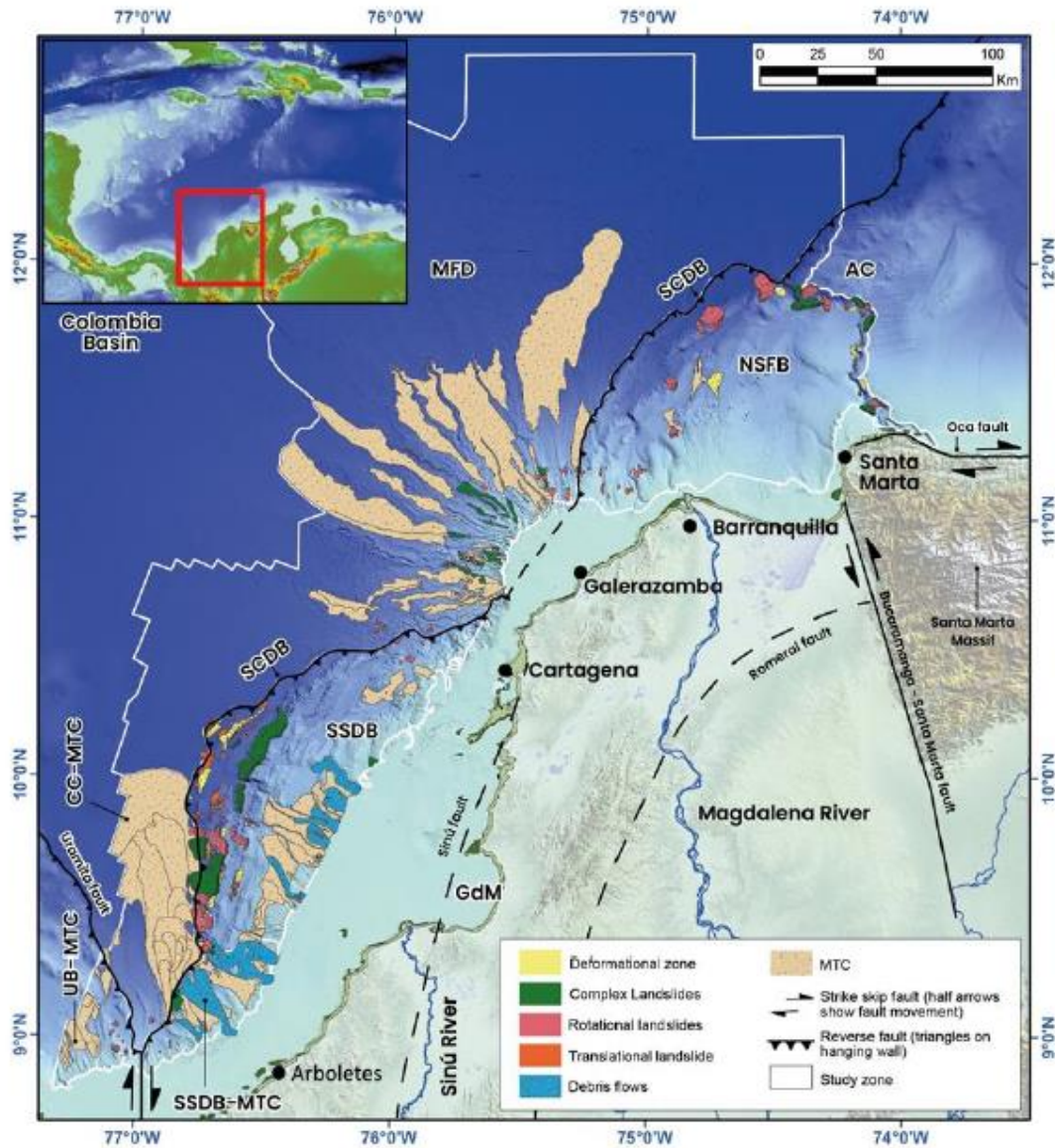


Figure. 2. Study zone. Topographic map of the northwest of Colombia, and bathymetric map of the southern Caribbean Sea highlighting the geographic distribution of landslides and MTCs. Note the relation between translational, rotational, and complex landslides with structural ridges in the SCDB (NSFB, SSFB). Likewise, a clear association between debris flows and the continental shelf break, seawards of the GdM, is observed. The main morphological zones are based on the proposal of Rincon et al. (2021). Geological features are based on proposals from Ruiz et al. (2000); Alfaro and Holz, 2014b; Martínez et al. 2015; Mora et al. (2018); Idárraga-

García et al.2019; Galindo y Lonergan (2020); and Rodríguez et al. (2021). South Caribbean Deformed Belt (SCDB). North Sinú Fold Belt (NSFB), Magdalena Fan Deposits (MFD). South Sinú Fold Belt (SSFB). Panama Fold Belt (PFB). South Sinú Fold Belt, a domain of MTC (SSFB-MTC). Colombian basin, a domain of MTC (CB-MTC). Urabá Basin, a domain of MTC (UB-MTC). Morrosquillo Gulf (GdM). b) The red box shows the location of the expanded information in the main panel. Ecopetrol S.A. supplied Multibeam bathymetry data. General bathymetry to complete areas without multibeam bathymetry was taken from the GEBCO grid (GEBCO., 2020).

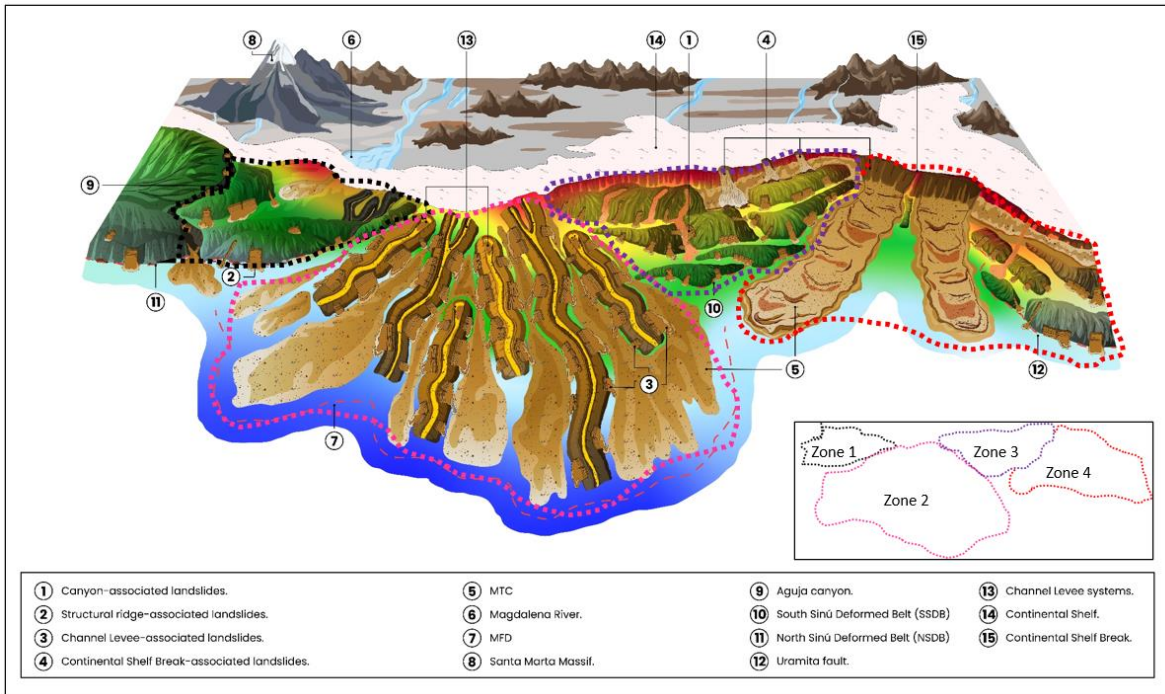


Figure. 3. Conceptual diagram of the south Caribbean Colombian margin showing four geomorphological zones (inset in the lower right corner highlights general shape and boundaries of each zone). Zones 1 and 3 relate the NSFB (11) and SSFB (10), respectively, where structural ridges and intraslope basins prevail. In these areas, landslides associate with canyons walls (9, 1), structural ridge limbs (2), and the continental shelf break (4). Zone 2 relates to MFD (7). There, channel-levee systems and MTCs (5) predominate. Landslides are linked to channels internal walls as to levees outer edges (3). Zone 4 includes the southern part of the SSFB and PFB. Landslides are associated with continental shelf break and structural ridge limbs.

2. DATA COLLECTION AND ANALYSIS

Based on the bathymetric model presented by Rincon et al (2021), the geomorphological analysis included four seismic cubes and seven multibeam bathymetry surveys. Data resolution ranged from 10 m to 100 m. These data involved areas from the continental shelf break to the continental rise which facilitated obtaining a regional image of the seabed in which the interpretation of landslides was extended toward areas without 3D seismic information. Based on their morphological parameters and seismic response of the displaced material,

landslides were interpreted, as described by Mateus et al, (2021) Table 1. Measured morphometry included Area (A), volume (V), total height drop (Ht), total length (Lt), scarp gradient (Ss), and natural slope angle (S) following the proposal by Clare et al. (2018).

Table 3. Submarine landslide types and characteristics used for identification. Based on what was described by Mateus et al, (2021) and Rincon et al., (2021).

Submarine Landslide type	Definition	Main characteristic used for identification
Traslational Landslide	Coherent mass movements characterized by presenting a planar failure surface on which the displaced material moves. (Cruden and Varnes, 1996; Highland and Bobrowsky, 2008)	Planar failure surface on seismic section
Rotacional Landslide	Coherent Mass movements formed by the failure of a solid or coherent material characterized by a semi-circular sliding surface (Cruden and Varnes, 1996; Highland and Bobrowsky, 2008)	Semi-circular sliding surface on seismic section
Complex Landslide	Mass movements formed by lateral or vertical superposition of sliding events (Hampton et al., 1996; He et al., 2014)	Multiple slide crowns on seafloor
Debris flows	Mass movement composed of disaggregated material in which the intergranular movement is greater than the shear movement on the slip surface (Shanmugam, 2016)	Erosive grooves, debris to megaclasts and hummocky texture on seafloor

After mapping the geographic distribution of submarine landslides reported by Rincon et al., 2021 (Figure 2), its relation with ground conditions including seafloor geomorphology, slope degree, and faults presence, was analyzed. For this purpose, we present bathymetric images and conceptual models (Serey A et al., 2020) to condense the main geomorphological features observed on the seafloor. In addition, looking for evidence connecting gas hydrate dissociation and submarine landslides, we analyzed the position of landslide glides concerning the Bottom Simulator Reflector (BSR) (McIver, 1982; Kayen and Lee, 1993; Kvenvolden, 1993; Miniert et al., 2005; Talling et al., 2014; Mountjoy, 2014; Wu et al., 2018). Finally, a preliminary map of landslides susceptibility was carried out following the landslide Weight index (Wi) method proposed by Van Westen in 1997 (Van Westen, 1997; Abella and Van

Westen, 2007; Borrell et al., 2016). This methodology quantifies the relation between landslides occurrence and physical factors such as topographic slopes, types of rock/soil, or the presence of faults. The way to quantify this relation is given through the W index, which is calculated by superimposing areas affected by landslides and areas of each factor (Class), the basic equation is listed below.

$$W_i = Ln \left[\frac{Densclass}{Densmap} \right] = Ln \left[\frac{\frac{Landslide\ area\ in\ a\ Class\ (i)}{Total\ area\ of\ Class\ (i)}}{\frac{Total\ landslide\ area\ in\ the\ study\ zone}{Total\ area\ of\ the\ study\ zone}} \right] \dots\dots\dots (1)$$

The total index Wt by adding the individual indices Wi is calculated.

$$W_t = \sum W_i \dots\dots\dots (2)$$

3. RESULTS

3.1. Morphometry of landslides

In total, 220 landslides were interpreted and grouped into 33 translational landslides, 138 rotational landslides, 37 complex landslides, and 12 debris flow zones (Figure 2).

Regarding landslide dimensions (Figure 4A), it was found that in translational landslides, the total length (Lt) ranges between 650 m to 6,450 m, while in rotational landslides, Lt fluctuates between 1,914 m and 12,772 m. However, just eleven landslides (6 % of singular events) exhibit Lt greater than 4,000 m (Figure 4B). Complex landslides show Lt ranging between 545 m and 13,941 m. Finally, debris flows exhibit Lt between 6,351 m and 31,657 m, demonstrating greater mobility in this type of mass movement. On the other hand, in translational landslides, vertical drop (Ht) ranges between 17 m and 860 m, in rotational landslides between 13 m and 1,186 m, in complex landslides between 129 m and 1,185 m, and in debris flows between 590 m and 1,642 m (Figure 4C).

Concerning landslides size (Figure 4D), translational slides were identified as the smallest events covering areas from 0.3 km² to 10.8 km² and volume between 0.004 km³ and 0.1 km³, followed by rotational landslides covering areas from 0.1 km² up to 52 km² and volumes between 0.01 km³ and 8.51 km³. On the other hand, complex landslides showed the greatest sizes covering areas from 0.47 km² to 209 km² and volumes from 0.009 km³ to 108 km³. Finally, debris flows exhibit areas between 7 km² and 195 km² even though it was impossible to estimate its volume because of the difficulty measuring the deposit thickness.

The estimated main scarp angles (S_s) in landslides ranged between 15° and 44°, and the natural slopes (S) close to this type of landslide, ranged between 5° and 13°.

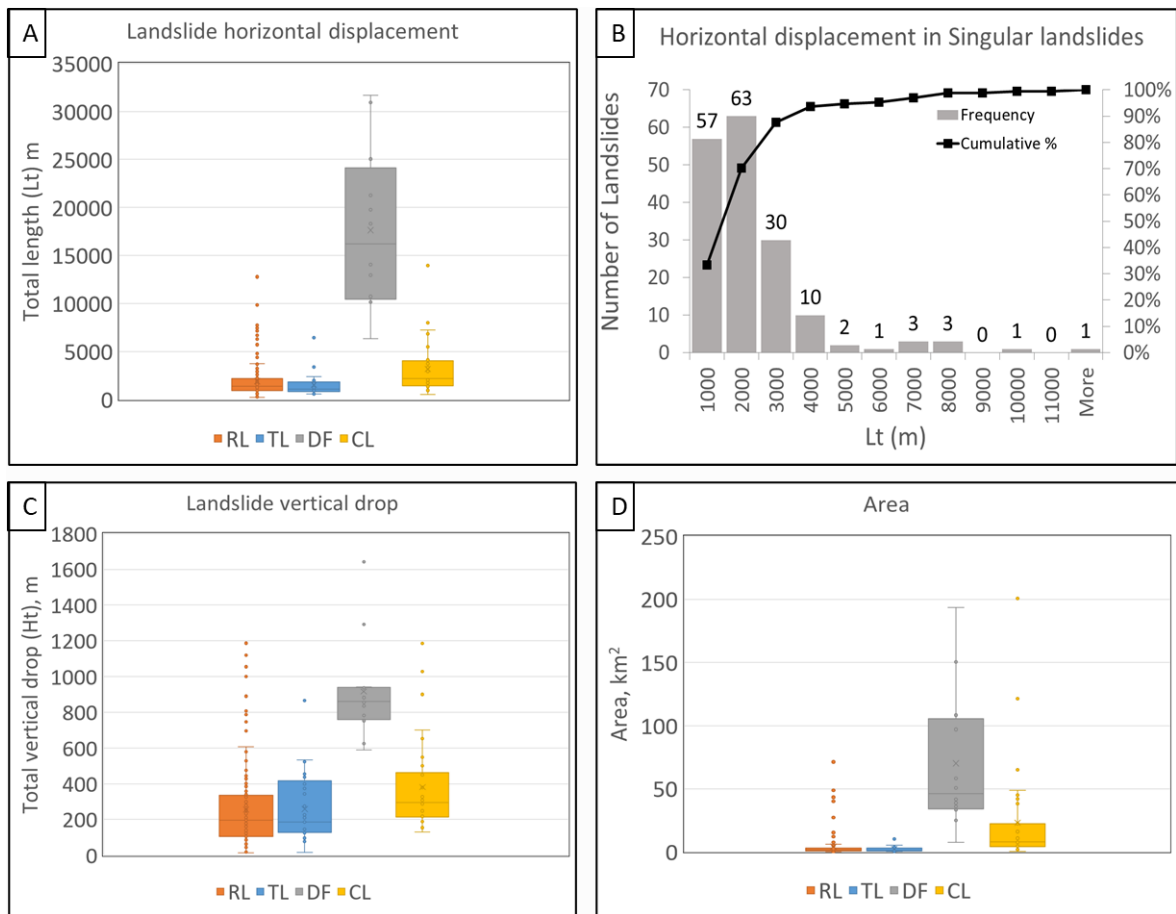


Figure. 12 Statistics for Morphometric parameters in landslides. A) box plot showing total length (Lt) observed in distinct types of landslides. B) Frequency histogram of Lt for singular landslides (translational and rotational). C) Box plot presenting total vertical drop (Ht). D) Box plot showing areas interpreted in all types of landslides.

3.2. Landslides occurrence and their relation with seafloor morphology

Ground conditions initially originated from tectonics, continental sediment supply, and ocean currents are affected by several types of submarine landslides which control the final geomorphology in each zone as follows.

3.2.1. Zone 1

This zone relates to the NSFB. It distinguishes itself by the predominance of intra-slope sub-basins, structural ridges, continental slope-associated hemipelagic sediments, and channeled systems. Submarine landslides in three main settings (Figure 5) were observed, i.e.: i) Rotational landslides eroding structural ridges and filling adjacent flat areas of the intraslope sub-basins. ii) landslides associated with the active canyons of the Magdalena River. These landslides are interpreted as the result of the instability of the low-consolidated sediments belonging to the current Magdalena River system. iii) Rotational and complex landslides on the Aguja canyon walls. These landslides widen the canyon edges and partially obstruct its thalweg. These landslides were interpreted as originating from the instability of the overstepped canyon walls ($>15^\circ$). Instability on the canyon walls generates deformational zones (Mateus et al, 2021) that progressively might become observed landslides. Other authors have suggested that faults influencing the evolution of the canyon (Shepard, 1973; Restrepo-Correa and Ojeda, 2010) also have an influence on the genesis of landslides (Restrepo-Correa and Ojeda, 2010; Vargas and Idárraga- García, 2014).

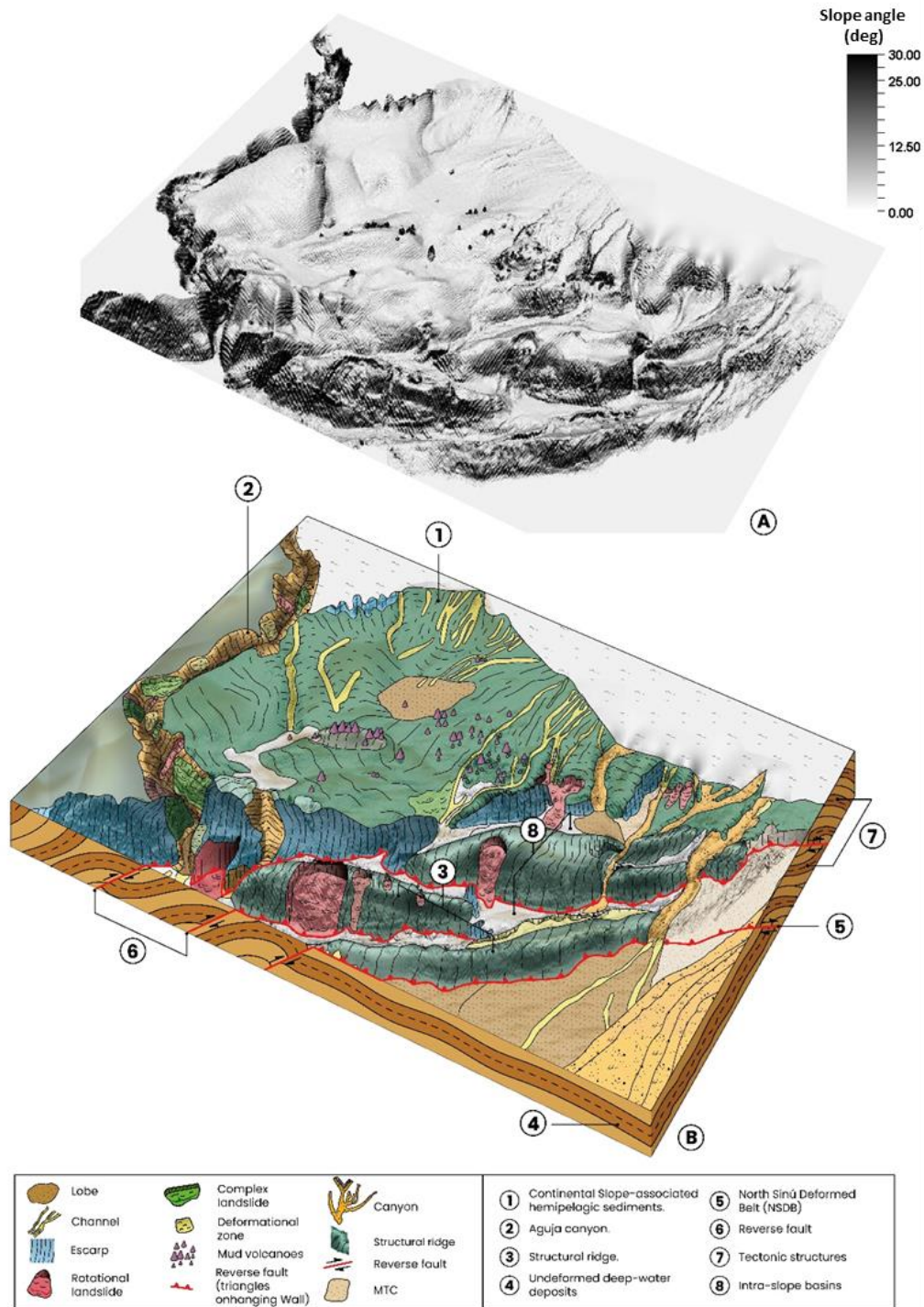


Figure 4. Conceptual ground model of zone 1 (for geographical location see Figure 3). A) Uninterpreted bathymetric relief where black tones represent the steepest slopes, and white tones correspond to flat areas. B) Three-dimensional conceptual ground model presenting the interpretation of the main geomorphological characteristics. Note that landslides are mainly associated with NSFB structural ridges and the Aguja canyon. No landslides in continental slope-associated hemipelagic sediments were observed except in those areas influenced by active Magdalena river systems. Likewise, in front of the NSFB, where lobes and canyons linked to the Magdalena Fan systems were interpreted.

3.2.2. Zone 2.

This zone corresponds to the MFD, where bathymetry is dominated by channel-levee systems, MTCs, abandoned channels, and sediment waves (Rincon et al., 2021). MTCs prevail in low-slope regions (<2 degrees) between the channel-levee systems (Figure 6). These MTCs interpreted as a consequence of landslides originating from both the upper continental slope (Idárraga-García et al., 2019; Leslie and Mann, 2016; Naranjo-Vesga et al., 2020; Ortiz-Karpf et al., 2017; Romero-Otero et al., 2015) and outer edges of channel-levee systems (Rincon et al., 2021). The lengths and widths of MTCs exceed 150 km and 25 km, respectively, in the continental rise. These highly erosive flows may have the ability to smooth and modify the relief of the continental slope and bottom of the Colombia Basin (Ercilla et al., 2002b; Flinch et al., 2003; Naranjo-Vesga et al., 2020; Ortiz-Karpf et al., 2015; Romero-Otero et al., 2015) and their deposits cover areas that reach 1,540 km² and have been reported with sizes of up to 34,700 km² in the subsurface (Leslie and Mann, 2016). Otherwise, landslides observed in the current bathymetry present rotational and translational dynamics and seem to evolve into areas of complex landslides located both on the inner edges of the channelized systems and the outer edges of the levees (Figure 6).

3.2.3. Zone 3.

In this area corresponding to the SSFB, morphology is characterized by intra-slope sub-basins, structural ridges, landslides, and MTCs. Landslides in this zone can be grouped in three geomorphological contexts, i.e.: i) Landslides associated with canyon walls. These landslides present rotational dynamics and a total length (Lt) of less than 4 km. The main effect they generate is the progressive widening of canyons and partial obstruction of the thalweg. ii) Landslides are linked to the system of reverse faults (thrust) and anticlines. Rotational and complex types are notable for their size. Rotational landslides reach 12.5 km of length (Lt) (Mateus et al., 2021). These landslides erode the structural ridges and are an important source of sediments for filling intra-slope sub-basins isolated from the continental shelf break. On the other hand, complex landslides involve areas exceeding 200 km² and are

linked to SSFB structures (Figure 7). iii) debris flows originated at the continental shelf break. The latter exhibit crowns and erosive scours that print hummocky texture on the seabed (Bornhold and Johns, 1984; Bell et al., 2013; Vanneste et al., 2013). According to measurements, debris flows present horizontal displacements that exceed 30 km, which is evidence of its high mobility. These flows were interpreted as the main feeder for MTCs identified in intraslope sub-basins having a direct connection with the continental shelf break as suggested by (Mateus al., 2021).

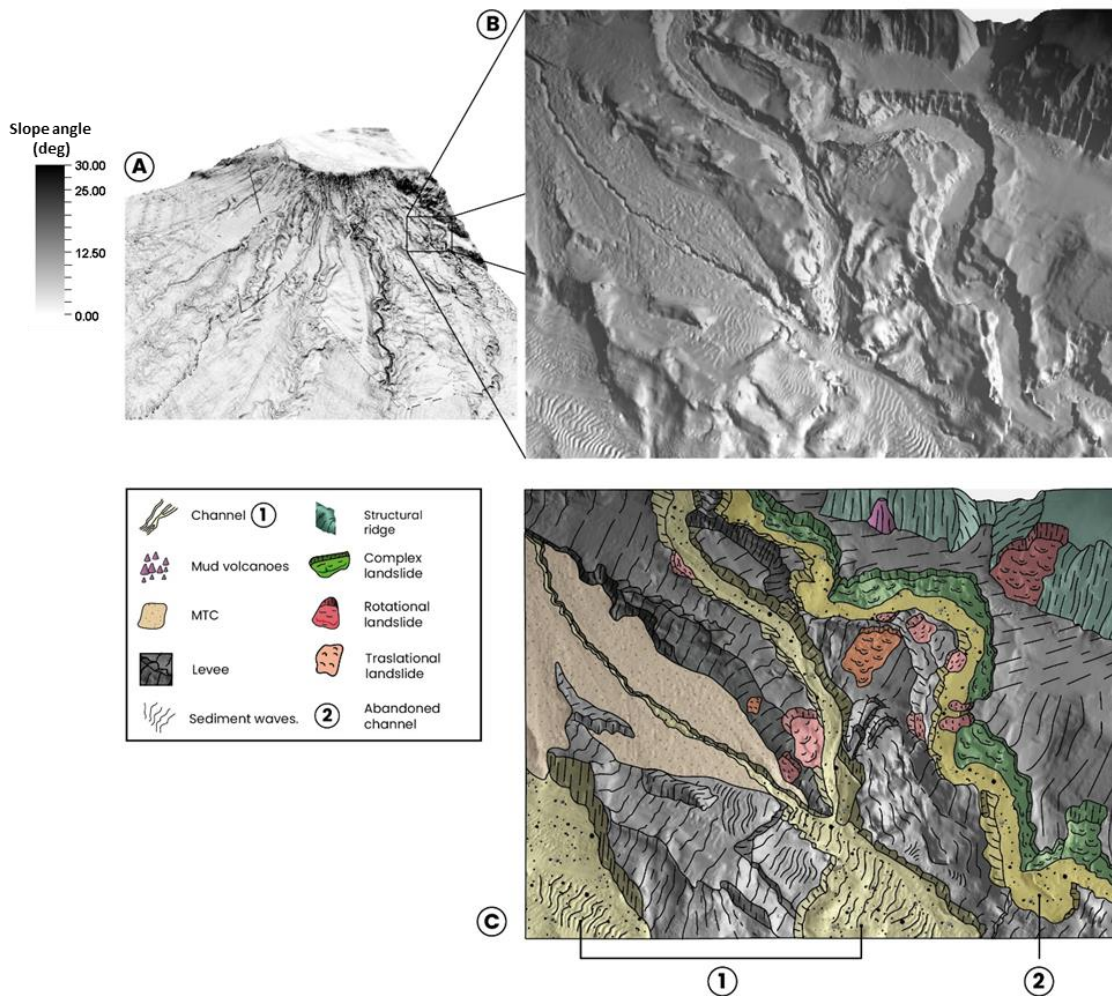


Figure. 5. Conceptual ground model of zone 2 (for geographical location see Figure 3). A) Uninterpreted bathymetry of MFD where black tones represent the steepest slopes and white tones correspond to flat areas. B) uninterpreted detailed seafloor relief in a zone with high-resolution bathymetry. C) Conceptual ground model that presents the Interpretation geomorphology of panel B. Note that a complex landslide affects the abandoned channel (labeled with number 2), while in active channels (labeled with number 1), displaced mass landslides, are not preserved. This observation suggests that displaced mass landslides are incorporated as part of MTCs observed in channelized systems.

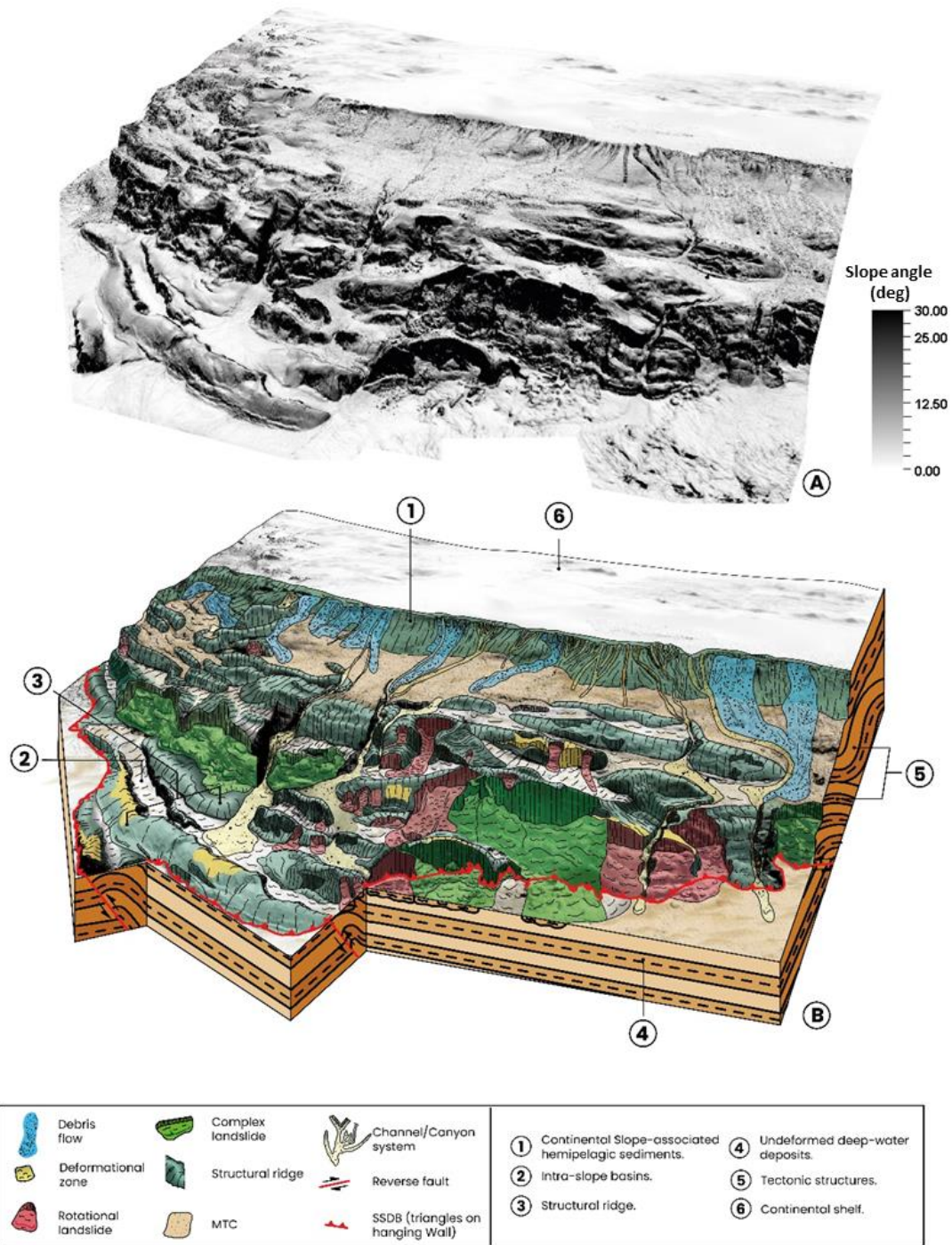


Figure. 6. Conceptual ground model of zone 3 (for geographical location, see Figure 3). A) Uninterpreted bathymetry where black tones represent the steepest slopes and white tones correspond to flat areas. B) Three-dimensional conceptual ground model that presents the interpretation of the main geomorphological features of Zone 3. Note that areas affected by rotational and complex landslides stand out for their sizes. Those cohesive landslides erode anticline structures of the SSFB. Debris flows originating from the continental shelf break are then deposited as MTCs filling adjacent intraslope sub-basins.

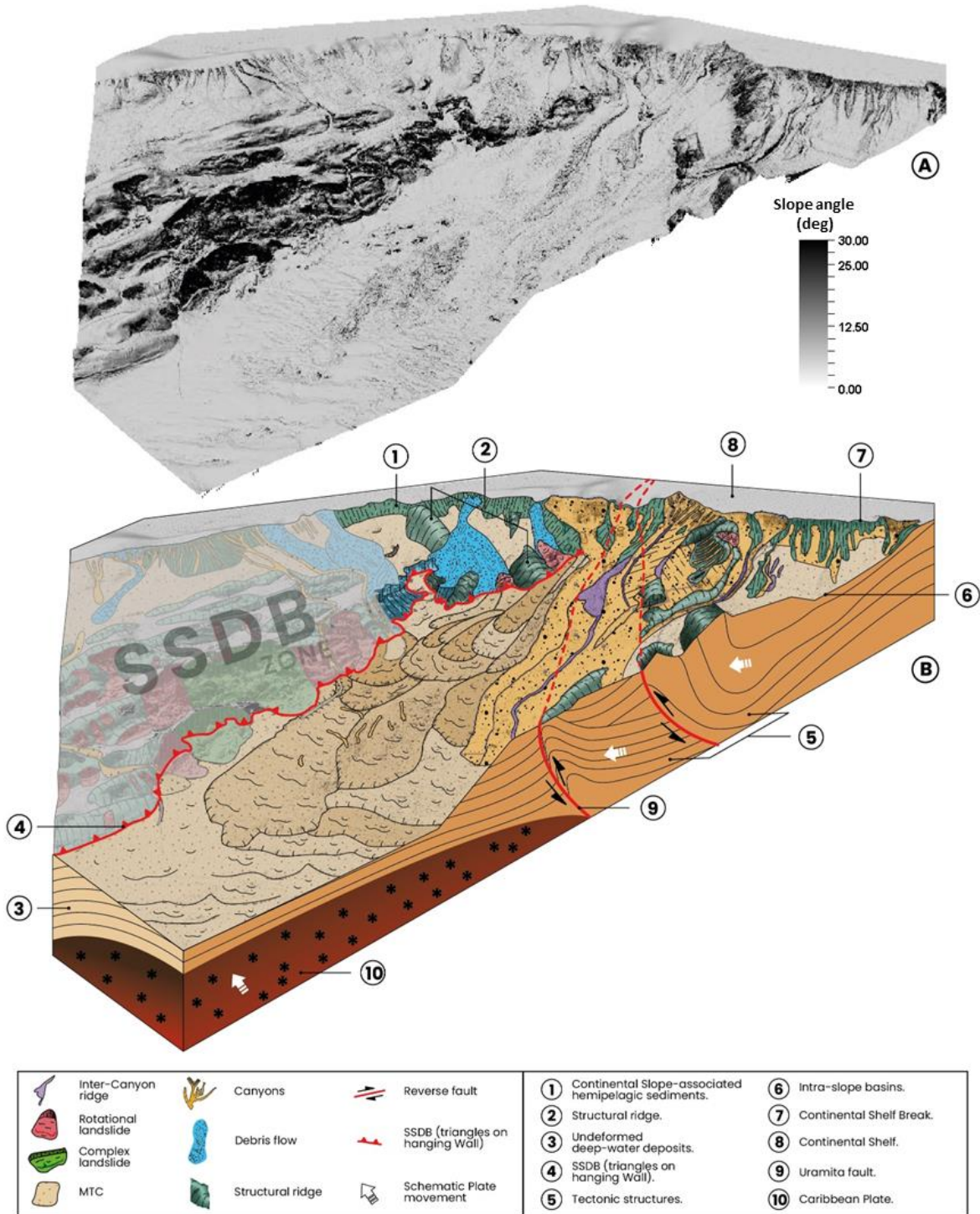


Figure 7. Conceptual ground model of zone 4 (for geographical location, see Figure 3). A) Uninterpreted bathymetry where black tones represent the steepest slopes and white tones correspond to flat areas. B) Three-dimensional conceptual ground model that presents the interpretation of the main geomorphological features of Zone 4. Note that the main canyons zone coincides with lineaments of the Uramita fault and the edge of Panama and South American plates. MTCs are the main feature in the sedimentary seismic record.

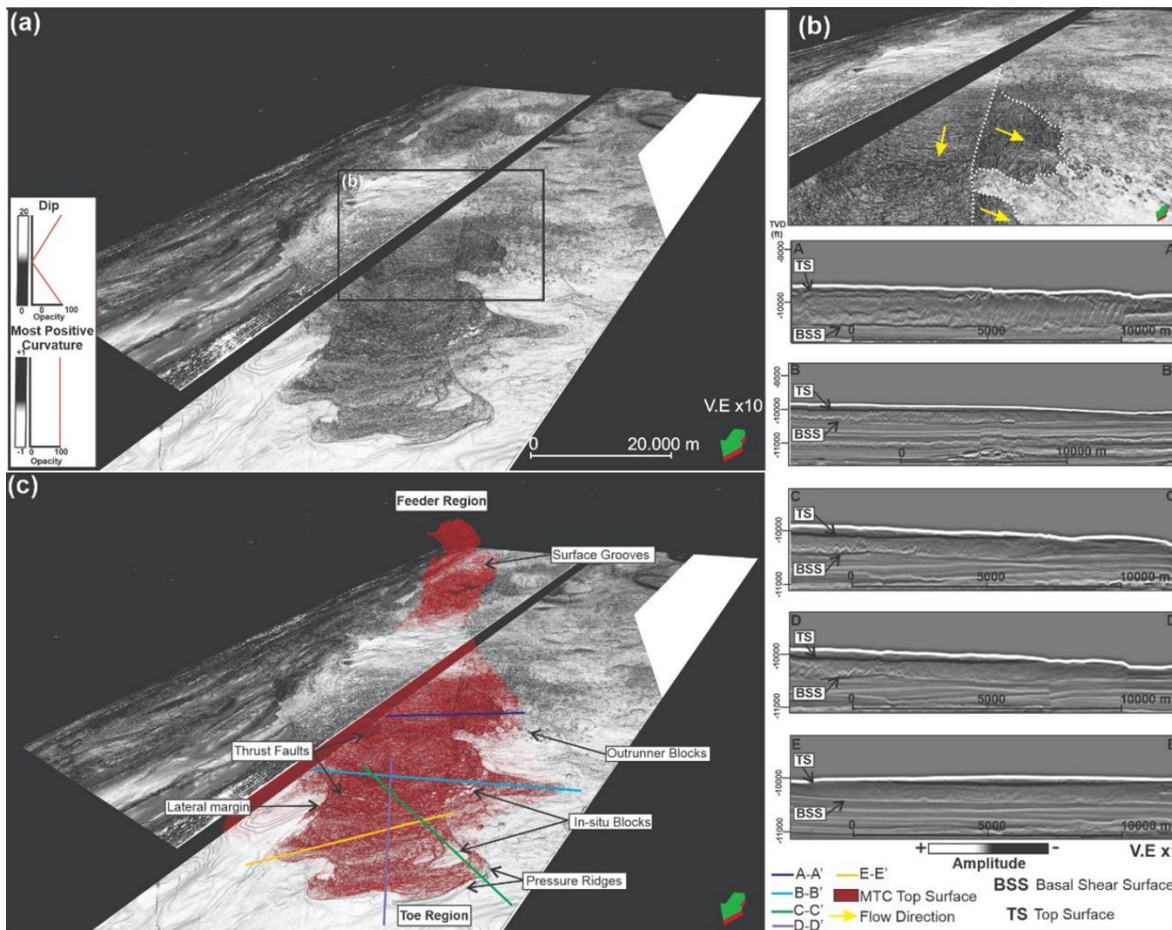


Figure. 8. MTCs in the subsurface in zone 4 (for geographical location, see Figure 3). A) Corendered vertical slices of Consistent Dip and Most Positive Curvature attributes highlighting edges of the biggest MTCs zone. It has a northwest deepening, and to get its whole geometry it was necessary to interpret tens of seismic sections in two seismic cubes surveys. B) An example of vergence change of thrust faults, which is an indicator of different movements blending in a unique deposit. C) Interpreted MTCs zone top surface. Note a coincidence between the interpreted feeder zone and debris flows observed in bathymetry (Figure 8). Pressure ridges and outrunner and in-situ blocks were also observed. Vertical Slices (A-A'), (B-B'), (C-C'), (D-D') and (E-E') show the MTCs zone top surface (TP), basal shear surface (BSS). Low-amplitude chaotic facies and thrust-fold belts characterize the MTCs Zone interlayered with flat-lying high amplitude seismic facies that identify low energy sediments.

3.2.4. Zone 4.

Figure 8 condenses seafloor features and ground conditions interpreted in the south of the Colombian Caribbean margin (Rincon et al, 2021; Mateus et al, 2021). In this zone, the subduction of the Caribbean plate beneath Panama and South American plates generates a depocenter in a southwest-northeast direction with a tilt to the south. This depocenter favors accommodation space which is filled by MTCs. These MTCs begin as landslides at the continental shelf break and evolve to canyons with a southeast-northwest orientation. Superposition of multiple MTCs difficult the identification and morphometric quantification of singular events;

however, it was possible to differentiate at least 26 overlapping MTCs. The largest of them reach an area of 1,200 km² and a volume of 183 km³ (Figure 9). It should be made clear that more than individual events, these MTCs are interpreted as a merge of successive landslides alternated by periods with low mass movement intensity. That alternation results in interlayered beds of low-energy sediments with MTCs, as shown in Figure 9C.

3.3. Submarine landslides and their relation with the Bottom Simulator Reflector (BSR)

The BSR is one of the characteristic features of the subsurface in the Colombian Caribbean. It is associated with the anticlinal structures of the SSFB but also (though to a lesser extent) with flat areas such as intraslope sub-basins (Rincón-Martínez et al., 2022). Figure 10 summarizes four types of spatial relationships evidenced between the BSR and submarine landslides in the study area as follows, i.e.: i) Landslides located above the BSR (Figure 10A). In this relation, most glide surfaces do not coincide with the BSR. That was observed in 95% of analyzed landslides, including those with areas larger than 10 km². ii) Glide surfaces coincide with the BSR reflector (Figure 10B). This relation in two landslides was observed. This relation in complex landslides related to SSFB structural ridges was observed. In this case, the interface between hydrate-cemented sediments and the free-gas-containing sediments might be a preferential surface for the development of landslide glide. To confirm this hypothesis, more data analyses are required. iii) The BSR crosscut the landslide displaced mass (Figure 10C). This relation suggests a hydrate stabilization after landslide development. That was identified only in two landslides. iv) The BSR crosscuts discontinuously the landslide displaced mass (Figure 10D). This relation observed in three landslides suggests reactivation of the movement, causing the destabilization of the hydrates and exhibiting an irregular BSR. The above suggests that there is no remarkable causal association between hydrate dissociation and landslide events in the study zone.

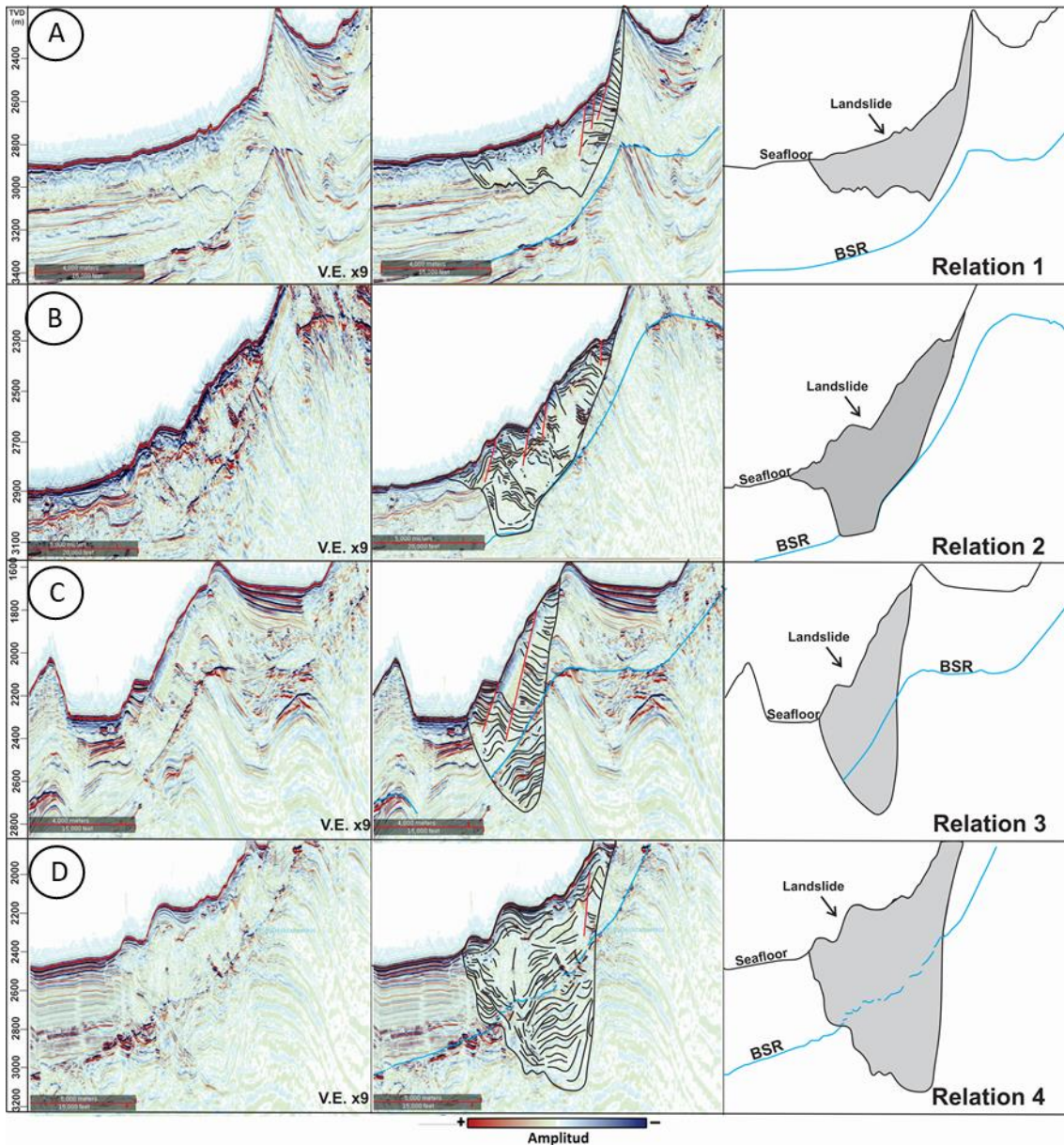


Figure. 9. Relation between submarine landslides and the BSR. A) landslide glide locates above BSR. This was observed in 95% of the analyzed landslides suggesting no direct linking exists between BSR level and landslide glide development. B) Glide surfaces coincide with the BSR reflector. This relation was observed in complex landslides in zone 3 suggesting that BRS could influence landslide development. C) BSR crosscut landslides displaced mass suggesting minor changes in landslides deformation allowing the BSR development. D) BSR crosscut discontinuously the landslide displaced mass suggesting internal movement that causes destabilization of the hydrates and resulting in an irregular BSR.

4. DISCUSSION

Regional interpretation of submarine landslides allowed us to analyze the association between these phenomena and other characteristics such as ground

conditions, the Bottom Simulator reflector (BSR), and MTCs. Likewise, a preliminary landslide susceptibility map is presented.

4.1. Landslides and their relation with ground condition

Submarine landslides were observed in four geomorphological contexts: i) Canyon walls. ii) channel-levee systems. iii) Tectonically Controlled ridges. iv) the continental shelf break.

4.1.1. Submarine landslides in canyon walls

Landslides in canyons present rotational dynamics. They are generated in canyons with overstepped walls ($>15^\circ$). These landslides may result in deposits with or without internal deformation. In the study area, these prevail in La Aguja canyon (CA) (Figure 11A, C, and E), where they generate U-canyon profiles (Naranjo et al, 2021). The probable trigger mechanism is seismic activity related to the SCDB tectonism (Vargas and Idarraga, 2014). In addition to the CA, this type of landslide was observed in slope incising canyons (Naranjo et al, 2021) in the NSF zone, where they are linked to the current Magdalena River fan system (Romero-Otero, 2009), as well as in the SSFB and associated with the PDB (Mateus et al, 2021)) (Figure 11 B, D, and F), where they erode canyon walls without direct connection to continental tributaries. An additional effect of these landslides is a partial obstruction of the canyon's thalweg which may affect the dynamics of internal flow patterns. The observed length was generally less than 4 km, which is similar to other landslides in canyon walls reported worldwide (Green and Uken, 2008; He et al, 2014; Casalbore et al, 2019).

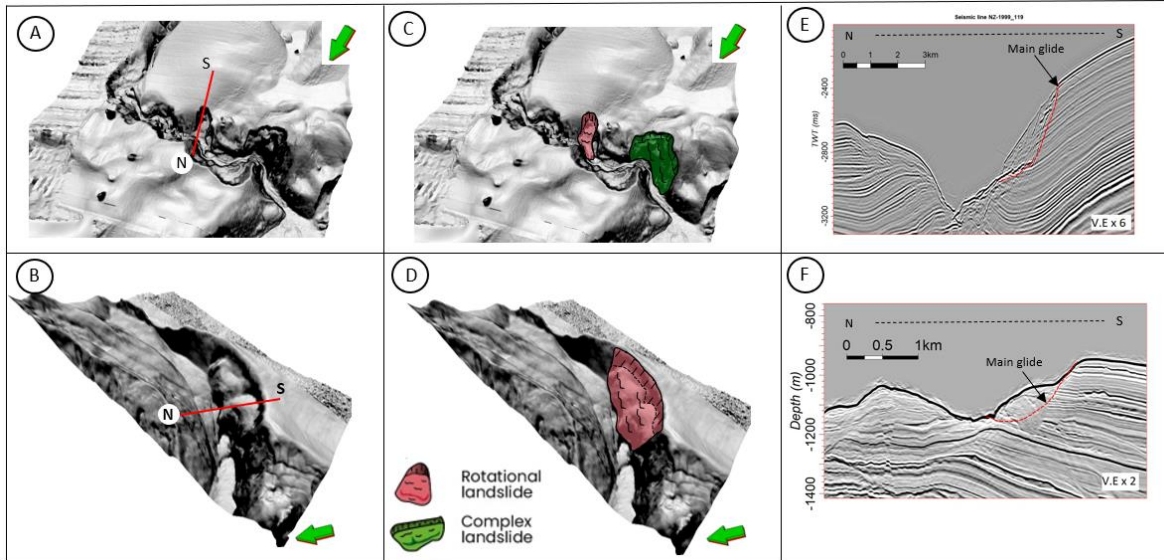


Figure. 10. Examples of submarine landslides in canyons walls. A) Bathymetry without interpretation showing La Aguja canyon (AC) and location of seismic section presented in panel E. B) Bathymetry without interpretation showing an incising canyon in the Panama Deformed Belt (PDB) and location of seismic section presented in panel F. C) Bathymetry interpretation showing two landslides associated with AC. D) Bathymetry interpretation showing the landslide observed in the PDB presented in panel B. E) Seismic sections showing the main glide of the landslide interpreted in AC. F) Seismic sections showing the main glide of the landslide interpreted in the PDB.

4.1.2. Submarine landslides in tectonically Controlled ridges.

Submarine landslides in tectonically controlled ridges are highly linked to faults and anticlines of the SSFB (Figure 12 A, C, E) and NSFB (Figure 12 B, D, F) (Idarraga J. and Vargas C, 2014; Mateus et al, 2021). These landslides present both translational and rotational kinematics. Translational landslides show a smaller size (maximum area = 10 km²) compared to rotational landslides that reach areas up to 52 Km². The maximum length observed was 12.5 km. However, 93% of the landslides exhibited lengths less than 4 km. These individual landslides are interpreted to grow up to be complex landslide areas reaching up to 200 km² along SSFB foothills (Mateus et al, 2021). They have a highly erosive effect that destroys the structural ridges originally raised by tectonism.

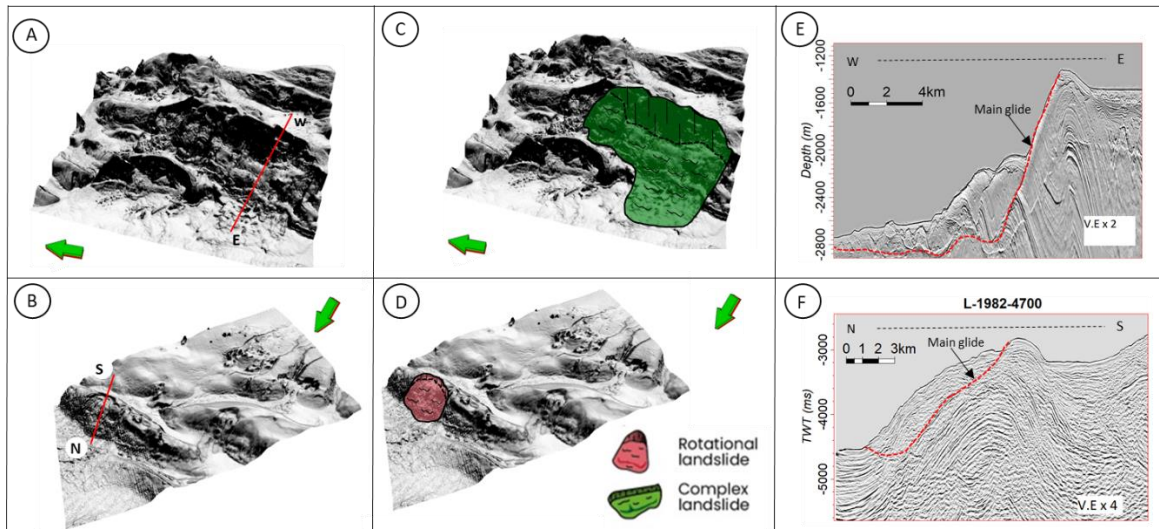


Figure. 11. Examples of submarine landslides in tectonically Controlled ridges. A) Bathymetry without interpretation showing structural ridges in the SSFB and location of seismic section presented in panel E. B) Bathymetry without interpretation showing rotational landslide affecting NSFb structural ridges. C) Bathymetry interpretation showing a complex landslide affecting structural ridges in the SSFB. D) Bathymetry interpretation showing a rotational landslide affecting a structural ridge in the NSFb. E) Seismic sections showing the main glide of the landslide interpreted in panel C. F) Seismic sections showing the main glide of the landslide are interpreted in panel D.

4.1.3. Submarine landslides in channel-levee systems.

Submarine landslides in channel-levee systems were mainly observed in the area influenced by the MFD. These present both translational and rotational dynamics and were detected in internal walls of channels and outer edges of levees. Since those are mainly disintegrative landslides (Idarraga J. and Vargas C, 2014), most of them do not preserve their displaced mass; on the contrary, only crown scarps are observed (Romero-Otero et al, 2015). Nonetheless, in some areas with high bathymetric resolution (15 m X 15 m) and 3D seismic information (Figure 6, Figure 13 A, C, E), it is possible to observe the effect of these landslides progressively widening channels and locally contributing to the filling inside them. So, they do not seem to be a significant source for large-scale MTCs reported in the MFD area (Ercilla et al, 2002b; Romero-Otero et al, 2015; Rincon et al, 2021; Lesly and mann, 2016; Ortiz-kraf, 2017).

4.1.4. Submarine landslides associated with the continental shelf break.

Submarine landslides associated with the continental shelf break are interpreted as debris flows (Rincon et al, 2021) or mixed slumps-turbidites-debrites (MSTD) (Alfaro and Holzt, 2014a). These were observed mainly in the continental shelf break, in front of the Morrosquillo Gulf (GdM) (Figure 2, Figure 13 B, D, F). These mass movements are considered to be the main source of the MTCs observed in intraslope sub-basins adjacent to the continental shelf break. They present horizontal displacements as long as 31 km; however, their horizontal displacements are stopped by structural ridges, and that is the reason why their mobility may be greater than the observed data.

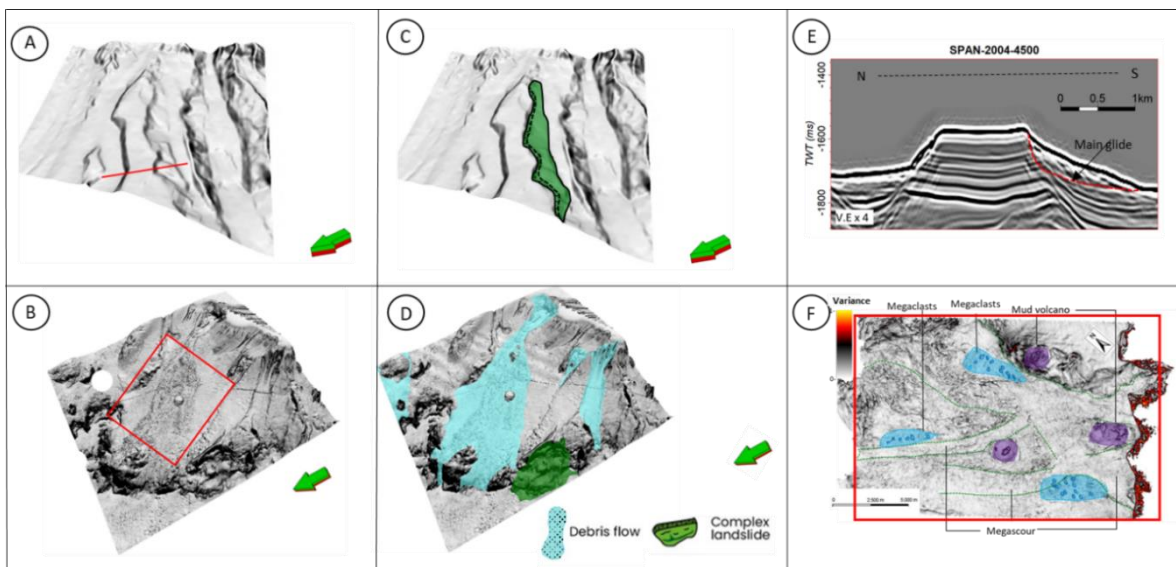


Figure. 12. Examples of submarine landslides in channel-levee systems and the continental shelf break. A) Bathymetry without interpretation showing channel-levee systems in the MFD and location of seismic section presented in panel E. B) hummocky appearance of debris flows associated with the continental shelf break and location of a seismic horizontal slide presented in panel F. C) Bathymetry interpretation showing landslides associated with channel-levee systems in the MFD. D) Bathymetry interpretation showing landslides associated with the continental shelf break. E) Seismic sections showing the main glide of the landslide interpreted in panel C. F) Interpreted horizontal slide highlighting megaclasts and mega scours observed in the variance attribute of a horizontal slide 100 ft below the seafloor (red box in panel B).

4.2. Insights on landslides size and their relation with MTCs

Cohesive landslides (translational, rotational, and complex) cover areas from 0.3 km² up to 209 km² and volumes between 0.004 km³ and 108 km³. Similarly, debris flow identified mainly in the southern region of the study area show areas ranging between 7 km² and 195 km². Otherwise, areas interpreted as MTCs in bathymetry

(Figure 2, Rincon et al., 2021) vary between 0.17km² to 1,540 km², alike the largest MTCs zone observed in the seismic record (Figure 9), whose area is around 1,200 km². The above supports that the dimensions of MTCs do not represent singular landslide movements appropriately (Mateus et al., 2021; Arthur and Gani., 2021). Our interpretation suggests that MTCs correspond to amalgamation events during periods with a high mass movement activity. Consequently, a hazard assessment should evaluate the potential for future movement by analyzing the observable individual events on the seafloor, likewise, those individualized events in the seismic record, but not the MTCs themselves, since their dimensions may overestimate the real material movement.

4.3. Submarine landslides susceptibility map

Table 2 presents the calculated W_i index carried out contrasting polygons representing landslides (Figure 2) and physical parameters such as i) bathymetric slope. ii) geomorphological interpretation. iii) presence of faults, and iv) natural seismicity (Figure 14). Due to their relevance in generating landslides (Borrell et al., 2016; Hearn et al., 2012; Hearn and Hart, 2011; Rapolla et al., 2012), the above-mentioned physical parameters, were selected. It was observed that landslides prevail on slopes greater than 10 °, showing the highest index (W_i) between 15 ° and 25° (Table 2). In this range, class density was greater than 0.4, that is, more than 40% of the area is affected by landslides. Regarding geomorphology, it was found that 38% of structural ridges and 16% of intraslope sub-basins are affected by landslides. These two groups are the most affected of all. In addition to the above, 21% of the area showing the presence of faults is affected by landslides. Finally, the connection between natural seismicity and the presence of landslides is not clear because of the difficulty of matching historical landslides to areas affected by the earthquakes recorded. Figure 15 presents a landslide susceptibility map for the study area. According to this, areas with less susceptibility (very low) occur in the continental rise where slopes less than 5 ° prevail, while areas with higher landslide susceptibility occur in structural ridges and adjacent intraslope sub-basin associated with SSFB and NSFB.

Table 4. Landslide Wi index. Wp=bathymetric index. Wf = presence of fault Wg = Geomorphological index. Ws = Natural seismicity index.

Factor: Slope gradient		Landslide area in class (Km ²)	Densclass	(Ws)
Class(°)	Class area (Km ²)			
0- 5	47068	1240,67	0,03	-1,05
5-10	7980,7	1442,93	0,18	0,88
10-15	2707,6	1001,1	0,37	1,59
15-20	1070	497,3	0,46	1,82
20-25	395,4	199,4	0,50	1,90
>25	249,43	98,6	0,40	1,66
TOTAL	59471,13	4480		

Factor: Fault		Landslide area in class (Km ²)	Densclass	(Wf)
Class	Area (Km ²)			
fault	2871	620	0,22	1,05
No fault	56600,13	3860	0,07	-0,10
Total	59471,13	4480		

Factor : Geomorphology		Landslide area in class (Km ²)	Densclass	(Wg)
Class	Class area (Km ²)			
Channalized systems (Channel-levee, Canyon, Gully, inter-channel ridge-Lobe)	10392,61	647,47	0,06	-0,19
Structural ridge, scarps	6316,62	2440,59	0,39	1,63
Intra slope basin	4684,50	786,69	0,17	0,80
Deep marine sedimentary systems (sediment waves, hemipelagic sediment, abandoned channel)	31416,74	119,86	0,00	-2,98
Continental slope hemipelagic sediments	6660,66	485,38	0,07	-0,03
TOTAL	59471,13	4480,00		

Factor: Earthquake influence		Landslide area in class (Km ²)	Densclass	(Ws)
Area affected by # Earthquake	Class area (Km ²)			
0 Earthquake	8903,19	673,59	0,08	0,00
1 Earthquake	38827,80	2213,83	0,06	-0,28
2 Earthquakes	5434,20	1293,01	0,24	1,15
5 Earthquakes	2678,25	65,38	0,02	-1,13
> 6 Earthquakes	3627,70	222,02	0,06	-0,21
TOTAL	59471,13	4467,83		

Total map Area (Km ²)	59471,13
Total Landslides (Km ²)	4480
Density map	0,08

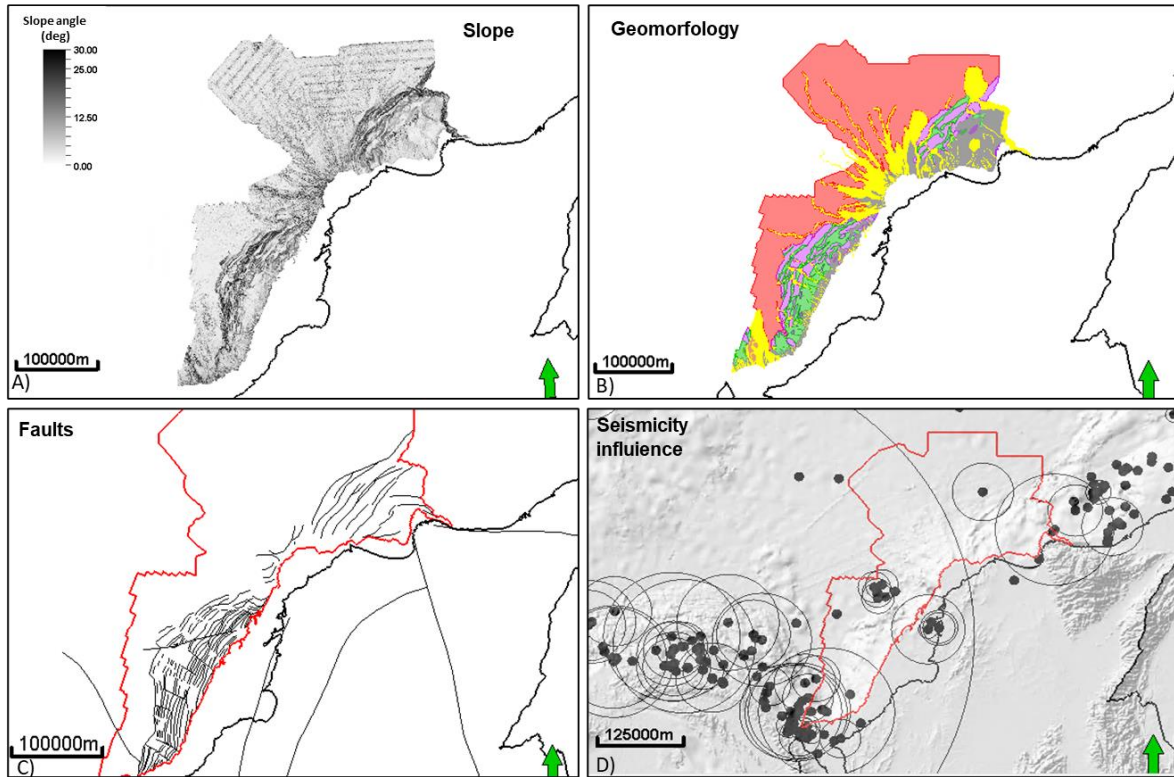


Figure. 13. Physical parameters are involved in the susceptibility assessment. A) The slope gradient taken from Rincon et al, (2021), was used. B) Geomorphology presented in Rincon et al, (2021) was grouped considering the genetic process as follows, i) Channeled flow systems (Channels, Canyons, Gullies, levees, inter-canyon ridges, and Lobes). ii) Structural ridge and escarpments. iii) Intra-slope sub-basins. iv) Deep marine sedimentary systems (sediment waves, hemipelagic sediments, abandoned channels). v) Continental slope hemipelagic deposits. C) Faults involved in the analysis were reported by Flinch et al., (2003) for the MFD, by Rodríguez et al., (2021) for the SSFB and by Galindo and Lonergan, (2020) for the NSFB. D) Areas influenced by natural seismicity (black circles) were estimated according to Keeper, D.K., (1984) methodology using earthquake epicenters (higher magnitudes than 3 on the Richter scale (black dots)) reported by the Colombian Geological Service (SGC) between 1993 and May 2019 (<https://www2.sgc.gov.co/sgc/sismos/Paginas/catalogo-sismico.aspx>).

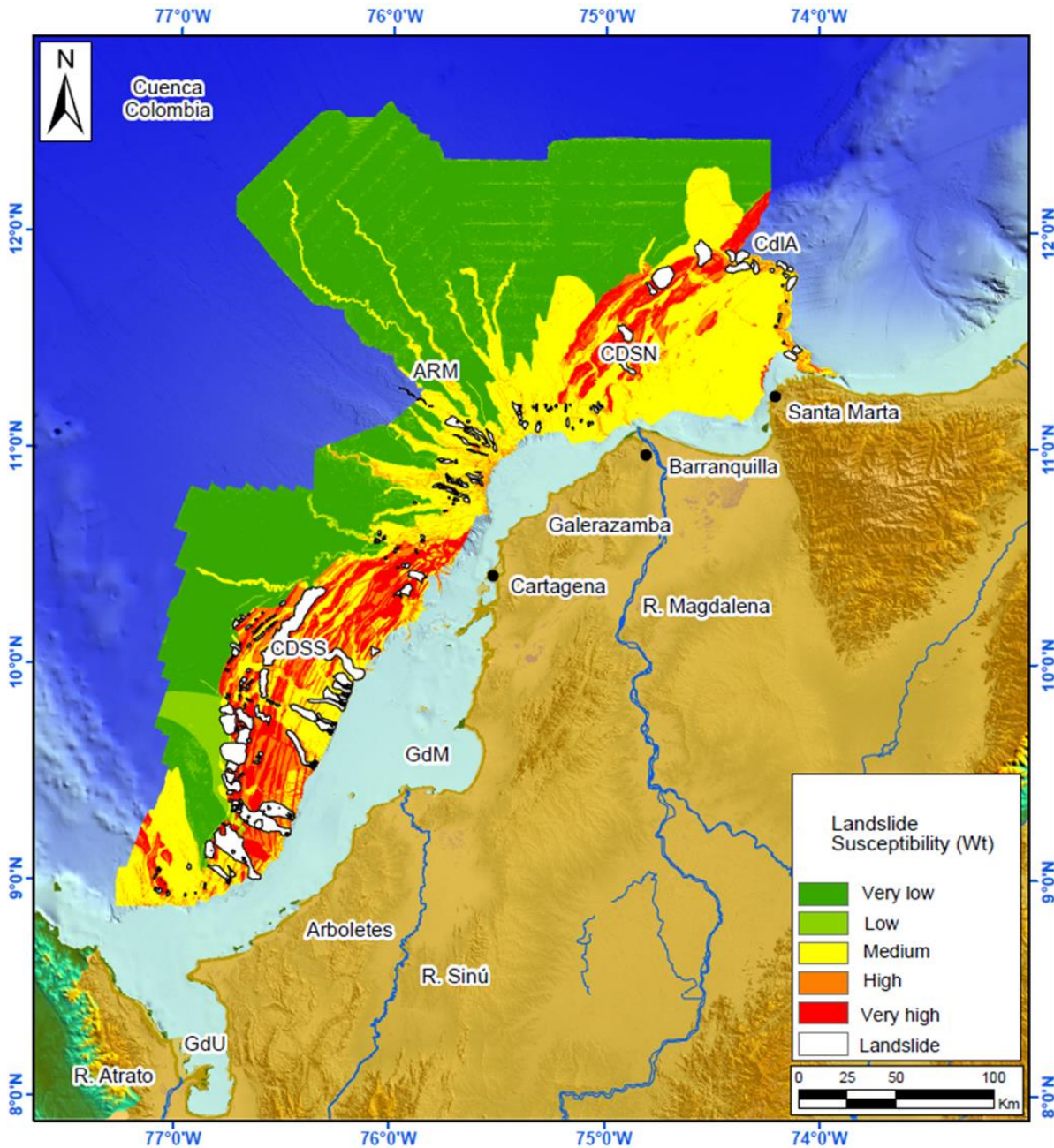


Figure. 14. Landslides Susceptibility map in the South Colombian Caribbean margin. The white polygons present the location of identify submarine landslides. The continental rise (green areas) where prevail slopes less than 5 ° present the lowest landslide susceptibility (very low). On the contrary, structural ridges and adjacent intraslope sub-basins associated with SSBF and NSFB present the highest landslide susceptibility (red areas). Channelized systems and hemipelagic sediments associated with the continental slope present a medium susceptibility to new landslides (yellow to orange areas).

5. CONCLUSIONS

The relief in the southern region of the Colombian Caribbean is the result of the interaction between geological factors such as structural deformation, continental sediments supply, ocean currents, and submarine landslides. Thus, in the areas where structural deformation prevails, the relief is dominated by structural ridges and intraslope sub-basins. Structural ridges are eroded by cohesive landslides that reach lengths up to 12.5 km and areas up to 209 km². Landslides are highly linked to the tectonic evolution of the NSFB and SSFB and contribute significantly to the filling of those intraslope sub-basins isolated from the continental shelf.

In Areas dominated by sediment supply, MFD, channeled systems and MTCs prevail. These MTCs are interpreted because mass movement accumulation originated both in the continental shelf break and in channel-levees systems. In contrast to what was observed in tectonically controlled zones, landslides do not limit their movement allowing the development of MTCs occupying large areas in the most distal channel-levée systems. Alike MFD, in front of the GdM (Figure 2), debris flows were observed associated with the continental shelf break reaching horizontal displacements that exceed 31 km, which indicates their high mobility. MTCs have overfilled intraslope sub-basins allowing sediments transport from the continental shelf to the deepest areas of the Colombia basin, where the biggest MTCs zone observed reaches an area up to 1,200 km² and 183 km³ volume.

Analysis of the relation between the BSR and landslide occurrence made it possible to suggest that there is not a remarkable causal association between hydrate dissociation and landslide events in the study zone. Otherwise, two processes are suggested as the main submarine landslide trigger mechanisms: First, overstepped slopes associated with the SSFB and NSFB result in rotational and translational individual landslides. These individual events then become complex landslide zones along structural ridges. Second, the continental shelf break erosion by debris flows which feed MTCs. Those MTCs fill intraslope sub-basins in the continental slope as flat areas in the continental rise.

Preliminary analyses of landslides suggest that structural ridges and adjacent intraslope sub-basins present the greatest potential to be affected by new landslides. Susceptibility increases with the presence of geological faults. The main hazards associated with submarine landslides, on the continental slope of the Colombian southern Caribbean margin are given: i) Cohesive landslides affecting areas at distances less than 4 km from the structural ridges of the NSFB and SSFB. ii) Debris flows originated from the continental shelf break in the MFD as in the SSFB (Figure 2). These mass movements can move tens of kilometers on the continental slope and eventually reach up to the continental rise. iii) remobilization of MTCs may occur in zones corresponding to the bottom of the Colombia basin.

The main limitation for the understanding of submarine landslides in the study zone is the lack of information about the frequency of occurrence of distinct types of landslides.

This would require the acquisition of new specialized data, such as deep piston core, underwater vehicle campaigns (Gliders / AUV / ROV), and seismic and high-resolution bathymetry in different periods. Likewise, computerized, and experimental modeling of these submarine landslides may allow obtaining movement predictive models to evaluate hazards in the southern Colombian Caribbean margin.

ACKNOWLEDGMENTS

This work was undertaken as part of Royal Academy of Engineering - Newton Fund grant IAPP1617/112 and the agreement FP44842-2017 Doctorado Empresa, ECOPETROL, EAFIT, COLCIENCIAS (MINTIC). Data were provided by Ecopetrol.

REFERENCES

Abella, E.A.C., Van Westen, C.J., 2007. Generation of a landslide risk index map for Cuba using spatial multi-criteria evaluation. *Landslides* 4, 311–325. <https://doi.org/10.1007/s10346-007-0087-y>

- Adams, M., 2020. Shell, Ecopetrol to develop gas province in Colombian Caribbean. OIL Gas J. 1. <https://doi.org/10.1017/CBO9781107415324.004>
- Alfaro, E., Holz, M., 2014a. Seismic geomorphological analysis of deepwater gravity-driven deposits on a slope system of the southern Colombian Caribbean margin. Mar. Pet. Geol. 57, 294–311. <https://doi.org/10.1016/j.marpetgeo.2014.06.002>
- Alfaro, E., Holz, M., 2014b. Review of the chronostratigraphic charts in the Sinú-San Jacinto basin based on new seismic stratigraphic interpretations. J. South Am. Earth Sci. 56, 139–169. <https://doi.org/10.1016/j.jsames.2014.09.004>
- ANH, 2018. Confirmada presencia de gas en aguas ultra profundas del Caribe colombiano.
- Arikawa T., Muhari A., Okumura Y., Dohi Y., Afriyanto B., Sujatmiko K.A. & Imamura F. 2018. Coastal subsidence induced several tsunamis during the 2018 sulawesi earthquake. Journal of Disaster Research, 13, sc20181204, <https://doi.org/10.20965/jdr.2018.sc20181204>
- Arthur, M., Gani, M., 2021. Submarine channel and lobe hidden inside mass-transport deposits in the northern Gulf of Mexico. Results in Geophysical Sciences. 5. 100013. [10.1016/j.ringsps.2021.100013](https://doi.org/10.1016/j.ringsps.2021.100013).
- Bell, K.L., Carey, S.N., Nomikou, P., Sigurdsson, H., Sakellariou, D., 2013. Submarine evidence of a debris avalanche deposit on the eastern slope of Santorini volcano, Greece. Tectonophysics 597–598, 147–160. <https://doi.org/10.1016/j.tecto.2012.05.006>
- Bernal-Olaya, R., Mann, P. y Vargas, C.A. (2015a). Earthquake, Tomographic, Seismic Reflection, and Gravity Evidence for a Shallowly Dipping Subduction Zone beneath the Caribbean Margin of Northwestern Colombia. En: Memoir 108: Petroleum Geology and Potential of the Colombian Caribbean Margin (247-270). <https://doi.org/10.1306/13531939m1083642>
- Bornhold, B.D., Johns, M.W., 1984. Depositional Characteristics of a Submarine Debris Flow Author. J. Geol. 92, 707–727.
- Borrell, N., Somoza, L., León, R., Medialdea, T., Gonzalez, F.J., Gimenez-Moreno, C.J., 2016. GIS Catalogue of Submarine Landslides in the Spanish Continental Shelf: Potential and Difficulties for Susceptibility Assessment, in: Submarine Mass Movements and Their Consequences, Advances in Natural and Technological Hazards Research 41. pp. 499–508. https://doi.org/10.1007/978-3-319-20979-1_50
- Cadena, A.F., Romero, G. y Slatt, R., 2015. Application of Stratigraphic Grade Concepts to Understand Basin-fill Processes and Deposits in an Active Margin Setting, Magdalena Submarine Fan and Associated Fold-and-Thrust

- Belts, Offshore Colombia. En: Memoir 108: Petroleum Geology and Potential of the Colombian Caribbean Margin (323-344). <https://doi.org/10.1306/13531942M1083646>
- Carter, L., Milliman, J.D., Talling, P.J., Gavey, R., Wynn, R.B., 2012. Near-synchronous and delayed initiation of long run-out submarine sediment flows from a record-breaking river flood, offshore Taiwan. *Geophys. Res. Lett.* 39. <https://doi.org/10.1029/2012GL051172>
- Clare, M.A., Le Bas, T., Price, D.M., Hunt, J.E., Sear, D., Cartigny, M.J.B., Vellinga, A., Symons, W., Firth, C., Cronin, S., 2018. Complex and Cascading Triggering of Submarine Landslides and Turbidity Currents at Volcanic Islands Revealed From Integration of High-Resolution Onshore and Offshore Surveys. *Front. Earth Sci.* 6, 1–24. <https://doi.org/10.3389/feart.2018.00223>
- Casalbore, D., Bosman, A., Casas, D., Chiocci, F., Martorelli, El., Domenico, R., 2019. Morphological Variability of Submarine Mass Movements in the Tectonically–Controlled Calabro–Tyrrhenian Continental Margin (Southern Italy). *Geosciences.* 9. 43. <https://doi.org/10.3390/geosciences9010043>.
- Corredor, F. 2003. Seismic strain rates and distributed continental deformation in the northern Andes and three-dimensional seismotectonics of northwestern South America. *Tectonophysics*, 372, 147–166. [https://doi.org/10.1016/S0040-1951\(03\)00276-2](https://doi.org/10.1016/S0040-1951(03)00276-2).
- Cortés, M. y Angelier, J. (2005). Current states of stress in the northern Andes as indicated by focal mechanisms of earthquakes. *Tectonophysics*, 403, 29–58. <https://doi.org/10.1016/j.tecto.2005.03.020>
- Cruden, D., Varnes, D., 1996. Landslides: Investigation and Mitigation. Chapter 3 - Landslide Types and Processes. *Transp. Res. Board Spec. Rep.*
- Devoli, G., Morales, A., Høeg, K., 2007. Historical landslides in Nicaragua-collection and analysis of data. *Landslides* 4, 5–18. <https://doi.org/10.1007/s10346-006-0048-x>
- Duque-Caro, H. 1979. Major structural elements and evolution of northwestern Colombia. En: Watkins, J.S., Montadert, L, y Dickerson, P.W. Memoir 29: Geological and Geophysical Investigations of Continental Margins. AAPG. <https://doi.org/10.1306/M29405C22>
- Duque-Caro, H. (1990). The choco block in the northwestern corner of South America: Structural, tectonostratigraphic, and paleogeographic implications, *Journal of South American Earth Sciences*, [https://doi.org/10.1016/0895-9811\(90\)90019-W](https://doi.org/10.1016/0895-9811(90)90019-W).

- Ercilla, G., Wynn, R. B., Alonso, B. y Baraza, J. (2002b). Initiation and evolution of turbidity current sediment waves in the Magdalena turbidite system. *Marine Geology* 192, 153-169.
- Flinch, J.F., Amaral, J., Doulcet, A., Mouly, B., Osorio, C., Pince, J.M., 2003. Structure of the Offshore Sinu Accretionary Wedge. Northern Colombia. VIII Simp. Boliv. - Explor. Pet. en las Cuencas Subandinas 76–83. <https://doi.org/10.1088/0953-8984/26/4/045302>
- Frey-Martínez, J., Cartwright, J., James, D., 2006. Frontally confined versus frontally emergent submarine landslides: A 3D seismic characterisation. *Marine and Petroleum Geology* 23, 585–604. <https://doi.org/10.1016/j.marpetgeo.2006.04.002>
- Frey-Martinez, J., 2010. 3D Seismic Interpretation of Mass Transport Deposits: Implications for Basin Analysis and Geohazard Evaluation, in: *Submarine Mass Movements and Their Consequences*, 553 *Advances in Natural and Technological Hazards Research*.
- Galindo, P., Lonergan, L., 2020. Basin evolution in an oblique subduction setting. Bahia Basin, Colombian Caribbean margin. *Tectonics*.
- GEBCO 2020. The GEBCO_2020 Grid - a continuous terrain model of the global oceans and land. British Oceanographic Data Centre. <https://doi.org/10.5285/a29c5465-b138-234d-e053-6c86abc040b9>.
- Glimsdal, S., L'Heureux, J.S., Harbitz, C.B., Løvholt, F., 2016. The 29th January 2014 submarine landslide at Statland, Norway—landslide dynamics, tsunami generation, and run-up. *Landslides* 13, 1435–1444. <https://doi.org/10.1007/s10346-016-0758-7>
- Green, A., and R. Uken, 2008, Submarine landsliding and canyon evolution on the northern KwaZulu-Natal continental shelf, South Africa, SW Indian Ocean: *Marine Geology*, 254, no. 2–3, 152–170, <https://doi.org/10.1016/j.margeo.2008.06.001>.
- Hampton, M.M. a. M., Lee, H.H.J., Locat, J., Bmar, S.U., Dsli, N.E., Hampton, M.M. a. M., Lee, H.H.J., Locat, J., Geological, U.S., Park, M., 1996. Submarine landslides. *Geophysics* 34, 35–59. <https://doi.org/10.1029/95rg03287>
- Hasegawa, H.S., kanamori, H., 1987. Source mechanism of the magnitude 7.2 grand banks earthquake of november 1929: double couple or submarine landslide? *Bull. Seismol. Soc. Am.* 77, 1984–2004. <https://doi.org/10.1190/1.1443742>
- He, Y., Zhong, G., Wang, L., Kuang, Z., 2014. Characteristics and occurrence of submarine canyon-associated landslides in the middle of the northern continental slope, South China Sea. *Mar. Pet. Geol.* <https://doi.org/10.1016/j.marpetgeo.2014.07.003>

- Hearn, G., Wise, D., Hart, A., Morgan, C., O'Donnell, N., 2012. Assessing the potential for future first-time slope failures to impact the oil and gas pipeline corridor through the Makarov Mountains, Sakhalin Island, Russia. *Q. J. Eng. Geol. Hydrogeol.* <https://doi.org/10.1144/1470-9236/10-033>
- Hearn, G.J., Hart, A.B., 2011. Geomorphological contributions to landslide risk assessment: Theory and practice. *Dev. Earth Surf. Process.* <https://doi.org/10.1016/B978-0-444-53446-0.00005-7>
- Heidarzadeh, M., Tappin, D.R., Ishibe, T., 2019. Modeling the large runup along a narrow segment of the Kaikoura coast, New Zealand following the November 2016 tsunami from a potential landslide. *Ocean Eng.* 175, 113–121. <https://doi.org/10.1016/j.oceaneng.2019.02.024>
- Heidarzadeh M., Muhari A. & Wijanarto A. 2018. Insights on the Source of the 28 September 2018 Sulawesi Tsunami, Indonesia Based on Spectral Analyses and Numerical Simulations. *Pure and Applied Geophysics*, 176, <https://doi.org/10.1007/s00024-018-2065-9>
- Highland, L.M., Bobrowsky, P., 2008. The Landslide Handbook — A Guide to Understanding Landslides. *Landslides* 28, 129. <https://doi.org/Circular 1325>
- Idarraga, J., Vargas, C.A., 2014. Morphological Expression of Submarine Landslides in the Accretionary Prism of the Caribbean Continental Margin of Colombia. *Submar. Mass Movements Their Consequences. Adv. Nat. Technol. Hazards Res. 6th Int. Symp. Vol. 37* 37, 391–401. https://doi.org/10.1007/978-3-319-00972-8_35
- Idárraga-García, J., Masson, D. G., García, J., León, H. y Vargas, C. A. 2019. Architecture and development of the Magdalena submarine fan (southwestern Caribbean). *Marine Geology*, 414, 18–33.
- INVEMAR & ANH, 2010. Biodiversidad del Margen Continental del Caribe Colombiano. *Ser. publicaciones especies* 20, 457.
- Kayen, R. E. and H. J. Lee, 1993, Slope stability in regions of sea-floor gas hydrate: Beaufort Sea continental slope. In W.C. Schwab, H.J. Lee, D.C. Twichell, eds., 2002, *Submarine landslides: selected studies in the U.S. exclusive economic zone: U.S. Geological survey bulleting*, 97-103.
- Keeper, D.K., 1984. *Geological Society of America Bulletin* Landslides caused by earthquakes. [https://doi.org/10.1130/0016-7606\(1984\)95<406](https://doi.org/10.1130/0016-7606(1984)95<406)
- Kvemvolden, K. A., 1993, Gas hydrates – geological perspective and global change: *Reviews of geophysics*, 31, 173-187.
- Kopf, A.J., Kasten, S., Bles, J., 2010. Geochemical evidence for groundwater-charging of slope sediments: The nice airport 1979 landslide and tsunami

- revisited. *Submar. Mass Movements Their Consequences - 4th Int. Symp.* 28, 203–214. https://doi.org/10.1007/978-90-481-3071-9_17.
- Lamarche, G., J. Mountjoy, S. Bull, T. Hubble, S. Krastel, E. Lane, A. Micallef, L. Moscardelli, C. Mueller, I. Pecher, and S. Woelz, 2016, Submarine mass movements and their consequences: progress and challenges, in G. Lamarche, G., J. Mountjoy, S. Bull, T. Hubble, S. Krastel, E. Lane, A. Micallef, L. Moscardelli, C. Mueller, I. Pecher, and S. Woelz, eds., *Submarine mass movements and their consequences – 7th International Symposium*: Springer, 41,1-13.
- Lastras, G., Del Blasio, F.V., Canals, M., Elverhøi, A., 2005. Conceptual and numerical modeling of the BIG'95 debris flow, western Mediterranean Sea. *J. Sediment. Res.* 75, 784–797. <https://doi.org/10.2110/jsr.2005.063>
- Leal Niño, C.A., 2019. La gran provincia gasífera del Caribe. *La Repub.*
- Leslie, S.C., Mann, P., 2016. Giant submarine landslides on the Colombian margin and tsunami risk in the Caribbean Sea. *Earth Planet. Sci. Lett.* 449, 382–394. <https://doi.org/10.1016/j.epsl.2016.05.040>
- Locat, J., Lee, H., 2009. *Submarine Mass Movements and Their Consequences: An Overview* 6 115–116.
- Martelloni, G., Segoni, S., Fanti, R., Catani, F., 2012. Rainfall thresholds for the forecasting of landslide occurrence at regional scale. *Landslides* 9, 485–495. <https://doi.org/10.1007/s10346-011-0308-2>
- Mateus Tarazona, D., Prieto J. A., Murphy, W., Naranjo Vesga, J. Identification of submarine landslides in the Colombian Caribbean Margin (Southern Sinú Fold Belt) using seismic investigations. *The Leading Edge* 2021;; 40 (12): 914–922. doi: <https://doi.org/10.1190/tle40120914.1>
- Martinez, J.A., Castillo, J., Ortiz-Karpf, A., Rendon, L., Mosquera, J.C., Vega, V., 2015. Deep Water Untested Oil-play in the Magdalena Fan, Caribbean Colombian Basin, in: Bartolini, C., Mann, P. (Eds.), *Petroleum Geology and Potential of the Colombian Caribbean Margin*. American Association of Petroleum Geologists, Memoir 108, pp. 251–260. <https://doi.org/10.1306/13531955m1083658>
- Masson, D., Harbitz, C., Wynn, R., Pedersen, G., Løvholt, F., 2006. Submarine landslides: processes, triggers and hazard prediction. *Philos. Trans. R. Soc. A Math. Phys. Eng. Sci.* 364, 2009–2039. <https://doi.org/10.1098/rsta.2006.1810>
- McAdoo, B.G., Pratson, L.F., Orange, D.L., 2000. Submarine landslide geomorphology, US continental slope. *Mar. Geol.* [https://doi.org/10.1016/S0025-3227\(00\)00050-5](https://doi.org/10.1016/S0025-3227(00)00050-5)

- Morley, C.K., Leong, L.C., 2008. Evolution of deep-water synkinematic sedimentation in a piggyback basin, determined from three-dimensional seismic reflection data. *Geosphere* 4, 939–962. <https://doi.org/10.1130/GES00148.1>
- Moscardelli, L., 2016. IGCP-640 – S4SLIDES- Significance of Modern and Ancient Subaqueous Slope Landslide Systems 614–615.
- Moscardelli, L., Wood, L., 2008. New classification system for mass transport complexes in offshore Trinidad. *Basin Res.* 20, 73–98. <https://doi.org/10.1111/j.1365-2117.2007.00340.x>
- Moscardelli, L., Wood, L., Mann, P., 2006. Mass-transport complexes and associated processes in the offshore area of Trinidad and Venezuela 7, 1059–1088. <https://doi.org/10.1306/02210605052>
- Mulder, T., Cochonat, P., 1996. Classification of offshore mass movements. *J. Sediment. Res.* <https://doi.org/10.1306/D42682AC-2B26-11D7-8648000102C1865D>
- Nadim, F., Kjekstad, O., Peduzzi, P., Herold, C., Jaedicke, C., 2006. Global landslide and avalanche hotspots. *Landslides* 3, 159–173. <https://doi.org/10.1007/s10346-006-0036-1>
- Naranjo-Vesga, J., Ortiz-Karpf, A., Wood, L., Jobe, Z., Paniagua-Arroyave, J.F., Shumaker, L., Mateus-Tarazona, D., Galindo, P., 2020. Regional controls in the distribution and morphometry of deep-water gravitational deposits along a convergent tectonic margin. Southern Caribbean of Colombia. *Mar. Pet. Geol.* 121, 1–30. <https://doi.org/10.1016/j.marpetgeo.2020.104639>
- Ortiz-Karpf, A., Hodgson, D.M., McCaffrey, W.D., 2015. The role of mass-transport complexes in controlling channel avulsion and the subsequent sediment dispersal patterns on an active margin: The Magdalena Fan, offshore Colombia. *Mar. Pet. Geol.* 64, 58–75. <https://doi.org/10.1016/j.marpetgeo.2015.01.005>
- Ortiz-Karpf, A., Hodgson, D.M., Jackson, C.A.-L. y McCaffrey, W.D. (2017). Influence of seabed morphology and substrate composition on mass-transport flow processes and pathways: Insights from the Magdalena Fan, Offshore Colombia. *Journal of Sedimentary Research*, 87, 189-209. <https://doi.org/10.2110/jsr.2017.10>
- Pindell, J.L. y Kennan, L. (2009). Tectonic evolution of the Gulf of Mexico, Caribbean and northern South America in the mantle reference frame: an update. *The Geological Society*, 328, 1-55. <https://doi.org/10.1144/sp328.1>

- Randolph, M.F., White, D.J., 2012. Interaction forces between pipelines and submarine slides - A geotechnical viewpoint. *Ocean Eng.* 48, 32–37. <https://doi.org/10.1016/j.oceaneng.2012.03.014>
- Rapolla, A., Di Nocera, S., Matano, F., Paoletti, V., Tarallo, D., 2012. Susceptibility regional zonation of earthquake-induced landslides in Campania, Southern Italy. *Nat. Hazards* 61, 115–126. <https://doi.org/10.1007/s11069-011-9790-z>
- Restrepo-Correa, I.C. y Ojeda, G.Y. (2010). Geologic controls on the morphology of La Aguja submarine canyon. *Journal of South American Earth Sciences*, 29, 861–870. <https://doi.org/10.1016/j.jsames.2010.07.001>
- Rincón, D. A., J. F. Naranjo, D. Mateus Tarazona, C. A. Hernández, H. D. Madero, J. De Bedout, A. Ortiz-Karpi, F. E. Malagón and C. O. Cabrera, 2021, Geomorfología del fondo marino profundo en la región sur del Caribe Colombiano: Instituto Colombiano del Petróleo, <https://doi.org/10.29047/9789589287361>.
- Rincón-Martínez, D., Ruge, S. M., & Silva Arias, A. (2022). Seismic analysis of the geological occurrence of gas hydrate in the Colombian Caribbean offshore. *Journal of South American Earth Sciences*, 116(April), 103800. <https://doi.org/10.1016/j.jsames.2022.103800>.
- Rodríguez, I., Bulnes, M., Poblet, J., Masini, M., Flinch, J., 2021. Structural style and evolution of the offshore portion of the Sinu Fold Belt (South Caribbean Deformed Belt) and adjacent part of the Colombian Basin. *Mar. Pet. Geol.* 125, 104862. <https://doi.org/10.1016/j.marpetgeo.2020.104862>
- Romero-Otero, G. A., 2009, Deepwater sedimentary processes in an active margin, Magdalena submarine fan, offshore Colombia: PhD Thesis, University of Oklahoma.
- Romero-Otero, G.A., Slatt, R.M. y Pirmez, C. (2015). Evolution of the Magdalena Deepwater Fan in a Tectonically Active Setting, Offshore Colombia. *Memoir 108: Petroleum Geology and Potential of the Colombian Caribbean Margin* (675–707). <https://doi.org/10.1306/13531953m1083656>
- Ruiz, C., Davis, N., Bentham, P., Price, A., Carvajal, D., 2000. Structure and tectonic evolution of the South Caribbean Basin, Southern Offshore Colombia: a progressive accretionary prism. *VII Simp. Boliv. - Explor. Pet. en las Cuencas Subandinas* 22.
- Sanchez, J., Mann, P., Carvajal-Arenas, L.C., Bernal-Olaya, R., 2019. Regional transect across the western Caribbean Sea based on integration of geologic, seismic reflection, gravity, and magnetic data. *Am. Assoc. Pet. Geol. Bull.* 103, 303–343. <https://doi.org/10.1306/05111816516>

- Serey, A., Sepúlveda, S.A., Murphy, W., Petley, D.N., De Pascale, G. Developing conceptual models for the recognition of coseismic landslides hazard for shallow crustal and megathrust earthquakes in different mountain environments – an example from the Chilean Andes. *Quarterly Journal of Engineering Geology and Hydrogeology*, 54, qjegh2020-023, 22 September 2020, <https://doi.org/10.1144/qjegh2020-023>
- Scarselli N., 2020. Chapter 16 - Submarine landslides – architecture, controlling factors and environments. A summary. In Scarselli, N., Adam, J., Chiarella, D., Roberts, D.G., Bally, A.W. *Regional Geology and Tectonics (Second Edition)*. Elsevier, 417-439, <https://doi.org/10.1016/B978-0-444-64134-2.00015-8>.
- Shanmugam, G., 2016. Slides, Slumps, Debris Flows, Turbidity Currents, and Bottom Currents.
- Shanmugam, G., Wang, Y., 2015. The landslide problem. *J. Palaeogeogr.* 4, 109–166. <https://doi.org/10.3724/SP.J.1261.2015.00071>
- Shepard, F. P. (1973). Seafloor off Magdalena Delta and Santa Marta area, Colombia. *Geological Society of America Bulletin* 84, 1955-1972.
- Symithe, S., Calais, E., Chabaliere, J.B. De, Robertson, R. y Higgins, M. 2015. Journal of Geophysical Research: Solid Earth Current block motions and strain accumulation on active faults in the Caribbean. *JGR Earth*, 3748-3774. <https://doi.org/10.1002/2014JB011779>.
- Tappin, D.R., 2010. Mass transport events and their tsunami hazard. *Submar. Mass Movements Their Consequences - 4th Int. Symp.* 28, 667–684. https://doi.org/10.1007/978-90-481-3071-9_54
- Tappin, D.R., Watts, P., McMurtry, G.M., Lafoy, Y., Matsumoto, T., 2001. The Sissano, Papua New Guinea tsunami of July 1998 - Offshore evidence on the source mechanism. *Mar. Geol.* 175, 1–23. [https://doi.org/10.1016/S0025-3227\(01\)00131-1](https://doi.org/10.1016/S0025-3227(01)00131-1)
- Tappin D.R. 2017. Tsunamis from submarine landslides. *Geology Today*, 33, 190–200, <https://doi.org/10.1111/gto.12200>
- Ter-Stepanian, G., 1977. TYPES OF COMPOUND AND COMPLEX LANDSLIDES. *Bull. Int. Assoc. Eng. Geol.* 16, 72–74.
- Vanneste, M., Forsberg, C.F., Glimsdal, S., Harbitz, C.B., Issler, D., Kvalstad, T.J., Løvholt, F., Nadim, F., 2013. Submarine landslides and their consequences: What do we know, what can we do? *Landslide Sci. Pract. Complex Environ.* 5, 5–17. <https://doi.org/10.1007/978-3-642-31427-8-1>

- Van Westen, C.J., 1997. Statistical landslide hazard analysis. ILWIS 2.1 for Windows application guide. ITC Publ. 2, 73–84.
- Varnes, D.J., 1978. Landslide Types and Processes. Highw. Res. Board Spec. Rep. 1–4.
- Vinnels, J.S., Butler, R.W.H., McCaffrey, W.D., Paton, D.A., 2010. Depositional processes across the Sinú Accretionary Prism, offshore Colombia. *Mar. Pet. Geol.* 27, 794–809. <https://doi.org/10.1016/j.marpetgeo.2009.12.008>
- Wu, X., Q. Liang, Y. Ma, Y. Shi, Z. Xia, L. Liu and M. Haeckel. Submarine landslides and their distribution in the gas hydrate area on the North Slope of the South China Sea: *Energies*, 11, 3481.

CHAPTER 3:

OVERPRESSURE IN THE SINÚ OFFSHORE BASIN, KNOWLEDGE, AND UNCERTAINTIES

This work was presented as: D. Mateus., M. Garcia., L Montilla. Overpressure in the Sinú Offshore basin. Knowledge and Uncertainties. Oral presentation at the 2022 AAPG International Conference and Exhibition (ICE), Cartagena, Colombia. 19–22 April 2022.

ABSTRACT

Pore pressure prediction is a critical issue in offshore operations due to the risks of causing loss of well control. The loss of well control can impact both the environment and the finance of companies, as well as a highly sensitive issue such as the safety of people in this type of operation. Between 1980 and 2015, more than 400 deaths have been associated with problems of well control that occurred in offshore operations. Consequently, the understanding of overpressures is a topic of the greatest relevance.

In the Colombian Caribbean margin, wells have experienced hydrostatic conditions and overpressures with values up to 12 ppg in most cases, but overpressure conditions above 15 ppg, which are considered very high, have also been observed.

This work summarizes the observations on overpressure made from the analysis of well data, seismic data, and basin modeling in the Sinú Offshore Basin.

We found that wells with the highest overpressures (greater than 15 ppg) are located in the south of the Sinú Offshore Basin. On the other hand, wells located in the northern area of the basin showed lower overpressure conditions (less than 15 ppg). We also notice that main zones of overpressure have been observed below a Pliocene-Pleistocene discordant level. despite that, we found evidence to conclude that this surface is not an absolute reference to identify the areas of overpressure. Finally, we suggest the distribution of overpressures seems to be affected not only by sub-compaction but also by the high tectonic compression setting.

This work improves the understanding of the distribution of overpressures in sedimentary sequences in the Sinú Offshore basin and presents those uncertainties that remain latent and await further studies leading to likely conclusive statements.

Keywords: Overpressure, Sinú offshore basin.

1. INTRODUCTION

Overpressures are part of the offshore geohazards that can affect operations (NGI, 2005). These Geohazards range from the shallow ones, such as landslides and flows to subsurface ones, within which overpressures are found, certainly being the main reason for this study.

Problems related to overpressures can trigger Loss of Well Control (LWC). The loss of well control can impact both the environment (when oil spills are produced) and the finance of companies, as well as a highly sensitive issue such as the safety of people in this type of operation. According to a study made by Holland (Holland, 2017), it is summarized that between 1980 and 2015, more than 400 deaths have been associated with problems of well control that occurred in offshore operations.

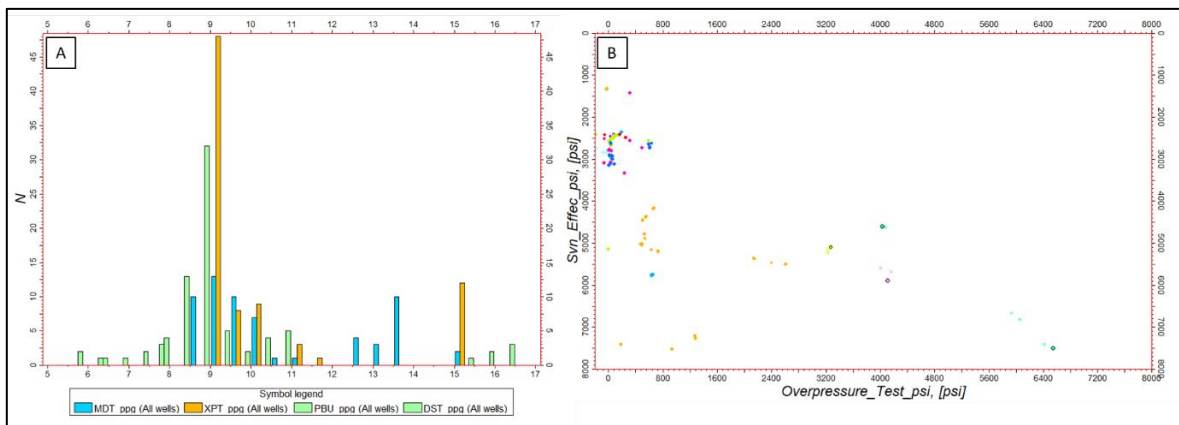


Figure. 13. Overpressure range according to well tests in the Colombian Caribbean Offshore. A) Frequency histogram showing pressure test in field-scale pound per gallon (ppg). Note that most of the tests range between 8 ppg and 12 ppg. However, values exceeding 15 ppg are also observed. B) Total overpressure on a scale of psi. Maximum values of excess pressure exceed 6000 psi.

Regarding the evidence of overpressures in the Caribbean, the frequency histogram (Figure 1) presents those wells which have been drilled in the Caribbean and already have pressure tests as well. The information shows that wells have experienced hydrostatic conditions and overpressures with values up to 12 ppg in most cases, but overpressure conditions above 15 ppg, which are considered very high, have also been observed. Likewise, by looking at the range of total

overpressures (Figure 1B), it is evident that most wells have overpressures below 800 psi, but in some cases, these can reach values exceeding 6,000 psi.

1.1. Theoretical frame

Methodologies for estimating pore pressure fall into three broad categories as follows: In the first category can be grouped conventional methodologies that are based on Terzaghi's general relationship (Terzaghi et al., 1996) (eq. 1). According to this relationship, total stress is seen as the weight on a point in depth which will be distributed, partly as effective stress and partly as pore pressure. The effective stress is the stress that is transmitted from grain to grain on the rock structure and the pore pressure is the part of the total weight receiving the fluids.

Early works based on Terzaghi's general relationship were carried out between the 1950s and 1970s using well logs to find an explanation for the high pressures in Louisiana fields, United States (Eaton, 1975; Fertl and Timko, 1971; Foster, J.B; Whalen, 1966; George Dickinson, 1953; Hottmann and Johnson, 1965; Hubbert and Rubey, 1959) Afterward, advances in seismic processing and new acquisitions technology allowed other authors to implement methods involving sound velocity (Bowers, 1995; Weakley, 1991). All these methods have a basic equation shape, in which the effective stress in the overpressured zone is represented by a univariable or multivariable exponential function, as shown in the Eq.(2) - (4), (Gutierrez et al., 2006). The main advantage of these equations is the use of typically available information in the petroleum industry, for example, well logs, seismic data, and drilling data.

$$\sigma = \sigma' + Pp \quad (1)$$

$$\sigma' = f(Vel) = a * Vel^b \quad (2)$$

$$\sigma' = f(Vel) = a * \ln Vel^b \quad (3)$$

$$\sigma' = f(Vel, T, \phi) = \sigma_0 e^{\left[- \left(\frac{\phi}{1-\phi} \right) * \frac{A(T)}{B(t)} \right]} \quad (4)$$

The second category consists of methods based on rock physics. These methods link wave propagation equations, and Hooke's law to get an estimation of pore pressure in sedimentary rocks (Carcione et al., 2003; Dvorkin, 2002).

The third group consists of methods based on basin modeling concepts. These methods consider the dynamic characteristics of the overpressure phenomenon involving rock permeability, and consequently, the ability of it to dissipate overpressures. (Borge, 2000; Mann and Mackenzie, 1990; Xiaorong et al., 2006; Xiaorong Luo and Vasseur, 1992) The latter included the interaction between the mechanisms of generation, distribution, and dissipation of pressures over geological time on a sedimentary basin scale.

The basic equation of pressure generation in basin modeling methods is the mathematical solution of Terzaghi, 1948 (Terzaghi et al., 1996) eq. (5). This differential equation is linear for the pore pressure variable; consequently, superposition of several overpressure mechanisms is admitted by adding them to the solution.

$$\frac{\partial \mu}{\partial t} = C_v * \frac{\partial^2 \mu}{\partial y^2} \quad (5)$$

The work published by Lou (Xiaorong Luo and Vasseur, 1992) reported one of the most complete differential equations, eq. (6) to represent the overpressure phenomenon. It considers the effects of thermal expansion and the ability of the rock to expel fluids. This model has been incorporated as the basis of the most recent algorithms for pore pressure prediction in basin modeling. This equation represents the balance between the cause of overpressure terms (e.g. compaction, change in temperature, etc.) and the diffusion terms. Letter q represents additional mechanisms that may be added.

$$\left(\phi \dot{B} + \frac{\alpha_\phi}{(1-\phi)} \right) \frac{dP}{dt} = \frac{1}{\rho} \nabla \left\{ \frac{\rho \cdot k}{u} (\nabla P - \rho \bar{g}) \right\} + \left(\frac{\alpha_\phi}{1-\phi} \frac{dS}{dt} \right) + \alpha_\phi \frac{\partial T}{\partial t} + q \quad (6)$$

1.2. Regional settings

The study area, known as Sinú offshore basin, corresponds to the red marked area in figure 2. The Sinú offshore basin is in the Colombian Caribbean Sea and forms part of the Sinú – San Jacinto sedimentary basin with which it limits to the west, to the north it limits with the Guajira Offshore basin, to the northwest with the Colombia basin, and to the southwest with the Uramita fault system and the Urabá basin. Tectonically, three main areas stand out: the South Sinú Fold Belt (SSFB); the Magdalena Fan Deposit (MFD); and the North Sinú Fold Belt (NSFB) (Flinch et al., 2003; Martinez et al., 2015).

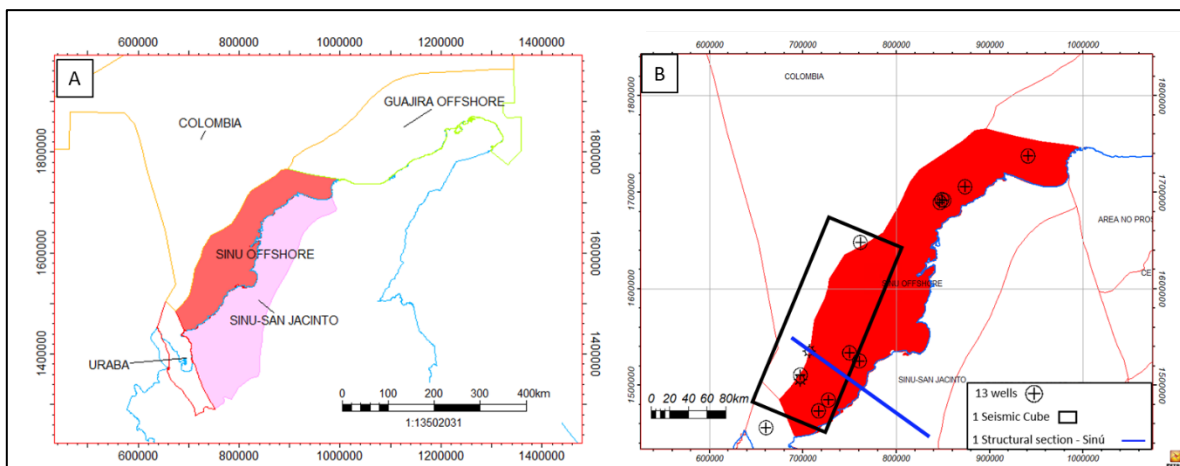


Figure. 14. Study area and data. A) Location and limits of the Sinú Offshore basin. B) Geographical location of the Information used in the present study. 13 wells (black circles), a seismic cube (black polygon), and a Structural section (blue line) were used.

Subsurface conditions are dominated by anticline-type compression structures, high-angle faults, and intraslope sub basins generated by tectonic interaction (Rincon Martinez et al., 2021). In the area, the Caribbean plate moves northeast subducting beneath the continental South America plate (Bernal-Olaya et al., 2016; Caro, 1978; Corredor, 2003; Pindell and tabbutt, 1995; Romero-Otero et al., 2015; Symithe et al., 2015) resulting in a slip strike stress field that controls the orientation of structures and faults (Bird, 2003).

2. DATA AND METHODOLOGY

For this analysis, information was obtained from 13 wells, 1 merged seismic survey which covers an approximate area of 9,000 km² and a structural section

represented by the blue line that is precisely located in that same geographical position (Figure 1B)

Methodologies based on the principle of effective stress and basin modelling were used.

The methodology base on the principle of effective stress, eq. (1) identifies the deviation in the effective stress trend, as compaction occurs, which in turn represents changes in pore pressure. The deviation in the effective stress is represented by the parameter “A” in eq. (8) which can be estimated from different porosity-dependent variables as; sound transit time or sound velocity, rock resistivity, and drillability. Sound transit time (DT) was used through the Eaton equation (Eaton, 1975) to quantify overpressure as presented in Eq. 10.

$$Pp = \sigma - \sigma' \quad (7)$$

$$\sigma' = \sigma'_N * A^B \quad (8)$$

$$A = \frac{DT_N}{DT_{OB}} \quad (9)$$

$$Pp = \sigma - \sigma'_N * \left(\frac{DT_N}{DT_{OB}}\right)^B \quad (10)$$

When the parameter “A” is 1, the observed effective stress (σ') is equal to the normal effective stress (σ'_N), indicating that the zone presents hydrostatic pressure. Otherwise, when having overpressures, the observed effective stress (σ') becomes lower than the expected normal effective stress (σ'_N), seeing this represented in that this parameter "A" will become less than 1.

The methodology consisted of three stages. The first stage had the objective of analyzing pressure profiles of 13 wells involved. The second stage of the study consisted in identifying areas with evidence of hydrostatic pressure, to establish a normal compaction trend that allow us to interpret overpressures in areas greater than those observed in wells, that is, to use other tools that offer greater coverage,

such as seismic cubes. The last stage consisted in carrying out a numerical simulation of the distribution of pore pressures in a cross section to understanding the conceptual distribution of these overpressures in an environment with the characteristics of the Southern Sinú Fold Belt (SSFB).

3. RESULTS

3.1. Pore pressure from wells

Figure 3 presents the pore pressure profile interpreted in two wells south of the Offshore Sinú basin. The second track shows that the blue line represents a Normal Compaction Trend (NCT) characterized by loss of porosity as sediments deepen. This loss of porosity is evidenced by the decrease in sound transit time, in other words, by the increase in sound velocity. As for the black line, it represents sonic logs of wells. This track shows the difference between these curves, whose separation is not very accentuated and therefore the curves remain a bit closer to each other. Interpretations related to pore pressure are presented in third track. There, the blue points indicate the estimated overpressure from the sonic log as the estimates of vertical stress (red line) and fracture gradient (green line). In this zone it is observed that these wells have overpressure ranging between 9 and 10 ppg, considered to be relatively small.

Otherwise, wells observed in figure 4 shows that as the blue line separates from the black line, the overpressure increases. The greater separation between the blue curve and the black curve confirms the growing overpressure observed in these wells, both located in the southern zone of the Sinú Offshore basin and whose observed values range between 15 and 18 ppg.

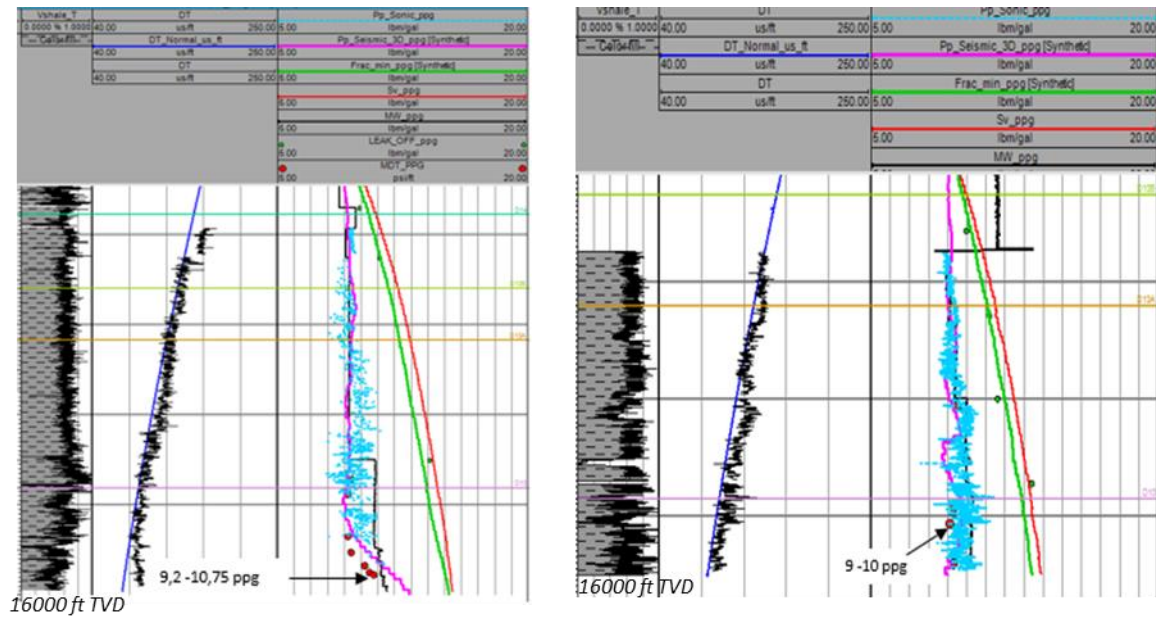


Figure. 15. Examples of wells South Sinú Offshore basin showing low overpressure profiles. Track 1, Interpreted clayness. Track 2, borehole sonic log (black line), compaction trend (blue line). Track 3, pore pressure estimation from well logs (cyan dots), pore pressure estimation from seismic velocities (magenta line), well mud density-Mw (black line), Vertical Stress (red line), Fracture gradient (Green line). integrity tests (green dots), pressure tests (red dots).

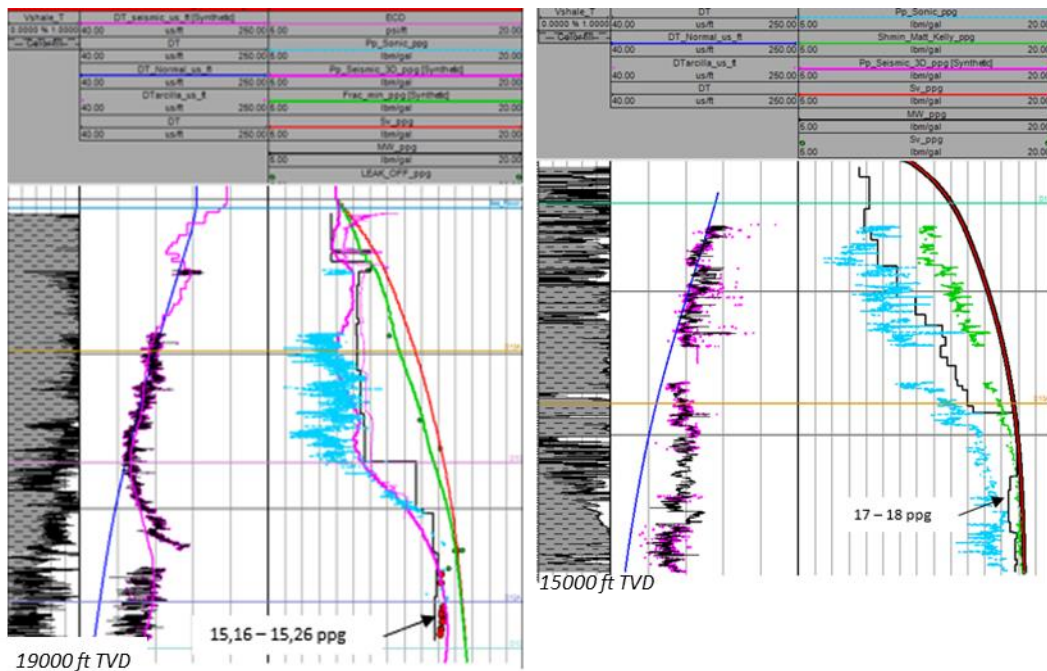


Figure. 16 Examples of wells South Sinú Offshore basin showing high overpressure profiles. Track 1, Interpreted clayness. Track 2, borehole sonic log (black line), seismic transit time (magenta line), compaction trend (blue line). Track 3, pore pressure estimation from well logs (cyan dots), pore pressure estimation from seismic velocities (magenta line), well mud density-Mw (black line), Vertical Stress (red line), Fracture gradient (Green line). integrity tests (green dots), pressure tests (red dots).

When observing the northern wells in influence of the Magdalena River fan, it is evident that the overpressures are generally lower than those observed in the south of the basin. For example, figure 5 presents wells in which values of the observed overpressures are lower than 14 ppg. These wells already have confirmatory pressure tests showing that despite the overpressure is relatively low. The presence of bulges indicates the existence of specific overpressured areas. However, such values would always be less than 13.5 ppg.

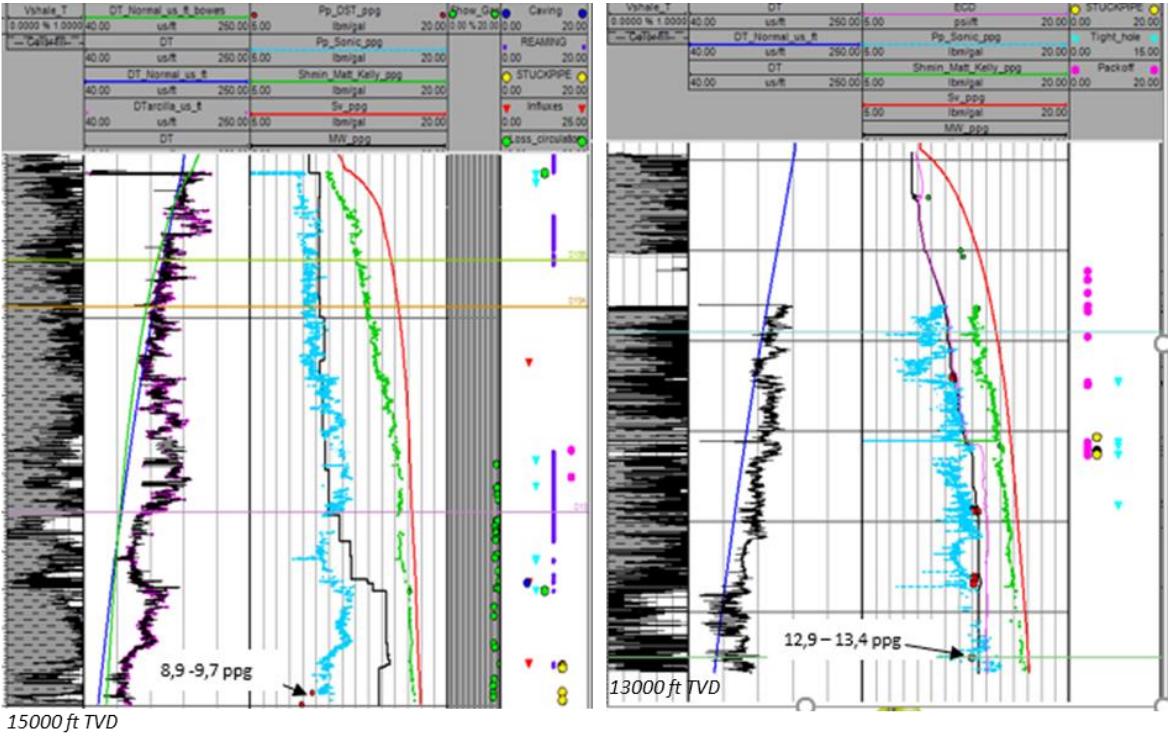


Figure. 17. Examples of wells North Sinú Offshore basin showing intermediate overpressure profiles. Track 1, Interpreted clayness. Track 2, borehole sonic log (black line), compaction trend (blue line). Track 3, pore pressure estimation from well logs (cyan dots), well mud density-Mw (black line), Vertical Stress (red line), Fracture gradient (Green line). integrity tests (green dots), pressure tests (red dots).

With the information obtained from wells we support that it is possible to identify the overpressured areas. This identification is the result of contrasting the difference between the normal compaction trend represented by the expected sonic transit time $DT_{(N)}$ and the observed sonic transit time in wells DT_{OB} (figure 6). The normal compaction trend was defined by selecting in wells sound transit time intervals under hydrostatic pressure conditions. After the compaction line was already defined, it was possible to interpret overpressures in areas greater than those observed in

wells, that is, it was feasible to use other tools that offer greater coverage, such as seismic cubes.

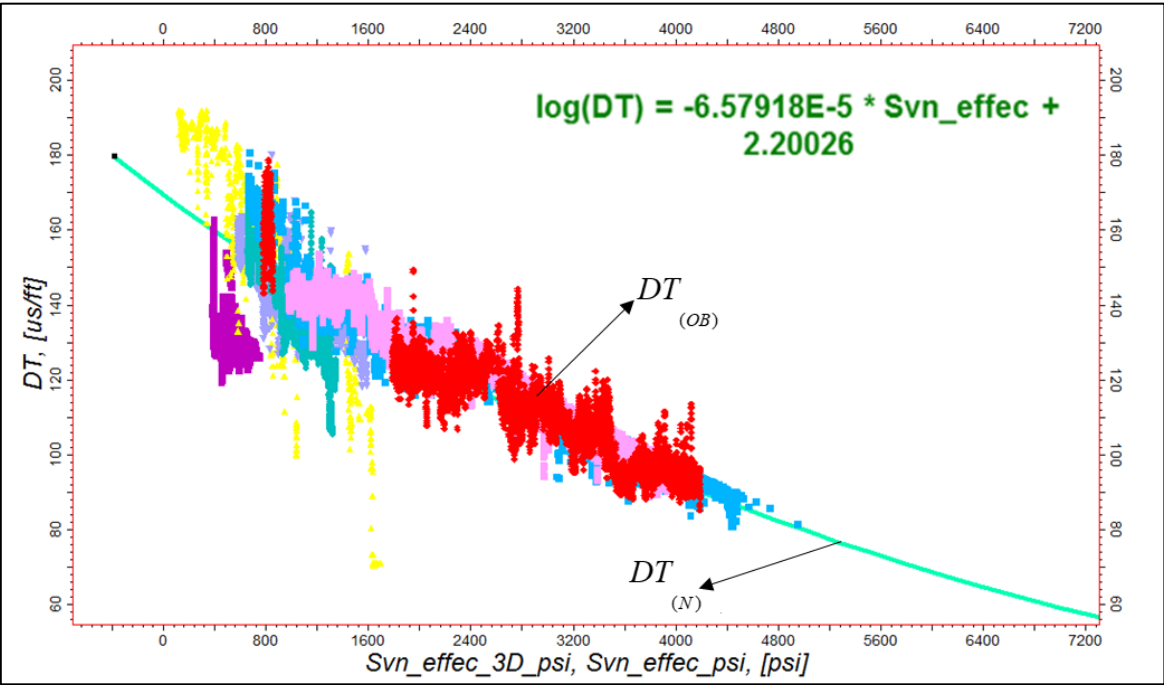


Figure. 18 Normal compaction curve defined for the sedimentary sequence in the Sinú Offshore basin. On the horizontal axis, the effective vertical stress under hydrostatic conditions (Svn_Effec) was plotted, while the vertical axis shows the reading of the sonic log (DT). The cyan colored line represents the compaction model for the study area.

3.2. Pore pressure from seismic data

Figure 7. presents the interpretation of pore pressure using a seismic cube for the Sinú offshore area. The color scale shows overpressures that can range from highly hydrostatic to pressures up to 15 ppg in certain areas.

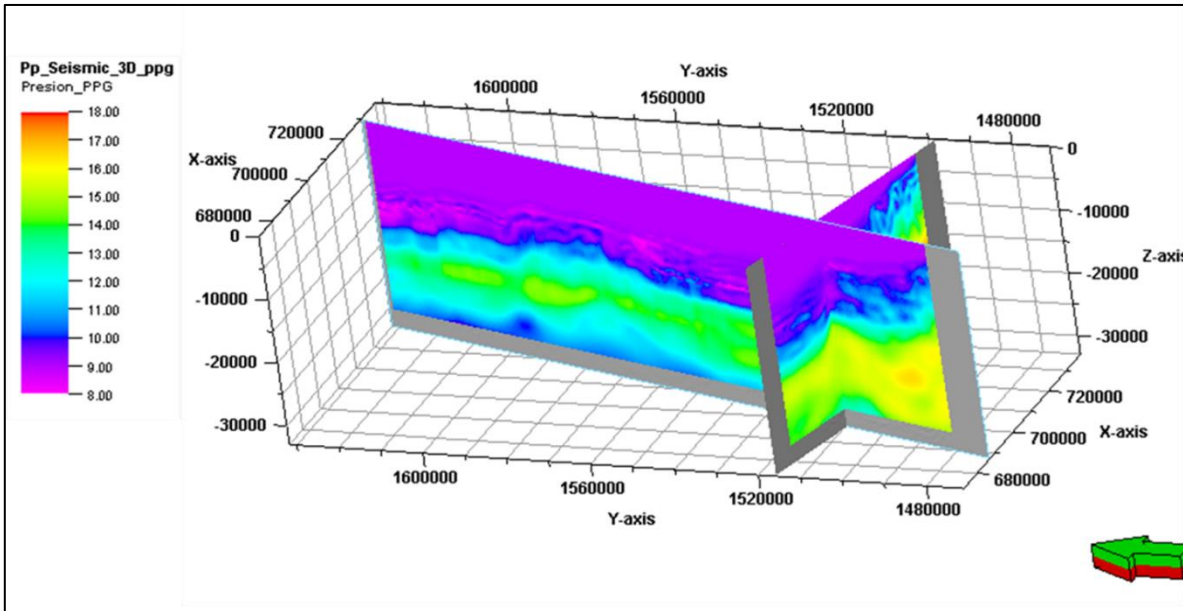


Figure. 19. Interpretation of pore pressure using a seismic cube for the Sinú offshore area. The color scale shows overpressures that can range from highly hydrostatic to pressures up to 15 ppg in certain areas.

By looking at a cross-section on the pore pressure interpretation cube, West to East (Figure 8) it is observed that overpressures represented with warm colors have a more direct relationship with compression structures (e.g. anticline-type) than with other geological phenomena such as: rapid sedimentation which is certainly more related to the characteristic Mass Transport Complexes (MTC) on the surface.

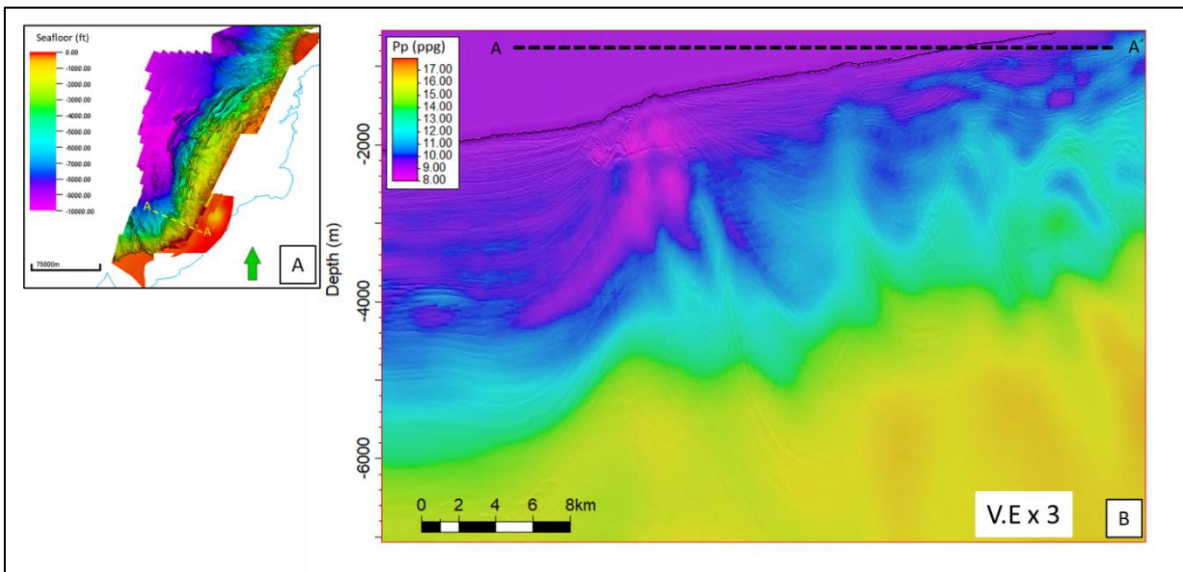


Figure. 20. East -West pore pressure distribution.

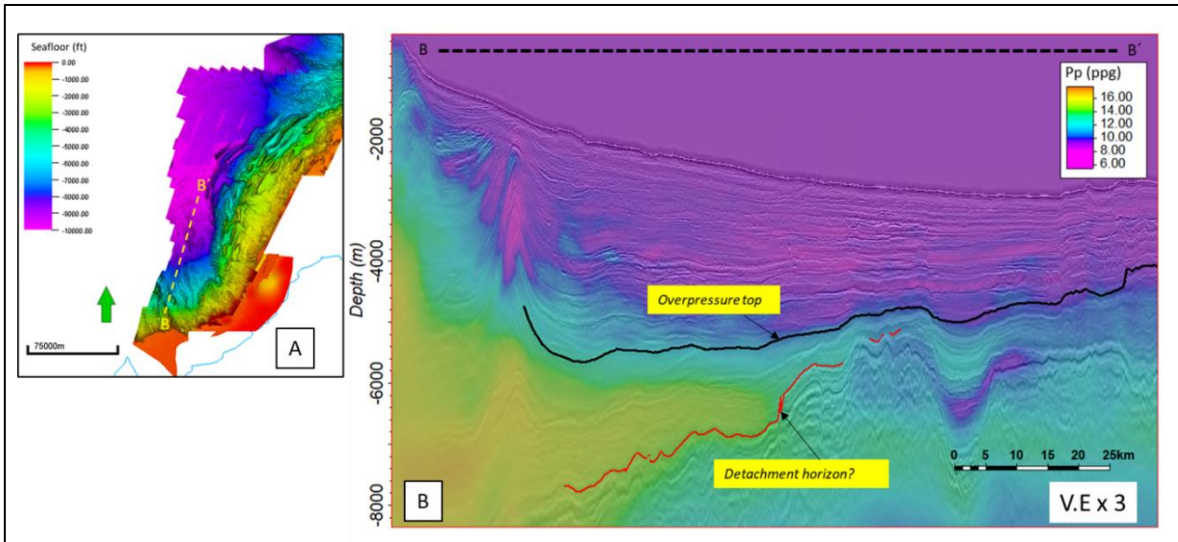


Figure. 21. South – North pore pressure distribution.

Reviewing the same information in a different direction, this time South to North (Figure 9) it is observed that overpressure, represented with warm colors, is related to a stratigraphic surface (e.g. Pliocene-Pleistocene discordance) up to a certain point, but from there, in this case with the presence of a structural high, the trace of that overpressure is lost. Likewise, sediments younger than the Pliocene - Pleistocene unconformity generally present a hydrostatic regime. From this observation it can be interpreted that in some areas the overpressure is related to a surface of Pliocene-Pleistocene regional discordance; despite that, this horizon is not an absolute reference to identify the areas of overpressure. This fact can be seen more clearly in figure 10 which is the interpretation of the regional discordance associated to the overpressure top presented in figure 9. It is observed that the overpressure is much more accentuated in the southern zone. Towards north, the overpressure in this discordance begins losing sight of its track and suddenly it vanishes.

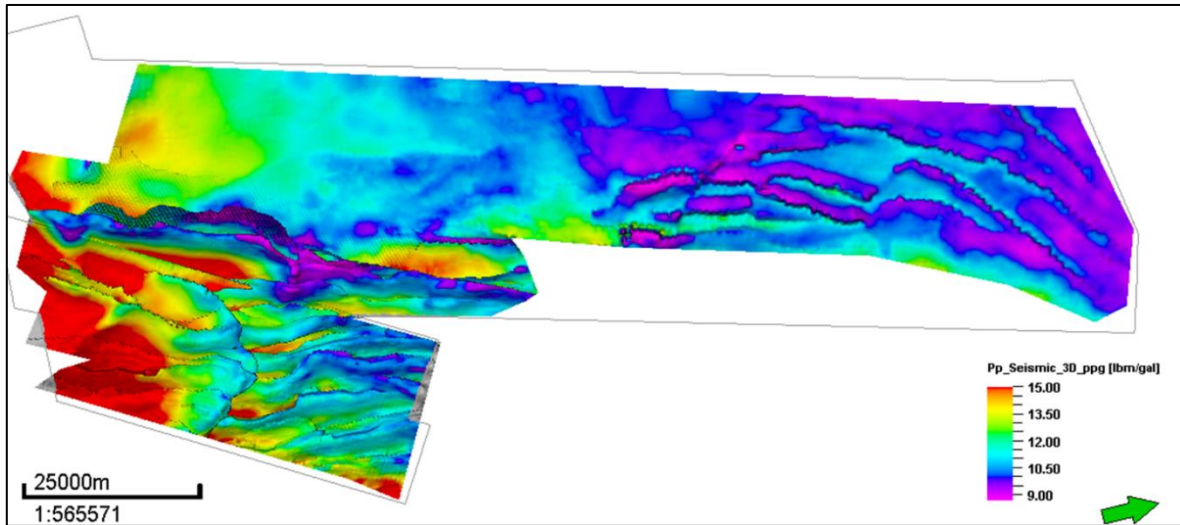


Figure. 22. Lateral pore pressure distribution along a Pliocene-Pleistocene regional discordance surface.

3.3. Pore pressure from 2D basin modelling

Understanding the conceptual distribution of these overpressures in an environment with the characteristics of the Southern Sinú Fold Belt (SSFB) was the fundamental reason why the 2D basin modeling was done.

The structural reconstruction of the last 10 million years in the evolution of the Southern Sinú Fold Belt was carried out considering the feasible component materials of this folded belt.

What this modeling suggests (figure 11) is that under current conditions overpressures are concentrated in the deformation front. The foregoing coincides very well with the data related to both the information of the well and the seismic information. According to this structural model, the overpressure coincides with important changes in both vertical and horizontal stresses. These horizontal stresses are interpreted to be associated with compression due to the tectonic interaction of the study area.

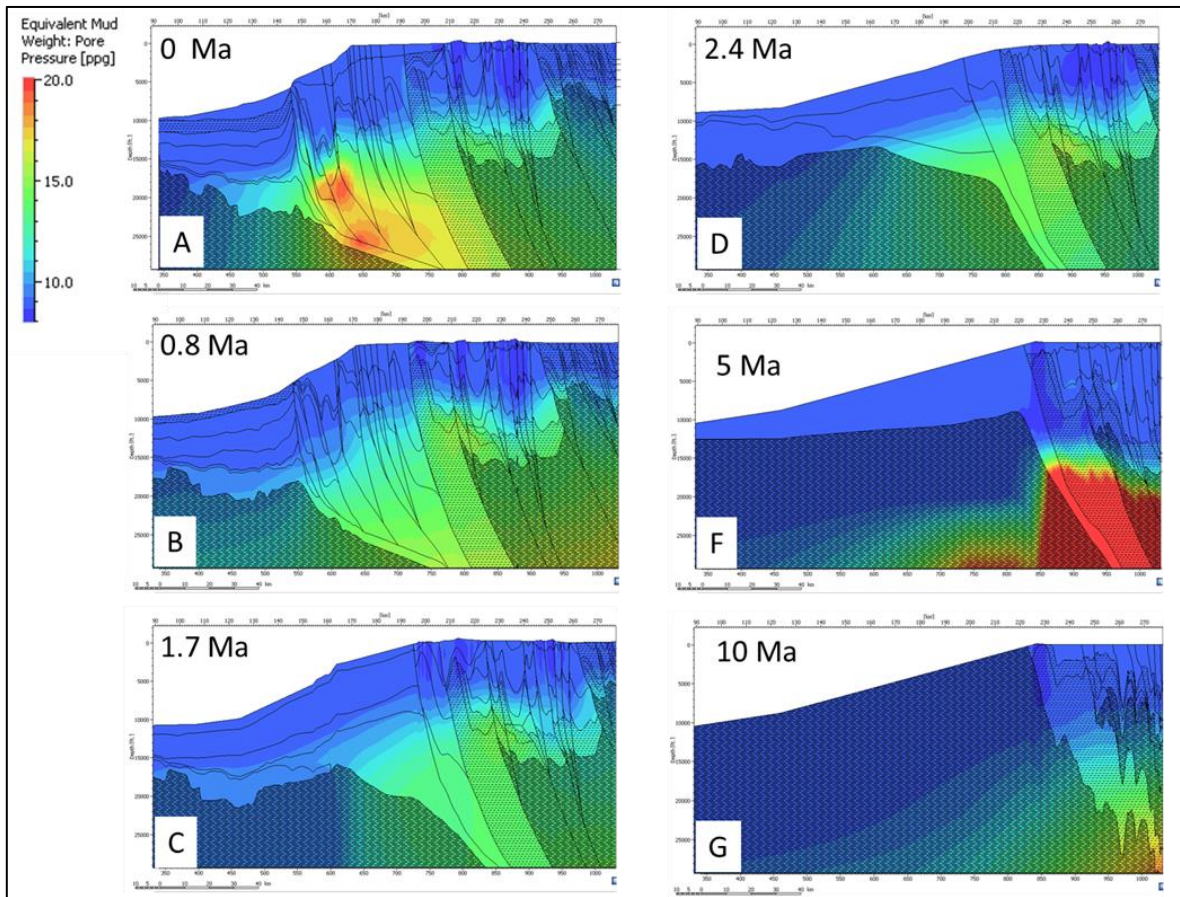


Figure. 23. Estimation of pore pressure from 2D Basin Modeling in the South Sinú fold Belt.

4. DISCUSSION

4.1. Adjusted factor for pore pressure and fracture gradient estimation

The exponent B in Eaton's equation (eq. 10) transforms an anomaly of the sound velocity into overpressure. That is, the same anomaly can be interpreted as greater overpressure as a greater exponent is used. For the study area, it was observed that areas of greatest compression require an exponent "B" between 2.5 and 3.0 to reflect the real condition of overpressure, while for areas with a predominance of gravitational stresses, an exponent "B" between 1.4 and 1.9 adequately predicts the observed overpressures.

The factor (K_0) of the fracture gradient equation (Mattews and Kelly) (eq. 11), represents the relationship between the minimum horizontal stresses and the vertical

stress. It can be calculated as the ratio between an effective LOT integrity test and the Effective vertical stress “ σ ” (Zhang and Yin, 2017). For this study, this relationship was estimated considering 24 LOT tests available in the analyzed wells, as shown in Figure 12. This model estimates conservative fracture gradient values, which is suitable for drilling mud window design. The equation that we suggest can represent the Ko for the sedimentary sequence of the Colombian margin of the Caribbean Sea is the following:

$$GF = K_o * \sigma' + Pp \tag{11}$$

$$K_o = 0.0672 * TVD_ft^{0.27} \tag{12}$$

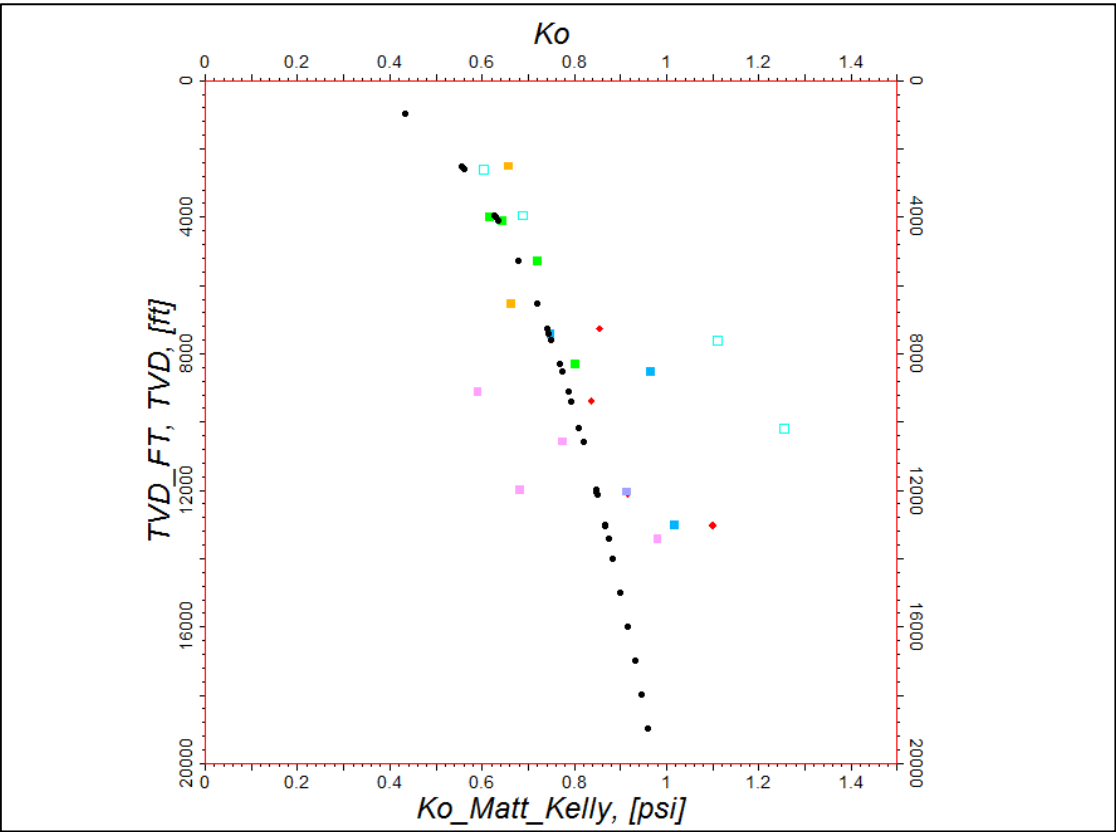


Figure. 15. Ko adjusted for pore pressure estimation in the Colombian Caribbean margin.

4.2. CONCLUSIONS

Wells with the highest overpressures (>15 ppg) are in the South of Sinú Offshore basin. On the other hand, wells located in the North area of the basin, showed less overpressure conditions (< 15 ppg).

Overpressure zones match with low velocities of sound from wells logs and seismic surveys.

Main overpressure zones are associated with levels older than a Pliocene-Pleistocene discordant level. However, we haven't found evidence about an absolute relation between overpressure and any specific stratigraphic unit.

Overpressure distribution in the South region of the Sinú Offshore basin seems to be affected not only by under compaction but also by high compressive tectonics setting.

Major identified uncertainties which are remaining are as follows:

- How overpressured are sediments far from the continental margin in the Colombia Basin? To learn more about this phenomenon in this area, either seismic cubes with interval velocity or data from wells should be used.
- Can the compaction curve be extended to other areas of the Colombian Caribbean Sea?
- Is it reasonable to use a regional compaction trend?
- How to involve horizontal compressive stresses for pore pressure estimation using methods based on the principle of effective stress?

ACKNOWLEDGMENTS

This work was undertaken as part the agreement FP44842-2017 Doctorado Empresa, ECOPETROL, EAFIT, COLCIENCIAS (MINTIC). Data were provided by Ecopetrol.

REFERENCES

- Bernal-Olaya, R., Sanchez, J., Mann, P., Murphy, M., 2016. Along-strike Crustal Thickness Variations of the Subducting Caribbean Plate Produces Two Distinctive Styles of Thrusting in the Offshore South Caribbean Deformed Belt, Colombia. *Mem. 108 Pet. Geol. Potential Colomb. Caribb. Margin* 295–322. <https://doi.org/10.1306/13531941m1083645>
- Borge, H., 2000. Fault controlled pressure modelling in sedimentary basins.
- Bowers, G.L., 1995. Pore Pressure Estimation From Velocity Data: Accounting for Overpressure Mechanisms Besides Undercompaction. *SPE Drill. Complet.* 10, 89–95. <https://doi.org/10.2118/27488-PA>
- Carcione, J.M., Helle, H.B., Pham, N.H., Toverud, T., 2003. Pore pressure estimation in reservoir rocks from seismic reflection data. *Geophysics* 68, 1569–1579. <https://doi.org/10.1190/1.1620631>
- Caro, H.D., 1978. Geotectonica y evolucion de la region noroccidental colombiana.
- Corredor, F., 2003. Seismic strain rates and distributed continental deformation in the northern Andes and three-dimensional seismotectonics of northwestern South America. *Tectonophysics* 372, 147–166. [https://doi.org/10.1016/S0040-1951\(03\)00276-2](https://doi.org/10.1016/S0040-1951(03)00276-2)
- Dvorkin, J., 2002. Pressure and Compaction in the Rock Physics Space.
- Eaton, B.A., 1975. The Equation for Geopressure Prediction from Well Logs. *Fall Meet. Soc. Pet. Eng. AIME*. <https://doi.org/10.2118/5544-MS>
- Fertl, W.H., Timko, D., 1971. Parameters for Identification of Overpressure Formations. *Drill. Rock Mech. Conf.* 12. <https://doi.org/10.2118/3223-MS>
- Flinch, J.F., Amaral, J., Doulcet, A., Mouly, B., Osorio, C., Pince, J.M., 2003. Structure of the Offshore Sinu Accretionary Wedge. Northern Colombia. VIII *Simp. Boliv. - Explor. Pet. en las Cuencas Subandinas* 76–83. <https://doi.org/https://doi.org/10.3997/2214-4609-pdb.33.Paper8>
- Foster, J.B; Whalen, H., 1966. Estimation of formation pressure From Electrical Surveys-Offshore Louisiana. *SPE* 1–7.
- George Dickinson, 1953. Geological Aspects of Abnormal Reservoir Pressures in Gulf Coast Louisiana. *Am. Assoc. Pet. Geol. Bull.* 37, 410–432. <https://doi.org/10.1306/5CEADC6B-16BB-11D7-8645000102C1865D>
- Gutierrez, M. a., Braunsdor, N.R., Couzens, B. a., 2006. Calibration and ranking of pore-pressure prediction models. *Lead. Edge* 25, 1516. <https://doi.org/10.1190/1.2405337>

- Hantschel, T., Kauerauf, A.I., 2009. Fundamentals of basin and petroleum systems modeling, *Fundamentals of Basin and Petroleum Systems Modeling*. <https://doi.org/10.1007/978-3-540-72318-9>
- Holand, P., 2017. Loss of Well Control Occurrence and Size Estimators, Phase I and II.
- Hottmann, C.E., Johnson, R.K., 1965. Estimation of Formation Pressures from Log-Derived Shale Properties. *J. Pet. Technol.* 17, 717–722. <https://doi.org/10.2118/1110-PA>
- Hubbert, M.K., Rubey, W.W., 1959. Role of fluid pressure in mechanics of overthrust faulting 1. Mechanics of fluid filled porous solids and its application of overthrust faulting. *Geol. Soc. Am. Bull.* 70, 115–166.
- Mann, D.M., Mackenzie, A.S., 1990. Prediction of pore fluid pressures in sedimentary basins. *Mar. Pet. Geol.* 7, 55–65. [https://doi.org/10.1016/0264-8172\(90\)90056-M](https://doi.org/10.1016/0264-8172(90)90056-M)
- Martinez, J.A., Castillo, J., Ortiz-Karpf, A., Rendon, L., Mosquera, J.C., Vega, V., 2015. Deep Water Untested Oil-play in the Magdalena Fan, Caribbean Colombian Basin, in: Bartolini, C., Mann, P. (Eds.), *Petroleum Geology and Potential of the Colombian Caribbean Margin*. American Association of Petroleum Geologists, Memoir 108, pp. 251–260. <https://doi.org/10.1306/13531955m1083658>
- NGI, 2005. Offshore geohazards 2, 72.
- Pindell, J.L., tabbutt, K., 1995. Mesozoic-Cenozoic Andean Paleogeography and regional control on hidrocarbon systems.
- Rincon Martinez, D.A., Naranjo-Vesga, J., Mateus-Tarazona, D., Hernandez Muños, C., Madero Pinzon, H., De Bedout Ordonez, J., Ortiz-Karpf, A., Malagon Rojas, F., Osorio Cabrera, C., 2021. Geomorfología del fondo marino profundo en la región sur del Caribe Colombiano. *Ecopetrol; Entrelibros S.A.S.* <https://doi.org/https://doi.org/10.29047/9789589287361>
- Romero-Otero, G.A., Slatt, R.M., Pirmez, C., 2015. Evolution of the Magdalena Deepwater Fan in a Tectonically Active Setting, Offshore Colombia. *Mem. 108 Pet. Geol. Potential Colomb. Caribb. Margin* 675–707. <https://doi.org/10.1306/13531953M1083656>
- Terzaghi, K., Peck, R.B., Mesri, G., 1996. *Soil mechanics in engineerin practice* 3rd edition. Wiley-Interscience.
- Weakley, R.R., 1991. Use of Surface Seismic Data To Predict Formation Pore Pressure Worldwide. *Proc. SPE West. Reg. Meet.* 37–42. <https://doi.org/10.2523/21752-MS>

- Xiaorong, L.U.O., Loujun, L.I.U., Xueyi, L.I., 2006. Overpressure distribution and pressuring mechanism on the southern margin of the Junggar Basin , Northwestern 51, 2383–2390. <https://doi.org/10.1007/s11434-006-2126-9>
- Xiaorong Luo, Vasseur, G., 1992. Contributions of compaction and aquathermal pressuring to geopressure and the influence of environmental conditions. Am. Assoc. Pet. Geol. Bull. 76, 1550–1559. <https://doi.org/10.1306/BDF8FB0-1718-11D7-8645000102C1865D>